GE Nuclear Energy

C.J. Deacon
Manager, Advanced Reactor Programs

General Electric Company
175 Curtner Avenue, M/C 365 San Jose, CA 95125-1014
408 925-2469 (phone) 408 925-5474 (facsimile)

MFN 03-013 Project 717

March 4, 2003

U.S. Nuclear Regulatory Commission
ATTN: Document Control Desk
One White Flint North
11555 Rockville Pike
Rockville, MD 20852-2738

Reference: Letter S. Hucik, GE to S. Collins, NRC, Pre-application Review of ESBWR, dated April 18, 2002

Subject: **SBWR Testing Summary Report, NEDO-32606 - Document Transmittal for Pre-Application Review of ESBWR – Non-Proprietary Report**

The CD accompanying this letter contains the GE non-proprietary report NEDO-32606, SBWR Testing Summary Report.

If you have any questions about the information provided here, please contact Atam Rao at (408) 925-1885, or myself.

Sincerely,

C.J.W. Deacon

cc: A. Cubbage USNRC (with CD)
J. Lyons USNRC (w/o CD)
G.B. Stramback - GE (with CD)

NEDO-32606
Class I
DRF 0000-0005-8040
August 2002

SBWR Testing Summary Report

P.F. Billig
J.D. Duncan
R.E. Gamble
M. Herzog
A. Hunsbedt
G.A. Wingate

Approved: _____
C.J.W. Deacon, Manager
Advanced Reactor Programs

IMPORTANT NOTICE REGARDING CONTENTS OF THIS REPORT

PLEASE READ CAREFULLY

The only undertakings of the General Electric Company (GE) respecting information in this document are contained in the contract between the customer and GE, as identified in the purchase order for this report and nothing contained in this document shall be construed as changing the contract. The use of this information by anyone other than the customer or for any purpose other than that for which it is intended, is not authorized; and with respect to any unauthorized use, GE makes no representation or warranty, and assumes no liability as to the completeness, accuracy, or usefulness of the information contained in this document.

ACKNOWLEDGMENT

The authors are indebted to the following people for providing valuable assistance, information, and comments on the draft of this report: R. Buchholz, J. Fitch, J. Healzer, T. Narazaki and A. Yang. Special thanks are extended to G. Yadigaroglu for his assistance with the scaling evaluation and to J. Dreier for his review of the sections on the PANDA program.

The authors also thank P. Bautista and Y. Espino for their efforts to compile everything into one document and M. Swope for his editorial assistance.

Finally, the authors would like to thank the international associates who developed and conducted the test programs described in this report. Specifically, these organizations are: Ansaldo SpA, ENEA, ENEL SpA, and SIET SpA in Italy for PANTHERS; the Paul Scherrer Institut in Switzerland for PANDA; and the Toshiba Corporation in Japan for GIRAFFE.

TABLE OF CONTENTS

LIST OF TABLES **ix**

LIST OF FIGURES **xi**

ACRONYMS **xv**

EXECUTIVE SUMMARY **xvii**

1. INTRODUCTION **1-1**

1.1 Background 1-1
1.2 Scope of Report 1-2

2. THERMAL-HYDRAULIC TESTS **2-1**

2.1 PANTHERS/PCC 2-3
2.1.1 Test Objectives 2-3
2.1.2 Test Description 2-3
2.1.3 Test Matrix 2-4
2.1.3.1 Steady-State Performance Tests 2-4
2.1.3.2 Transient Test Conditions 2-5
2.1.4 Applicability of Data to SBWR 2-5
2.1.4.1 SBWR PCC Operational Modes 2-6
2.1.4.2 PCC Purge and Vent Process 2-8
2.1.4.3 PANTHERS PCC Operation 2-9
2.1.4.4 Summary of Data Applicability 2-13
2.1.5 Key Results 2-14
2.1.5.1 Steady-State Tests 2-14
2.1.5.2 Transient Tests 2-15
2.1.5.3 Closure with TAPD 2-16
2.1.6 Component Demonstration Tests 2-16
2.2 PANTHERS/IC 2-38
2.2.1 Test Objectives 2-38
2.2.2 Test Description 2-38
2.2.3 Test Matrix 2-39
2.2.3.1 Steady-State Performance Tests 2-39
2.2.3.2 Transient Test Conditions 2-39
2.2.4 Applicability of Data to SBWR 2-40
2.2.4.1 Steady-State Tests 2-40
2.2.4.2 Transient Tests 2-40
2.2.5 Key Results 2-41
2.2.5.1 Steady-State Tests 2-41
2.2.5.2 Transient Tests 2-41
2.2.5.3 Closure with TAPD 2-42
2.2.6 Component Demonstration Tests 2-43

2.3 PANDA 2-51
2.3.1 Test Objectives 2-51
2.3.2 Test Description 2-51
2.3.3 Test Matrix 2-52
2.3.3.1 Steady-State Performance Tests 2-52
2.3.3.2 Transient Integral Systems Tests 2-53
2.3.4 Applicability of Data to SBWR 2-55
2.3.4.1 Steady-State Tests 2-55
2.3.4.2 Transient Integral Systems Tests 2-56
2.3.5 Key Results 2-62
2.3.5.1 Steady-State Tests 2-62
2.3.5.2 Transient Integral Systems Tests 2-62
2.3.5.3 Closure with TAPD 2-68
2.4 GIST 2-88
2.4.1 Test Objectives 2-88
2.4.2 Test Description 2-88
2.4.3 Test Matrix 2-88
2.4.4 Applicability of Data to SBWR 2-89
2.4.4.1 Introduction 2-89
2.4.4.2 GDCS Driving Pressure 2-89
2.4.4.3 RPV Water Level 2-90
2.4.4.4 Summary of Data Applicability 2-90
2.4.5 Key Results 2-90
2.4.5.1 Series BDLB 2-91
2.4.5.2 Series MSLB 2-91
2.4.5.3 Series GDLB 2-91
2.4.5.4 Series NB 2-91
2.4.5.5 Closure with TAPD 2-92
2.5 GIRAFFE/Helium 2-99
2.5.1 Test Objectives 2-99
2.5.2 Test Description 2-99
2.5.3 Test Matrix 2-99
2.5.3.1 Helium Test Series 2-99
2.5.3.2 Tie-Back Test Series 2-100
2.5.4 Applicability of Data to SBWR 2-101
2.5.4.1 Test Facility Design 2-101
2.5.4.2 Choice of the Base Case (H1) 2-102
2.5.4.3 Other Tests 2-102
2.5.5 Key Results 2-102
2.5.5.1 Nitrogen vs. Helium Tests (H1 and H2) 2-102
2.5.5.2 Nitrogen with Helium Tests (H3 and H4) 2-103
2.5.5.3 Tie-Back Tests (T1 and T2) 2-103
2.5.5.4 Closure with TAPD 2-104
2.6 GIRAFFE/SIT 2-112
2.6.1 Test Objective 2-112

2.6.2 Test Description 2-112
2.6.3 Test Matrix 2-113
2.6.4 Applicability of Data to SBWR 2-114
2.6.4.1 Test Facility Design 2-114
2.6.4.2 Choice of the Base Case Test (GS1) 2-114
2.6.4.3 Other Tests 2-114
2.6.4.4 Test Initiation 2-115
2.6.5 Key Results 2-115
2.6.5.1 Effect of IC/PCC (GS1 and GS2) 2-115
2.6.5.2 Effect of Break Type (GS2 and GS3) 2-115
2.6.5.3 Effect of Single Failure Assumption (GS2 and GS4) 2-116
2.6.5.4 Effect of GDCS Flow on PCCS Operation (GS2) 2-116
2.6.5.5 Closure with TAPD 2-117

3. PIRT EVALUATION 3-1

3.1 PANTHERS/PCC 3-5
3.1.1 PCC Flow and Pressure Drop (PC1) 3-5
3.1.2 Condensation on Primary Side - Degradation by Noncondensible Gases (PC2) 3-6
3.1.3 Secondary Side Heat Transfer (PC3) 3-6
3.1.3.1 Pool Temperature Distribution 3-7
3.1.3.2 Pool Void Distribution 3-7
3.1.3.3 Natural Circulation 3-7
3.1.4 Parallel PCC Tube Effects (PC4) 3-8
3.1.5 Parallel PCC Module Effects (PC5) 3-9
3.2 PANTHERS/IC 3-14
3.2.1 IC Pressure Drop (Q1) 3-14
3.2.2 IC Capacity (Q2) 3-14
3.2.3 Stratification in IC Drums (Q3) 3-14
3.2.4 IC Pool Stratification (Q4) and Secondary Side Heat Transfer (Q5) 3-15
3.3 PANDA 3-16
3.3.1 PCC Flow and Pressure Drop (PC1) 3-16
3.3.2 Condensation on Primary Side-Degradation by Noncondensible Gases (PC2) 3-16
3.3.3 Secondary Side Heat Transfer (PC3) 3-16
3.3.3.1 Pool Temperature Distribution 3-17
3.3.3.2 Pool Void Distribution 3-17
3.3.3.3 Natural Circulation Distribution 3-17
3.3.4 Parallel PCC Tube Effects (PC4) 3-17
3.3.5 Three-Dimensional Effects (DW3) 3-18
3.3.5.1 Phase Distribution 3-19
3.3.5.2 Noncondensible Gas Distribution 3-19
3.3.5.3 Buoyancy/Natural Circulation 3-20
3.3.6 Condensation on Reactor Outflows (DW4) 3-20
3.3.7 Wetwell Free Surface Condensation/Evaporation (WW4) 3-20

3.3.8 Pool Mixing and Stratification (WW6) 3-21
3.3.9 Three-Dimensional Effects in Gas Space (WW7) 3-21
3.3.9.1 Temperature Distribution 3-22
3.3.9.2 Noncondensible Gas Distribution 3-22
3.3.10 Drywell Spray Condensation (FPS1, WW8) 3-22
3.3.11 Parallel PCC Unit Effects (PC5/XC5) 3-23
3.3.12 PCCS Startup with Noncondensible Gas (PC8) 3-24
3.3.13 Leakage between Drywell and Wetwell (DWB1) 3-24
3.3.14 System Interactions - IC/GDCS/PCC (XC2) 3-25
3.3.15 System Interactions - Multiple PCC units (XC5) 3-26
3.4 GIRAFFE/Helium 3-30
3.4.1 System Interaction - Light Noncondensible Gas DW/PCCS/WW (XC6) 3-30
3.4.2 Three-Dimensional Effects (DW3) 3-31
3.4.2.1 Phase Separation (DW3) 3-31
3.4.2.2 Noncondensible Gas Stratification (DW3) 3-31
3.4.2.3 Buoyancy/Natural Circulation (DW3) 3-32
3.4.3 PCCS Startup with Noncondensible Gas (PC8) 3-33
3.5 GIRAFFE/SIT 3-35
3.5.1 Break Uncovery (E1) 3-35
3.5.2 Void Profile/Two-Phase Level in Downcomer (E2) 3-36
3.5.3 Cold Water Injection Below Two-Phase Level (E3) 3-36
3.5.4 Cold Water Injection Above Two-Phase Level (E7) 3-36
3.5.5 Void Distribution/Two-Phase Level in Chimney (F1) 3-37
3.5.6 System Interaction - GDCS/System Depressurization (XL3) 3-37
3.5.7 System Interaction - RPV/DW/WW/IC/DPV/PCCS/GDCS (XL4) 3-37

4. INTEGRATION OF TESTS AND CONFIRMATION OF SCALING 4-1

4.1 Steady-State Component Tests 4-3
4.1.1 Pure Steam Tests 4-3
4.1.2 Heat Removal Degradation by Noncondensible Gas 4-4
4.1.3 Correlating the PCC Performance Data 4-5
4.2 Integral System Transient Tests 4-12
4.2.1 Short-term RPV Behavior 4-13
4.2.1.1 RPV Liquid Mass 4-13
4.2.1.2 RPV Blowdown Pressure 4-17
4.2.2 Containment Performance 4-20
4.2.2.1 Containment Behavior Overview 4-21
4.2.2.2 Wetwell Behavior 4-23
4.2.2.3 DW Behavior 4-29
4.2.2.4 Summary of Containment Behavior and Scaling 4-35
4.3 Helium Tests 4-57
4.4 Scaling Distortions 4-59
4.4.1 Background 4-59
4.4.2 Scaling Issues Considered 4-60

4.4.3 Scaling Issue Evaluation 4-60
4.4.3.1 Heat Release from RPV Structures 4-60
4.4.3.2 Heat Release from DW Structures 4-64
4.4.3.3 Drywell Mixing 4-66
4.4.4 Discussion of Safety Parameters 4-69

5. CONCLUSIONS 5-1

6. REFERENCES 6-1

APPENDIX A A-1

LIST OF TABLES

Table 2.0-1	Roadmap of the SBWR Test Programs	2-2
Table 2.1-1	PANTHERS/PCC Steady-State Performance Matrix – Steam Only Tests	2-18
Table 2.1-2	PANTHERS/PCC Steady-State Performance Matrix – Air-Steam Mixture Tests	2-19
Table 2.1-3	PANTHERS/PCC Noncondensible Buildup – Test Matrix	2-23
Table 2.1-4	PANTHERS/PCC Pool Water Level Effects – Test Matrix	2-23
Table 2.2-1	PANTHERS/IC Steady-State Performance Test Matrix	2-45
Table 2.2-2	PANTHERS/IC Startup and Operation Test Matrix	2-45
Table 2.2-3	PANTHERS/IC Transient Performance Test Matrix	2-45
Table 2.3-1	PANDA Steady-State PCC Performance Test Matrix	2-69
Table 2.3-2	PANDA Transient System Performance Test Matrix	2-70
Table 2.4-1	GIST Test Matrix Initial Conditions (RPV at 791 kPa)	2-93
Table 2.5-1	GIRAFFE/Helium Test Series Test Matrix	2-105
Table 2.5-2	GIRAFFE/Helium Test Series Initial Conditions	2-105
Table 2.5-3	GIRAFFE/Helium Tieback Tests Initial Conditions	2-106
Table 2.6-1	GIRAFFE/SIT Test Matrix	2-118
Table 2.6-2	GIRAFFE/SIT Test Conditions	2-119
Table 2.6-3	Basis for GIRAFFE/SIT Test Conditions	2-120
Table 3.0-1	TRACG Qualification Needs from PANTHERS	3-2
Table 3.0-2	TRACG Qualification Needs from PANDA	3-3
Table 3.0-3	TRACG Qualification Needs from GIRAFFE	3-4
Table 3.1-1	Key Results from PANTHERS/PCC Tests with 5 kg/sec Steam Flow and 330 kPa Inlet Pressure	3-10
Table 3.1-2	PANTHERS/PCC Pool Temperatures	3-11
Table 3.1-3	PANTHERS/PCC Tube Temperatures (Test T09-9)	3-12
Table 3.4-1	GIRAFFE/Helium Drywell Temperatures at 7200 sec	3-34
Table 4.1-1	GIRAFFE Phase 1, Step 1 Test Matrix	4-8
Table 4.1-2	Deduced Scale Factors for the PCC at SBWR Test Facilities	4-8
Table 4.2-1	Reference Values and PI-Groups for RPV Liquid Mass	4-36

Table 4.2-2	Reference Values and PI-Groups for RPV Pressure During Late Blowdown and GDCS Transition Phases	4-37
Table 4.2-3	Reference Values and PI-Groups for WW Pressure During PCC Phase	4-38
Table 4.2-4	Reference Values and PI-Groups for DW Pressure During PCC Phase	4-39
Table 4.4-1	List of Perceived Scaling Distortions and Evaluation Results for SBWR Related Test Facilities	4-71
Table 4.4-2	Calculated Specific Time Ratios for Drywell Mixing	4-73

LIST OF FIGURES

Figure 1.0-1:	Key Variables and Test Coverage During SBWR LOCA Phases	1-3
Figure 2.1-1:	PANTHERS/PCC Test Article	2-24
Figure 2.1-2:	PANTHERS/PCC Test Facility Schematic	2-25
Figure 2.1-3:	PCC Operational Modes	2-26
Figure 2.1-4:	PANTHERS Representation of PCC Operational Modes	2-27
Figure 2.1-5:	TRACG PANTHERS/PCC Qualification Points	2-28
Figure 2.1-6:	PANTHER/PCC Power for Saturated Steam Tests	2-29
Figure 2.1-7:	PANTHERS/PCC Power for Air/Steam Tests	2-30
Figure 2.1-8:	Effect of Superheat on Condensation Efficiency for PANTHERS/PCC Air/Steam Tests	2-31
Figure 2.1-9:	Effect of Air Mass Fraction on Condensation Efficiency for PANTHERS/PC4 Air/Steam Tests	2-32
Figure 2.1-10:	PANTHERS/PC5 Test T54 Inlet Pressure Response to IC Pool Water Level	2-33
Figure 2.1-11:	PANTHER7/PCC Test T51 Tube Temperature Response with Air Injection	2-34
Figure 2.1-12:	PANTHERS/PCC Test T76 Tube Temperature Response with Helium Injection	2-35
Figure 2.1-13:	PANTHERS/PCC Test T76 Tube 5Q Temperature Response with Helium Injection	2-36
Figure 2.1-14:	PANTHERS/PCC Pressure Transients for Air (Test T51) and Helium (Test T76) Buildup	2-37
Figure 2.2-1:	Isolation Condenser Test Article	2-46
Figure 2.2-2:	PANTHERS/IC Test Facility Schematic	2-47
Figure 2.2-3:	PANTHERS/IC Power for Saturated Steam Tests	2-48
Figure 2.2-4:	PANTHERS/IC Test T15 Inlet Pressure Response to PCC Pool Water Level	2-49
Figure 2.2-5:	PANTHERS/IC Inlet Pressure Response During Noncondensible Gas Venting Tests	2-50
Figure 2.3-1:	Isometric View of the PANDA Facility	2-71
Figure 2.3-2:	PANDA Facility Schematic	2-72
Figure 2.3-3:	PANDA Facility: IC/PCC Test Units	2-73
Figure 2.3-4:	Effect of Air Mass Fraction on PANDA S-series Tests	2-74

Figure 2.3-5:	PANDA Tests M3, M3A, M3B Drywell Pressure Response	2-75
Figure 2.3-6:	PANDA Test M3 PCC1 Inside Tube Gas Temperatures	2-76
Figure 2.3-7:	PANDA Test M3 PCC1 Inside Gas and Wall Tube Temperatures	2-77
Figure 2.3-8:	PANDA Test M3B PCC1 Inside Tube Gas Temperatures	2-78
Figure 2.3-9:	PANDA Tests M3 and M2 Drywell Pressure Response	2-79
Figure 2.3-10:	PANDA Tests M10A, M10B, & M3 Drywell Pressure Response	2-80
Figure 2.3-11:	PANDA Tests M10A & M10B WW1 Upper Gas Temperature Response	2-81
Figure 2.3-12:	PANDA Test M10A PCC2 Inside Tube Gas Temperatures	2-82
Figure 2.3-13:	PANDA Test M10B PCC2 Inside Tube Gas Temperatures	2-83
Figure 2.3-14:	PANDA Test M6/8 and M3 Drywell Pressure Response	2-84
Figure 2.3-15:	PANDA Test M6/8 IC and PCC Pool Levels	2-85
Figure 2.3-16:	PANDA Tests M9 and M3 Drywell Pressure Response	2-86
Figure 2.3-17:	PANDA Test M9 GDCS and Average PCC Pool Levels	2-87
Figure 2.4-1:	GIST Facility Schematic	2-95
Figure 2.4-2:	GIST Facility Piping Arrangement	2-96
Figure 2.4-3:	GIST RPV Pressure for GDCS Line Break Base Case Test (C01A)	2-97
Figure 2.4-4:	GIST RPV Inventory and GDCS Flow for GDCS Line Break Base Case Test (C01A)	2-98
Figure 2.5-1:	GIRAFFE/Helium Test Facility Schematic	2-107
Figure 2.5-2:	PCC Unit for GIRAFFE /Helium and SIT Tests	2-108
Figure 2.5-3:	GIRAFFE /Helium Tests Drywell Pressure Response	2-109
Figure 2.5-4:	GIRAFFE /Helium Test H1 PCC Tube Bulk Fluid Temperatures	2-110
Figure 2.5-5:	GIRAFFE /Helium Test H2 PCC Tube Bulk Fluid Temperatures	2-111
Figure 2.6-1:	GIRAFFE/SIT Test Facility Schematic	2-121
Figure 2.6-2:	GIRAFFE/SIT IC Unit	2-122
Figure 2.6-3:	GIRAFFE/SIT RPV Pressure Response to IC/PCCS Operation	2-123
Figure 2.6-4:	GIRAFFE/SIT RPV Inventory Response to IC/PCCS Operation	2-124
Figure 2.6-5:	GIRAFFE/SIT RPV Pressure Response to Break Location	2-125
Figure 2.6-6:	GIRAFFE/SIT RPV Inventory Response to Break Location	2-126
Figure 2.6-7:	GIRAFFE/SIT RPV Pressure Response to Single Failure Assumption	2-127
Figure 2.6-8:	GIRAFFE/SIT RPV Inventory Response to Single Failure Assumption	2-128

Figure 2.6-9:	Effect of GDCS Flow on Containment Pressure and PCCS Operation in GIRAFFE/SIT Test GS2	2-129
Figure 3.1-1:	PCC Module Pressure Drops at PANTHERS	3-13
Figure 3.3-1:	PANDA Test M3 PCC1 Mid-Tube Wall Temperatures	3-27
Figure 3.3-2:	PANDA Test M3 PCC Feed Mass Flow Rates	3-28
Figure 3.3-3:	PANDA Test M7 Drywell 1 Air Mass Fraction and PCC Pool Water Level	3-29
Figure 3.5-1:	GDL Break Uncovery In Giraffe/SIT Test GS2	3-38
Figure 3.5-2:	RPV Temperatures In Giraffe/SIT Test GS2	3-39
Figure 4.1-1:	Effect of Pressure on Pure Steam Condenser Tests	4-9
Figure 4.1-2:	Effect of Noncondensible Concentration on Normalized Power	4-10
Figure 4.1-3:	Scaling Comparison of Air/Steam Condenser Tests Using a Simple Heat Transfer Correlation	4-11
Figure 4.2-1:	PI-Group Magnitudes for RPV Liquid Mass Equation During Three Early Phases	4-40
Figure 4.2-2:	Nondimensional Comparison of RPV Liquid Mass Equation for SBWR, GIST and GIRAFFE	4-41
Figure 4.2-3:	PI-Group Magnitudes for RPV Depressurization - Late Blowdown	4-42
Figure 4.2-4:	Nondimensional Comparison of RPV Pressure for SBWR, GIST and GIRAFFE	4-43
Figure 4.2-5:	Comparison of WW Pressures for SBWR, PANDA and GIRAFFE - MSLB	4-44
Figure 4.2-6:	Comparison of DW Pressures for SBWR, PANDA and GIRAFFE - MSLB	4-45
Figure 4.2-7:	Comparison of SP Temperatures for SBWR, PANDA and GIRAFFE - MSLB	4-46
Figure 4.2-8:	Comparison of WW Pressures for SBWR and GIRAFFE - GDLB	4-47
Figure 4.2-9:	Comparison of DW Pressures for SBWR and GIRAFFE - GDLB	4-48
Figure 4.2-10:	Comparison of SP Temperatures for SBWR and GIRAFFE - GDLB	4-49
Figure 4.2-11:	Nondimensional Comparison of WW Pressure for SBWR, PANDA and GIRAFFE	4-50
Figure 4.2-12:	PI-Group Magnitudes for WW Pressure Phenomena - PCCS Phase	4-51

Figure 4.2-13:	WW Pressure Increases with Increases in Noncondensible Partial Pressures	4-52
Figure 4.2-14:	Time Dependent Behavior of Dominant WW Phenomena for SBWR, PANDA and GIRAFFE - PCCS Phase	4-53
Figure 4.2-15:	Nondimensional Comparison of DW Pressure for SBWR, PANDA and GIRAFFE - PCCS Phase	4-54
Figure 4.2-16:	PI-Group Magnitudes for DW Pressure - PCCS Phase	4-55
Figure 4.2-17:	Time Dependent Behavior of Dominant Phenomena for SBWR, PANDA and GIRAFFE - PCCS Phase	4-56
Figure 4.4-1:	SBWR Heat Release Rates for Blowdown Transient	4-74
Figure 4.4-2:	Comparison of Structural Heat Release Rates for SBWR and GIRAFFE	4-75
Figure 4.4-3:	Comparison of Structural Heat Release Rates for SBWR and GIST	4-76
Figure 4.4-4:	SBWR DW Heat Loss Rates for Transient	4-77
Figure 4.4-5:	Comparison of DW Structural Heat Loss Rates for SBWR and PANDA	4-78
Figure 4.4-6:	PANDA DW Axial Temperatures for Asymmetry Tests at 20,000 s	4-79
Figure 4.4-7:	PANDA DW Air Partial Pressures for Asymmetry Tests at 20,000 s	4-80

ACRONYMS

ADS	Automatic Depressurization System
BDLB	Bottom Drain Line Break
BWR	Boiling Water Reactor
CRD	Control Rod Drive
DBA	Design Basis Accident
DPV	Depressurization Valve
DW	Drywell
ECCS	Emergency Core Cooling System
GDCS	Gravity-Driven Cooling System
GDLB	GDCS Line Break
GE	General Electric Company
GIRAFFE	Gravity-Driven Integral Full-Height Test for Passive Heat Removal
GIST	GDCS Integral System Test
IC	Isolation Condenser
ICS	Isolation Condenser System
LOCA	Loss-Of-Coolant Accident
LDW	Lower Drywell
MSLB	Main Steam Line Break
NB	No Break
N/C	Noncondensible
NDT	Nondestructive Test
PANDA	Passive Nachwarmeabfuehr-und Drueckabbau-Testanlage (Passive Decay Heat Removal and Depressurization Test Facility)
PANTHERS	Performance Analysis and Testing of Heat Removal Systems
PCC	Passive Containment Condenser
PCCS	Passive Containment Cooling System
PIRT	Phenomena Identification and Ranking Tables
PSI	Paul Scherrer Institut
RHR	Residual Heat Removal
RPV	Reactor Pressure Vessel
SBWR	Simplified Boiling Water Reactor

SIET	Societa Informazioni Esperienze Termoidrauliche
SIT	Systems Interaction Tests
SP	Suppression Pool
SRV	Safety/Relief Valve
SSAR	Standard Safety Analysis Report
TAF	Top of Active Fuel
TAPD	Test and Analysis Program Description
TRAC	Transient Reactor Analysis Code
TRACG	Transient Reactor Analysis Code, GE Version
UDW	Upper Drywell
VB	Vacuum Breaker
WL	Water Level
WW	Wetwell

EXECUTIVE SUMMARY

This *SBWR Testing Summary Report* summarizes the extensive database generated by GE and its associates from the SBWR-unique thermal-hydraulic test programs. These test programs were defined in the SBWR Test and Analysis Program Description [1.1] and accepted by the U.S. Nuclear Regulatory Commission Staff [1.7]. A major objective of these test programs was to provide test data to qualify the GE computer code TRACG for SBWR applications. The results of these qualification studies will be reported in a separate TRACG Qualification Supplement. Both component and integral systems transient tests were conducted to gather this data and study the phenomena of interest. The following summarizes these test programs:

Component Tests:

PANTHERS/PCC:	Performance tests of a full-scale prototype of the Passive Containment Condenser
PANTHERS/IC:	Performance tests of a full-scale prototype of the Isolation Condenser
PANDA S-series:	Performance tests of a 1/25 volume, full-height, section-scaled Passive Containment Condenser
GIRAFFE Phase 1, Step 1:	Performance tests of a 3-tube, full-height, Passive Containment Condenser

Integral Systems Transient Tests:

PANDA M-series:	Simulation of steam line break LOCAs in a 1/25 volume, full-height scaled SBWR with RPV, containment, GDCS, PCCS, and ICS.
GIST:	Simulation of steam and water line break LOCAs in a 1/508 volume, full-height scaled SBWR with RPV, containment, and GDCS.
GIRAFFE/Helium:	Simulation of steam line break LOCAs in a 1/400 volume, full-height scaled SBWR with RPV, containment, GDCS and PCCS.
GIRAFFE/SIT:	Simulation of water line break LOCAs in a 1/400 volume, full-height scaled SBWR with RPV, containment, GDCS, ICS and PCCS.

These test programs satisfied a number of needs for the eventual qualification of the TRACG computer code by simulating specific phenomena and combinations of phenomena and, in some cases, quantifying the effect of a particular phenomenon.

Each of the component tests yielded data on the performance of vertical tube steam condensers. Three of the tests (PANTHERS/PCC, PANDA S-series, and GIRAFFE Phase 1, Step 1) modeled the operation of the SBWR Passive Containment Condenser. These tests had as a major goal the study of steam condensation with an air/steam or nitrogen/steam mixture at post-LOCA containment conditions. The PANTHERS/PCC tests also investigated the differences in condenser performance with heavier-than-steam (air) and/or lighter-than-steam

(helium) noncondensible gases present with the steam. Results from these tests will be useful in the qualification of TRACG for SBWR containment analysis.

The PANTHERS/IC tests modeled steam condensation in a prototype SBWR Isolation Condenser over a range of pressures encompassing normal RPV operating pressure down to containment post-LOCA pressures. The PANTHERS/IC tests also investigated the degradation in condenser performance with the buildup of noncondensible gases (representing radiolytic gases) and demonstrated the ability of the IC to vent these gases. Results from these tests will be useful in the qualification of TRACG for SBWR transient analysis.

The integral systems transient tests covered three major SBWR post-LOCA periods: (1) late RPV blowdown into the start of the GDCS injection phase, (2) late GDCS injection phase into the PCCS cooling phase, and (3) long-term PCCS cooling phase.

[

Redacted

]

[

Redacted

]

[

Redacted

]

Results of this scaling evaluation demonstrate that the test components or test facilities were properly scaled to capture the dominant phenomena for various LOCA phases and that the experimental observations are representative of expected SBWR behavior.

The results from the SBWR test programs confirmed the operation of the SBWR safety systems (GDCS, PCC, and IC), as well as the robustness of the RPV and containment configurations. No unexpected results were observed in the simulated SBWR system response. No adverse system interactions of these or other plant systems (e.g., safety/relief valves, depressurization valves, vacuum breakers) were observed.

The SBWR Testing Program validated the performance of the passive safety systems in the 670 MWe SBWR design. The data from these tests are now available for other applications of this technology.

1. INTRODUCTION

1.1 Background

In the 1980's, GE began a project to design and certify a new Boiling Water Reactor (BWR) design which incorporates advanced, passive safety features. The Simplified BWR (SBWR) experienced design evolution from its beginning until 1996.

The final design was a natural circulation reactor rated at 670 MWe with a typical BWR pressure suppression containment system. The major safety systems are:

- Gravity-Driven Cooling System (GDCS), which during a postulated loss-of-coolant accident (LOCA), supplies makeup water to the reactor core from a pool located above the core.
- Isolation Condenser System (ICS), which during an isolation transient, uses natural circulation to remove core decay heat from the reactor pressure vessel (RPV) by condensing steam from the RPV and returning condensate to the RPV.
- Passive Containment Cooling System (PCCS), which during a postulated LOCA, removes heat from the containment by condensing steam from the drywell and returns the condensate to the GDCS pool.

A comprehensive experimental program was carried out to demonstrate the thermal-hydraulic performance of these passive systems and their components. The philosophy of testing was to focus on those features and components that are SBWR-unique or performance-critical, and to test over a range that spans and bounds the SBWR parameters of importance. In addition to demonstrating the performance of these systems, these tests were conducted to provide test data to be used to qualify the TRACG computer code for SBWR application. TRACG is the GE version of TRAC-BWR.

Major SBWR test programs were conducted at the GIST, GIRAFFE, PANTHERS, and PANDA test facilities. GIST, GIRAFFE, and PANDA were integral systems tests focusing on different aspects of the SBWR response to LOCAs. Figure 1.0-1 shows the relationship of these tests to the LOCA phases. These facilities also simulated the SBWR at different system scales (1:500 for GIST, 1:400 for GIRAFFE and 1:25 for PANDA). PANTHERS tests were full-scale component tests of prototypical ICS and PCCS condensers.

The *SBWR Test and Analysis Program Description* (TAPD) [1.1] described a comprehensive integrated plan that addressed the testing elements needed for analysis of SBWR performance. The TAPD provided the technical basis for determining the performance of the plant during transients and accidents. It provided the rationale for the diverse experimental and analytical efforts in support of SBWR certification based on the Phenomena Identification and Ranking Tables (PIRT). These tables listed the phenomena and interactions between systems important to SBWR transient and accident analysis.

The *Scaling of SBWR Related Tests* [1.2] provided an evaluation of the test facilities with respect to the scaling of the important phenomena and processes identified in the SBWR PIRT. The study demonstrated that the experimental observations from the test programs were representative of SBWR behavior and that the data were useful for TRACG qualification.

In March 1996, GE redirected the focus of SBWR programs from plants of the 670 MWe size to plants of 1000 MWe or larger. However, GE completed key ongoing test and analysis activities to make this data available for other applications of the SBWR technology.

1.2 Scope of Report

This *SBWR Testing Summary Report* provides a summary of the SBWR-unique thermal-hydraulic test programs.

Section 2 gives a summary description of the testing performed for the 670 MWe SBWR and presents the key results of those test programs. A roadmap is presented to guide the reader to individual test reports and other test documentation which completely describe these test programs.

Section 3 evaluates key PIRT phenomena from TAPD [1.1] against the results seen in the tests. TAPD presented a roadmap of the then remaining activities to qualify TRACG for SBWR application. Those qualification needs are discussed in this section to show that each of the specified phenomena was present in its respective test program. In some cases, additional data are presented in this section to supplement the discussion of the PIRT parameters.

Section 4 evaluates the scaling approach of the SBWR tests [1.2]. Where test programs were similar but performed at different scales, results are compared using non-dimensional parameters, and conclusions are drawn as to the effect of scale on the system or component performance. For the integrated transient tests, the parameters chosen for comparison are those most important to the type of test performed (e.g., containment pressure for the long-term containment study tests and RPV water inventory for the short-term reactor study tests).

This *SBWR Testing Summary Report* does not include all test programs applicable to the SBWR. GE also conducted component performance and reliability tests on other components which have been developed for SBWR, such as the depressurization valve (DPV) and vacuum breaker (VB). In addition, because the SBWR design is an evolution of earlier BWR designs, many of the test programs conducted for those BWRs are also applicable to the SBWR. TAPD presented a summary of all these other test programs and how they are useful to the SBWR.

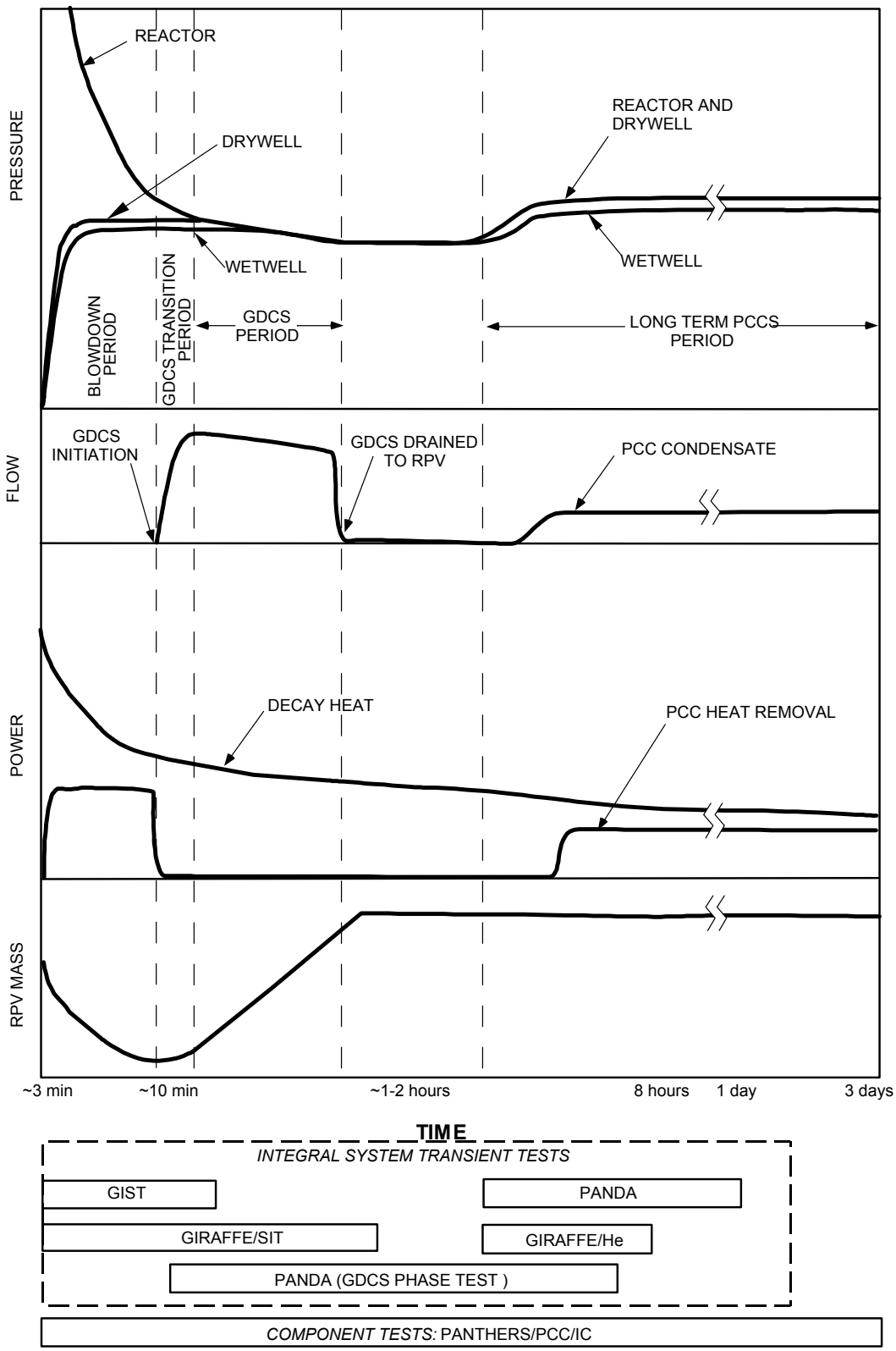

Figure 1.0-1: Key Variables and Test Coverage During SBWR LOCA Phases

2. THERMAL-HYDRAULIC TESTS

Each of the thermal-hydraulic test programs conducted for the SBWR program is described in this section. Brief summaries of the test objectives, descriptions, applicability to SBWR, and key results are given. Some additional data are also presented in Section 3 to support discussion of PIRT parameters.

Table 2.0-1 presents a roadmap of these programs and identifies references for more detailed information. Section 6 lists the references given in Table 2.0-1.

Table 2.0-1
Roadmap of the SBWR Test Programs
[Reference*] {Section number}

	PANTHERS/ PCC	PANTHERS/ IC	PANDA	GIST	GIRAFFE/ Helium	GIRAFFE/ SIT
Test Requirements	[2.1]	[2.1]	[3.1]	[4.1]	[5.1]	[6.6]
Test Objectives	[2.5] {2.}	[2.9] {2.}	[3.1]-[3.6]	[1.1]{A.3.1.4.2}	[5.2] {2}	[6.1] {2.1}
Facility Description	[2.5] {3.}	[2.9] {3.}	[3.23]	[4.3] {3.1}	[5.2] {3}	[6.1] {3.0}
Test Plan	[2.2]	[2.7]	[3.2]-[3.6]	[4.2] {App. A}	[5.2] {App. A}	[6.1] {App. A}
Test Procedure	[2.2]	[2.8]	[3.2], [3.7]-[3.11]	[4.2] {App. A}	[5.2] {App. A}	[6.1] {App. A}
Facility Instrumentation	[2.3], [2.4]	[2.3], [2.7] {4.}	[3.23]	[4.2] {3.3}	[5.2] {4}	[6.1] {4.0}
Data Acquisition System	[2.5] {5.}	[2.9] {5.}	[3.23]	[4.2] {3.4}	[5.2] {5}	[6.1] {5.0}
Apparent Test Results	[2.10]	[2.11], [2.12]	[3.12]-[3.22]	**	[5.3]	[6.2]-[6.5]
Final Test Results	[2.5] {7.}	[2.9] {8.}	[3.24]-[3.33]	[4.3] {3.3}	[5.2] {6}	[6.1] {6.0}
Data Evaluation	[2.6] {3.}	[2.9] {8.}	[3.24]-[3.33]	[4.3] {4.}	[5.2] {6}	[6.1] {6.0}
Conclusions	[2.5] {8.}	[2.9] {9.}	[3.24]-[3.33]	[4.3] {2.}	[5.2] {7}	[6.1] {7.0}

* See Section 6 for listing of References.
** Results stored in Design Record File.

2.1 PANTHERS/PCC

2.1.1 Test Objectives

The test objectives of the PANTHERS/PCC (Passive Containment Condenser) Test Program were:

1. Demonstrate that the prototype PCC heat exchanger is capable of meeting its design requirements for heat rejection. (Component Performance)
2. Provide a sufficient database to confirm the adequacy of TRACG to predict the quasi-steady heat rejection performance of a prototype PCC heat exchanger, over a range of air (similar to nitrogen in SBWR) flow rates, steam flow rates, operating pressures, and superheat conditions that span and bound the SBWR range. (Steady-State Separate Effects)
3. Determine and quantify any differences in the effects of noncondensible buildup in the PCC heat exchanger tubes between lighter-than-steam and heavier-than-steam gases. (Concept Demonstration)

The PANTHERS/PCC test program also included an additional objective for structural component qualification. This is discussed in Section 2.1.6.

2.1.2 Test Description

PANTHERS/PCC testing was performed as a joint effort by GE, Ansaldo, ENEA and ENEL at Societa Informazioni Esperienze Termoidrauliche (SIET) in Piacenza, Italy. The test facility consisted of a prototype PCC unit, steam supply, air supply, and vent and condensate volumes sufficient to establish PCC thermal-hydraulic performance.

The PCC was a full-scale, two-module vertical tube heat exchanger designed and built by Ansaldo. Figure 2.1-1 is an outline drawing of the heat exchanger assembly. The heat exchanger was a prototype unit, built using prototype procedures and with prototype materials. The SBWR has three heat exchanger units (6 modules). The PCC was installed in a water pool having the appropriate volume for one SBWR PCC assembly. Figure 2.1-2 is a schematic of the PANTHERS/PCC facility.

For the steady-state performance tests, the facility was purged with steam and placed in a condition where steam or an air/steam mixture was sent to the PCC, and the flows of the condensate and vented gases were measured. Once steady-state conditions were established, data were collected for a period of approximately 15 minutes. The time-averaged data were reported [2.5] and evaluated [2.6].

Transient tests were conducted by first establishing steady-state conditions and then either varying the water level in the PCC pool or allowing the unit to fill up from an injection of noncondensible gases with the vent line closed off by a spectacle flange.

2.1.3 Test Matrix

2.1.3.1 Steady-State Performance Tests

Table 2.1-1 shows the PANTHERS/PCC Steady-State Performance Matrix for steam-only tests. Thirteen test conditions were included.

- Data from Tests T37 through T43 (Test Group P1) were used to determine the baseline heat exchanger performance over a range of saturated steam flow rates without the presence of noncondensible gases. Test Group P1 data were compared with design requirements to meet Test Objective 1.

- Tests T44 through T49 (Test Group P2) addressed the effect of superheat conditions in the inlet steam. Tests T38, T44, T45 and T46 can be used to establish the effects of superheat at a relatively low steam flow condition, while Tests T41, T47, T48 and T49 give the same information at a steam flow rate near rated conditions.

Table 2.1-2 shows the PANTHERS/PCC Steady-State Performance Matrix for air/steam mixture tests. The independent variables are steam mass flow rate, air mass flow rate, steam superheat conditions, and absolute operating pressure.

- Tests T09, T15, T18 and T23 (Test Group P3) were used to compare heat rejection rates over a range of air flow rates to the saturated, steam-only condition determined from Test T41 in the pure steam series. Holding steam flow constant at near rated conditions, these tests yield the effect of air and pressure on the condensation process.

- Tests T02, T13, T16, T17, T19, T22 and T25 (Test Group P4) supplemented Test Group P3, in that they defined condensation performance at the extremes of the SBWR air/steam mixture ranges, and at several intermediate points. These tests were used to quantify noncondensible effects at off-rated conditions.

- Tests T35 and T36 (Test Group P5) further supplemented Test Group P4 by extending the effect of noncondensible gases over the superheated steam range. These tests can be compared to Tests T48 and T49 to establish the effect of air content at the same superheat condition, and to Test T23 at the same air flow, but with saturated steam.

- Tests T01, T03, T04, T05, T06, T07, T08, T10, T11, T12, T14, T20, T21 and T24. (Test Group P6) were lower priority tests. They were run at only a single inlet pressure to supplement the previously identified tests by increasing the data density within the already established air/steam flow map.

- Test Groups P3 through P6 support Test Objective 2.

2.1.3.2 Transient Test Conditions

Table 2.1-3 shows the PANTHERS/PCC Noncondensible Buildup Test Matrix. Eight test conditions are specified as Test Group P7. In these tests, steam was supplied at a constant rate, and steady-state conditions were established in a manner similar to that of the steady-state performance tests. Air, helium, or air/helium mixtures were then injected into the steam supply, with the vent line closed. The transient degradation in heat transfer performance was measured, as a function of the total noncondensible mass injected.

- Tests T50 and T51 provided a baseline condition with air as the only noncondensible. Air is similar to nitrogen in molecular weight, and is heavier than steam. Tests T52 and T53 were similar to Tests T50 and T51, but with the steam supply superheated. Tests T75 and T76 repeated Tests T50 and T51, but utilized helium as the noncondensible gas instead of air. Helium is lighter than steam and is expected to mix in a manner similar to hydrogen. The results of Tests T50 through T53 plus T75 and T76 can be compared to establish performance differences between lighter-than-steam and heavier-than-steam gases as they build up in the heat exchanger tubes. Tests T77 and T78 can be used to evaluate the effect of an air and helium mixture flowing into the heat exchanger.

- Test Group P7 data were evaluated to meet the requirements of Test Objective 3.

Table 2.1-4 shows the PANTHERS/PCC Pool Water Level Effect Test Matrix. Three test conditions are specified as Test Group P8. In these tests, steam and air/steam mixtures were supplied to the PCC heat exchanger, and steady-state conditions were established in a manner similar to the steady-state performance tests. In these tests, however, the water level in the PCC pool was allowed to drop and uncover the PCC tubes. Both the PCC pool level and the PCC heat rejection rate were monitored as a function of time.

- Tests T54, T55 and T56 established the effect of water level in the PCC pool for a range of steam and air/steam supply rates to the PCC. Data from Tests T54, T55 and T56 can be compared to Tests T41, T15 and T25, respectively, to obtain the effect of lowered water level on condensation performance. Tests T54 and T55 can be compared to establish the effect of air content on the rate of pool boiloff.

- Test Groups P1 through P5, P7 and P8 provided a database for TRACG qualification and met the requirements of Test Objective 2.

2.1.4 Applicability of Data to SBWR

In the SBWR, the post-LOCA function of the PCC is to remove decay heat from the drywell and reject this energy to the atmosphere. This is the major difference between the SBWR and earlier pressure suppression containment designs. In earlier designs, the decay heat is transferred from the drywell to the wetwell via main vent flow, and is subsequently transferred to the ultimate heat sink by the Residual Heat Removal (RHR) System.

As in previous pressure suppression containment designs, following the initial main vent-clearing transient, the maximum drywell pressure is limited to the wetwell pressure plus the vent submergence head and vent system flow losses. For design basis accidents, the peak long-term drywell pressure occurs when essentially all the noncondensible gases are present in the wetwell and, consequently, the drywell is nearly pure saturated steam. The wetwell pressure is the sum of the partial pressures of nitrogen and water vapor. The resultant drywell pressure is in the range of 300 to 330 kPa.

During a LOCA in the SBWR, the PCCS and GDCS form a circuit to keep the core covered with water and remove the decay heat. Steam coming off the core leaves the RPV through the DPVs, enters the drywell, and flows to the PCCS. Condensate flow from the PCCS heat exchangers drains to the GDCS pools in the drywell. The GDCS delivers the water to the RPV, where the decay heat of the core converts it to steam and starts the loop again.

2.1.4.1 SBWR PCC Operational Modes

The operational modes of the PCC heat exchanger can best be described in terms of the pressure difference across the unit. Figure 2.1-3 illustrates several of a family of possible pressure trajectories along the flow path from the drywell to the suppression pool via the PCC heat exchanger. Note that the drywell-to-wetwell pressure difference can vary only between the negative value required to open the vacuum breaker and the positive value required to open the main vent. The individual curves in Figure 2.1-3 can be categorized as follows:

Reference LOCA Condition

Curve 1 of Figure 2.1-3 illustrates the SBWR post-LOCA condition with the PCC carrying the decay heat load. In this case, the drywell pressure is slightly greater than the PCC vent submergence pressure, but less than the main vent submergence pressure. Thus, water is forced out of the PCC vent line, clearing a gas venting path to the suppression pool. The flow is forced through the PCC heat exchanger by the drywell-to-wetwell pressure difference, and noncondensible gases are vented into the suppression pool.

PCC Capacity Greater Than The Decay Heat

Curves 2 and 3 of Figure 2.1-3 illustrate a situation where most of the noncondensible gases have been vented to the wetwell. These two curves illustrate cases where the drywell is supplying nearly pure steam to the heat exchanger. Curve 3 represents PCCS inlet conditions with a lower mass fraction of noncondensible gases than Curve 2. As the degrading effects of noncondensible gases on the heat transfer process are reduced, the heat exchanger can reject more energy than is supplied to the drywell by decay heat, and the drywell pressure is reduced. The reduced pressure is no longer sufficient to keep the PCC vent open, so suppression pool water partially refills the PCC vent pipe. The flow into the PCC heat exchanger is no longer driven by the drywell-to-wetwell pressure difference, but by the lowered pressure in the heat exchanger

tubes due to the condensation process. The limit of this type of operation is shown on Curve 4, where the drywell pressure has fallen below the wetwell pressure by an amount equal to the vacuum breaker opening pressure. Here, the vacuum breaker opens, returning noncondensible gases to the drywell, where they can re-enter the PCCS. When this happens, the capacity of the PCCS to remove energy is temporarily degraded, and the drywell pressure rises, as necessary, to vent the noncondensible gases and increase the heat transfer.

PCC Capacity Less Than The Decay Heat

Finally, Curve 5 of Figure 2.1-3 illustrates the other extreme of PCC operation. In this case, PCC heat transfer is insufficient to reject the decay heat even with PCC venting. The drywell pressure rises, and flow is forced through the PCC by the drywell-to-wetwell pressure difference. However, the magnitude of the PCC driving pressure difference is limited by the presence of the main LOCA vents. If the main LOCA vents clear, then mass and energy will flow to the suppression pool via the main vent system to limit the drywell pressure. This pressure difference will determine the amount of parallel flow through the PCCS.

In summary, PCCS performance in the SBWR is characterized by two relatively distinct operating modes: (1) a pressure-driven mode, with the PCC vent cleared to accommodate throughput of a mixture of steam and noncondensible gases; and (2) a condensation-driven mode with the PCC vent partially filled with water and no throughput to the wetwell. Characteristics of these PCC operational modes can be summarized and contrasted as follows:

1. Pressure-Driven Mode

   - PCC capacity < core decay heat
   - PCC flow is forced by the DW-to-WW pressure difference
   - PCC flow typically includes both steam and noncondensible gas

2. Condensation-Driven Mode

   - PCC capacity $\geq$ core decay heat
   - PCC flow is induced by DW-to-PCC pressure difference due to condensation
   - PCC flow is essentially pure steam

For completeness, it should be noted that condensation always plays some role in moving a steam-gas mixture through the PCC unit. The distinction is that, in the pressure-driven mode, it is of secondary importance and, by itself, would not be able to sustain flow.

2.1.4.2 PCC Purge and Vent Process

A PCCS purge event can occur as a result of the system being called upon to remove decay heat after an extended period of inactivity or by an increase in the mass fraction of noncondensible gas in the region of the drywell from which the system draws its inlet mixture. If the system is starting up after a period of inactivity, the condensers will contain a mixture of steam and noncondensible gas in near thermal equilibrium with the surrounding pool. The partial pressure of the steam will be approximately saturation pressure at the pool temperature and the remainder of the mixture will be noncondensible gas. This mixture must be expelled from the condenser tubes before heat removal can begin. As steam is added to the drywell by the RPV, the drywell pressure will rise until the PCCS vents are cleared and the initial steam/noncondensible gas inventory of the condensers is vented. The movement of the initial inventory out of the condenser tubes will be accompanied by ingestion of a fresh steam/noncondensible gas mixture at the existing drywell conditions in the neighborhood of the PCCS inlets. Depending upon the fraction of noncondensible gas in the inlet mixture, and the decay power, the system may or may not be able to condense steam at the rate that it is being added to the drywell by the RPV.

Consider, first, the case where the PCCS heat removal rate at the existing inlet conditions is less than decay power. The situation is the same whether the PCCS is starting up from a period of inactivity or, while operating, the PCCS is confronted with an increased noncondensible fraction in the inlet mixture. The drywell pressure will rise, thereby increasing the flow rate through the condensers from the drywell to the wetwell. The rise in drywell pressure also slightly increases the condensation rate. Additionally, as steam is continuously added to the drywell by the RPV, and a steam/gas mixture is transported through the condensers, the mass fraction of noncondensible gas in the inlet mixture will start to decrease. At some point, the combination of increasing drywell pressure and decreasing noncondensible inlet mass fraction enables the PCCS heat removal rate to match decay power and the drywell pressure stops rising.

Next, consider the case where the PCCS heat removal rate at the existing inlet conditions is greater than decay power. Again, the situation is the same whether the PCCS is starting up from a period of inactivity or, while operating, the PCCS is confronted with a decreased noncondensible fraction in the inlet mixture. The drywell pressure will start to drop, allowing water to re-enter and close the vents. Unless the inlet conditions are pure steam, the PCCS will then start to accumulate noncondensible gas. Gas can accumulate in the vent pipes above the water level, in the lower headers, and in the condenser tubes. The combination of accumulating noncondensible gas and, to a lesser extent, decreasing drywell pressure results in a decreasing condensation rate. Eventually, the condensation rate will drop below decay power and the drywell pressure will start to rise, initiating a new purge cycle.

The presence of vacuum breakers in the SBWR leads to a potential interaction between PCCS purging and vacuum breaker operation. As discussed above, if the instantaneous PCCS heat removal exceeds decay power, the drywell pressure will decrease. When the difference between DW and WW pressure drops below the submergence head of the PCCS vents, water

will enter the vents and noncondensible gas will start to accumulate in the PCCS. The drywell pressure will continue to decrease until the combination of the lower pressure and the noncondensible gas accumulation drops the PCCS heat removal rate below decay power. If the PCCS noncondensible gas inventory is relatively small when the vents close, and the mass fraction of noncondensible gas in the inlet mixture is also small, the drywell pressure can continue to fall until it drops below the wetwell pressure by a sufficient amount to allow the vacuum breakers to open. The noncondensible gas which flows back to the drywell via the vacuum breakers increases the mass fraction of noncondensible gas in the inlet mixture, degrades condenser performance and leads to a new purge cycle. Thus, depending on the attendant circumstances, a PCCS purge event may or may not lead to a vacuum breaker opening. In discussing these two possibilities, GE has introduced the nomenclature "strong purge" to identify a purge event which leads to opening of a vacuum breaker and "weak purge" to identify one which does not.

2.1.4.3 PANTHERS PCC Operation

The basic feature of PANTHERS/PCC tests is that the PCC test unit is subjected to boundary conditions which determine its performance in a directly analogous manner to the PCC unit in the SBWR. Steam for the tests is supplied by a neighboring power plant. The facility has a condensate tank which collects the condensate from the PCC and returns it to the power plant, thereby performing the function of the GDCS in closing the loop between the PCC and the RPV. The water level in the condensate tank is held at a position corresponding to the top of the loop seal on the drain line in the SBWR. The pressure in the tank is equal to the PCC steam inlet pressure which is similar to the SBWR where the pressure above the GDCS pool is the drywell pressure. The PANTHERS PCC vent configuration differs between the types of tests performed. Figure 2.1-4 shows how the different test conditions simulate the two operational modes of the PCC as discussed below.

2.1.4.3.1 Steady-State Tests

As noted in the earlier discussion, the PCC can perform in two distinct modes: pressure-driven and condensation-driven. Both of these conditions are simulated in the PANTHERS/PCC steady-state tests, as discussed below. The pure-steam steady-state tests simulate the condensation-driven mode and the steam-air tests simulate the pressure-driven mode.

- **Steam Only Tests**

The pure steam tests are performed with the PCC vent tank closed. Since there is negligible heat loss from the vent tank, all the steam is condensed within the PCC and steam is drawn into the heat exchanger by the condensation process. These tests simulate the condensation-driven mode. With no noncondensible gases present in the heat exchanger, the pressure is determined as being that necessary to maintain complete condensation for the prescribed inlet steam flow.

- **Air/Steam Mixture Tests**

In the steam-air steady-state tests, flow is permitted from the vent tank to the atmosphere. The vent tank pressure is controlled such that the PCC inlet pressure matches a specified value at prescribed inlet steam and air flows. These tests simulate the pressure-driven mode. In this case, there is flow through the heat exchanger, with the flow rate determined by the difference in pressure between the inlet supply and the vent tank.

The independent variables for the PANTHERS/PCC steady-state steam-air tests are steam flow rate, air flow rate, and PCC inlet pressure. Dependent variables include condenser efficiency (ratio of steam condensed to steam in) and system pressure drop. Figure 2.1-4 illustrates how the test conditions model SBWR post-LOCA conditions.

As noted in the previous discussion of operating modes, with the exception of the main vent clearing transient, which occurs within a few seconds of the LOCA, the pressure drop from the drywell (through the PCC heat exchanger to the PCC vent exit) cannot exceed a value equivalent to the difference in hydraulic head between the main vent submergence and the PCCS vent submergence. This pressure drop limit is approximately 9 kPa.

In PANTHERS, the pressure drop depends on the PCC performance for the prescribed pressure and flow inlet conditions. The PCC pressure drop is one of the dependent variables measured during the testing. Figure 2.1-4 shows that two of the inlet conditions prescribed for Test T23 resulted in an overall pressure drop about equal to the limit at which main vent flow would initiate. These tests represent the upper limit for PCC inlet gas mass fraction at the given steam flow rate. In the SBWR, if the gas mass fraction was higher, a portion of the flow would be diverted to the main LOCA vents.

Test T09 models conditions where a large fraction of the steam is condensed while noncondensible gases are continually vented to the wetwell. The pressure drop through the system is less than the submergence head between the PCC vent exit and the top main vent, so all of the flow would be through the PCCS.

In the SBWR, as the steaming rate decreases at a relatively constant inlet pressure, the steam in the inlet steam/gas mixture is completely condensed, and the pressure drop through the system is near the lower boundary of the pressure-driven range. (It should be noted that "complete condensation" is used to describe a situation in which the temperature of the gas mixture in the bottom of the condenser is close to the pool temperature. Such a mixture, in direct contact with the condensate film, is likely to contain water vapor at a partial pressure near one bar.) This condition is closely modeled by Test T02, where the efficiency is over 90%. As the fraction of noncondensible gases in the inlet flow approaches zero, the PCC operating mode transitions to the condensation-driven range.

From the above discussion, it can be seen that the PANTHERS/PCC test matrix included conditions which produced flows up to the limit of what the unit could experience at any time during the post-LOCA transient. This provides a basis for qualification of the TRACG code for

simulation of PCCS performance over the full range of post-LOCA conditions. The only exception is the first few seconds of the LOCA during which the PCCS flow would be dictated by the pressure difference associated with the initial main vent clearing transient. This regime is not important for TRACG qualification since the flow is almost pure noncondensible gas and, consequently, PCCS heat removal is insignificant.

The design basis of the PCCS (three heat exchangers) provides the ability to reject all SBWR decay heat at approximately one hour post-LOCA. Figure 2.1-5 compares the range of test conditions for PANTHERS/PCC with the air and steam flow conditions for the SBWR main steam line, bottom drain line, and GDCS line break scenarios after one hour into a LOCA. The triangles representing the three breaks are constructed as the intersection of a vertical line, bounding the maximum steam flow, and a line drawn from the origin with a slope sufficient to envelope the calculated steam and noncondensible flow rates. The triangles are not one-to-one maps or time histories but, rather, represent bounds of the steam/noncondensible gas inlet conditions throughout the calculated SBWR LOCA scenario.

The triangles can be used to explain the progression of inlet conditions as the transient proceeds. This progression starts at the origin. In the period immediately following one hour, subcooled GDCS water is absorbing the decay heat power and there is no flow to the PCCS. This period is represented by the region near the origin. When the RPV water again reaches saturation, flow to the PCCS resumes and, at first, follows an approximately linear steam/noncondensible gas flow trajectory corresponding to the noncondensible gas mass fraction in the region of the drywell which feeds the PCCS. This initiates the purging process which transports the drywell noncondensible gas to the wetwell via the PCC units. At some point during the purge, the concentration of noncondensible gas in the drywell starts to drop and the steam/noncondensible gas trajectory turns over. The steam flow continues to increase as the noncondensible gas concentration in the inlet mixture decreases. The end of the purging process is represented by the extreme lower right corner of the triangle. The steam flow has now increased to its maximum value (matching the decay power) and the noncondensible gas flow has dropped to essentially zero. From this point, the steam flow “walks” backward along its axis as the decay power slowly drops.

The difference in the steam/noncondensible gas envelopes for the GDCS line and main steam line break accident scenarios results from the behavior during the GDCS injection phase of the transient. For the main steam line break, a large fraction of the subcooled GDCS water is retained in the pools as the RPV two-phase water level rapidly recovers to the main steam line elevation and equilibrates with the water in the GDCS pools. There is very limited vacuum breaker activation and, accordingly, there is a small noncondensible gas fraction in the drywell at the initiation of PCCS flow. At about one hour from the instant of LOCA, RPV steaming and PCCS flow resume. Also at this time, the core decay power is about equal to the heat removal capacity of the PCCS. Since there is a low drywell noncondensible gas inventory, the PCCS heat removal rate rises rapidly to match decay power.

For the GDCS break, the pools drain completely and RPV steaming does not resume until about 2.5 hours after the LOCA initiation. During the GDCS injection period, there are multiple

vacuum breaker activations leading to a relatively large noncondensible gas fraction in the drywell when PCCS flow initiates. With the larger noncondensible fraction, PCCS steam flow does not match decay power until about 3.5 hours from the LOCA. Thus, the maximum PCCS steam flow is significantly reduced from the main steam line break case.

A bottom drain line (BDL) break behaves similarly to the GDCS line break as shown in Figure 2.1.5.

[

Redacted

]

Although there is no specific relationship between Figures 2.1-3 and 2.1-5, an association can be made by considering the variation in steam-air inlet conditions associated with Curves 1 through 4 of Figure 2.1-3. At the end of the purge (Curve 1), drywell pressure exceeds wetwell pressure by slightly more than the head required to clear the PCCS vents. If the purging process has left the condensers relatively free of noncondensible gas (a "strong" purge), a reduction in the inlet noncondensible flow will result in a decrease in drywell pressure as the PCCS removes slightly more than the decay power. Eventually, as it moves through the sequence from Curves 1 to 4, the drywell pressure will decrease to the point where the vacuum breakers open. This will reintroduce noncondensible gas to the drywell and drive the PCCS inlet conditions to the left and upwards in the triangular regions of Figure 2.1-5.

2.1.4.3.2 Transient Tests

Transient tests are performed to assess two phenomena: (1) the buildup of noncondensible gases of differing molecular weights in the heat exchanger, and (2) the reduction of PCC pool water level as the inventory is boiled away.

- **Noncondensible Gas Buildup Tests**

The noncondensible gas buildup tests are initiated by establishing steady-state pure-steam condensation. Air and/or helium, representing heavier-than-steam and lighter-than-steam gases, are then introduced at low volume flow rates. The flow rate is low enough such that the performance may be considered quasi-steady. Noncondensible gases are added until the

pressure required for complete condensation is approximately the design pressure of the PCC. These tests do not simulate PCCS transient behavior in the SBWR. As described above, any degradation in PCCS performance caused by the presence of noncondensible gases would be quickly relieved by the opening of the PCC vents.

The early part of these tests is representative of the performance of the PCCS near the boundary of the pressure-driven range and the condensation-driven range. The mixture is almost pure steam compared to the steady-state tests. Complete condensation takes place in the condenser. The spectacle flange on the vent line simulates the blockage of the vent in SBWR by the submergence in the suppression pool. In PANTHERS, the pressure continues to rise as the gases build up in the system. In the SBWR, the pressure would also rise until the water level in the vent reaches the elevation of the vent exit. At this point, the PCCS would transition to the pressure drop driven mode as the gases bubble out and enter the wetwell.

- **Water Level Tests**

The PANTHERS/PCC water level tests begin with test conditions similar to those of a steady-state steam or air/steam test. In these tests, through a combination of normal boil-off and draining of the pool, the PCC pool level is lowered through a range that exceeds the SBWR inventory loss over a 72-hour period. The drop in water level is sufficiently slow to yield quasi-steady behavior at any given time.

Data from these tests can be used to qualify TRACG for PCC performance over a broad range of water levels. It should be noted that the performance of the unit varies little as the water level drops from normal pool water level to the top of the tubes. This range covers the expected water level variation for a 72-hour design basis accident (DBA) condition in the SBWR.

2.1.4.4 Summary of Data Applicability

The conditions tested in PANTHERS/PCC are representative of conditions predicted in SBWR containment analyses for PCC operation. These include the ranges for DW pressure, inlet steam, and inlet steam/air mixture conditions. The tests capture both pressure-driven and condensation-driven operating modes of the PCC. The steady-state tests simulate the pressure-driven mode from the upper limit of maximum pressure loss through the system (corresponding to flow through the top main vent in SBWR) to the transition to condensation-driven mode. The transient tests demonstrate the condensation-driven flows both with and without the presence of noncondensible gases in the PCC.

2.1.5 Key Results

2.1.5.1 Steady-State Tests

- **Pure Steam Tests**

For the pure steam tests, the heat rejection rate increases almost linearly with pressure (Figure 2.1-6). The intersection of the linear regression with the x-axis represents the limiting steam temperature at which condensation would occur and is slightly higher than the bulk pool temperature. This limit is consistent, since the steam temperature must be higher than the PCC pool temperature so that condensation can occur. The linear regression also demonstrates that the prototype PCC meets the design requirement of 10 MW at 308 kPa, which satisfies Test Objective 1.

While the PANTHERS tests showed that an individual prototype PCC meets its design capacity with minimal margin, excess system capacity is demonstrated in the PANDA transient tests where less than full capacity of the three PCC units was required. Section 2.3.5.2 discusses the results from the PANDA transient tests.

- **Air/Steam Tests**

For tests conducted with a constant air/steam mixture flow rate, the amount of steam condensation varies with varying inlet pressure until complete condensation occurs. The heat rejection rate increases as the pressure increases, because the increase in pressure raises the difference between the tubeside average fluid temperature and the poolside water temperature. Figure 2.1-7 illustrates this effect for various tests, all conducted with 5 kg/sec inlet steam flow and different air mass fractions. Figure 2.1-7 shows that the heat rejection rate increases to an asymptote at higher pressures. The asymptotic limit is the energy removal required to condense all the steam and bring the condensate and gas to the pool temperature.

As expected, the increase in air concentration results in a decrease in condensation at a given pressure for all tests. In the tests with the higher air mass fractions (T18 and T23), the PCC does not reach complete condensation at the tested conditions.

The results with superheated steam basically agree with those from the saturated steam tests because the unit was able to remove most of the superheat in the steam riser and headers before reaching the tubes. Figure 2.1-8 shows tests that were conducted at the same inlet steam and air flow rates but different initial superheated steam temperatures. The three superheat conditions follow essentially the same curve as a function of inlet pressure. Figure 2.1-8 shows no difference in condenser efficiency with inlet conditions up to 30 °C superheat.

Figure 2.1-9 illustrates the effect that the air mass fraction has on the condenser efficiency. All the tests in Figure 2.1-9 were run at the same inlet steam flow and pressure. The pressure corresponds to that required to condense all of the given steam at zero air mass fraction. As expected, as the air mass fraction decreases to zero, the PCC is able to condense more steam, and the efficiency rises. It should be noted that the curve generated in Figure 2.1-9 corresponds

to a specific set of inlet conditions. For a given air mass fraction at different inlet steam flows or pressures, the condenser efficiency will change.

The stable results from the steady-state performance tests demonstrate that the PCC is well behaved over a broad range of test conditions. The database generated by these tests satisfied Test Objective 2.

2.1.5.2 Transient Tests

- **Pool Water Level Effects Tests**

Figure 2.1-10 shows how the PCC inlet pressure varies for different pool water levels for a test with pure steam and no venting (Test T54). The neighboring IC pool is used to measure the water level because it was quiescent and gave a more steady reading. As the pool water level decreased, the inlet pressure decreased until the water level in the PCC pool reached the top of the condenser tubes. This shows that the performance of the PCC improves slightly because of the decreasing water head and resulting decreased bulk pool boiling temperature. As the tubes uncover, the inlet pressure increased because of the smaller available heat transfer surface.

Another phenomenon that can be observed from Figure 2.1-10 is a slight hysteresis on the water level decrease-increase cycle. This can be explained by the fact that the pool water level is increased by the addition of cold make up water, resulting in an increased pool average density. Therefore, for a given measured collapsed water level, the two-phase level in the PCC pool is lower when the water is increasing than when it is decreasing. This means that, during the pool refilling, less tube surface is wetted and the tube inlet pressure is higher.

- **Noncondensible Gas Buildup Tests**

The noncondensible gas buildup tests show how the molecular weight of the gas relative to that of steam affects the buildup location of the gas in the PCC.

When air, a heavier-than-steam gas, is used, the air builds up in the lower regions of the condenser and steam condensation occurs in the top part of the tubes. This is illustrated in Figure 2.1-11 from Test T51, which shows tube wall temperatures measured near the outside surface. Where condensation is occurring, the tube wall temperature is higher than the PCC pool temperature. When the tube wall temperature decreases to that of the PCC pool, this indicates that the tube at this level is filling with air. As the air builds up, the air/steam interface in the tubes rises causing the measured temperature to decrease at lower elevations. Some temperature fluctuations occur as the interface crosses over the elevation of the sensor, causing a variation in the local gas concentration. By the end of the test, all of the steam condensation is occurring in the upper levels of the tubes.

When helium, a lighter-than-steam gas, is used, the helium is more evenly distributed within the tubes. This is illustrated in Figures 2.1-12 and 2.1-13 from Test T76. For most of the test, the tube wall temperatures along the tubes are fairly constant and high, indicating that

condensation is occurring along the entire tube length. This indicates that the upward buoyancy of the helium can overcome the downward momentum of the condensing steam. The steam condensation is evenly distributed along these condenser tubes. In Figure 2.1-12, for a short time near the start of the test, the tube temperatures are more spread out and lower. This indicates a greater concentration of helium within the tube, causing reduced condensation. This phenomenon is also observed in another instrumented tube (Figure 2.1-13) but not at the same time, which indicates that the helium is moving from one region of the PCC to another. In other tubes, the measured temperatures are sometimes much lower indicating that very little condensation is occurring in those tubes. However, these changes in local heat transfer characteristics do not result in simultaneous degradation of the overall condenser performance. This is evident in Figure 2.1-14, which is indicative of the total heat rejection characteristics for this same test. Figure 2.1-14 shows no sudden changes in the operating pressure required to condense the steam. Section 3.1.4 provides additional discussion of tube-to-tube variations observed in the PANTHERS/PCC tests The impact of lighter-than-steam gases on the PCC performance is discussed further in Section 4.3.

Figure 2.1-14 shows how the pressure increases as noncondensible gases buildup in the PCC. Higher pressure implies increased degradation. For a given molar mass injected, the helium appears to degrade the condenser more than does air; however, the amount of gas injected does not correspond directly to the amount residing in the PCC tubes. A significant fraction of the air accumulated in the lower header and vent pipe (down to the spectacle flange), while only a small fraction of the helium accumulated in the upper header. In addition, some of the air may have been entrained in the condensate, while helium is less likely to get entrained because of its upward buoyancy. All of these factors must be considered in order to evaluate the effect of these gases on the PCC performance.

The results from these tests quantify the differences in the effects of heavier-than-steam and lighter-than-steam noncondensible gases building up in the PCC tubes and, thus, satisfy Test Objective 3.

2.1.5.3 Closure with TAPD

All the PANTHERS/PCC thermal-hydraulic tests presented in TAPD [1.1], which covers the expected SBWR range of conditions, were conducted. Each test objective given in Section 2.1.1 was met. The PCC was very well behaved, and there were no performance anomalies.

2.1.6 Component Demonstration Tests

Component testing of the prototype PCC heat exchanger was also performed as part of the PANTHERS/PCC test program. The component demonstration tests were very similar in conduct to the thermal-hydraulic testing. The test article (PCC module “A”) was instrumented with strain gages, accelerometers, and thermocouples. Data were collected during the thermal-hydraulic tests, as well as the structural performance tests described in this section.

The test objective of the PANTHERS/PCC Component Demonstration Tests was to confirm that the mechanical design of the PCC heat exchanger is adequate to assure its structural integrity over a period that exceeds that required for lifetime application of this equipment to the SBWR.

The original approach taken to address the test objective was to subject the condenser to a total number of pressure and temperature cycles well in excess of that expected over the anticipated SBWR lifetime [1.1]. The test matrix was composed of 10 LOCA cycles and 300 pressure test cycles. This matrix represented five times the design requirement number of hypothetical LOCAs (2) and nearly 17 times the number of expected pneumatic test cycles in accordance with 10CFR50, Appendix J over the 60-year design life of the PCC.

The simulated LOCA cycles were performed by pressurizing the PCC units with steam to simulate both the temperature and pressure effects of a LOCA. The PCC pool was at ambient temperature at the beginning of a test, but was allowed to heat up to saturation as each cycle proceeded. Each of the ten LOCA cycles lasted approximately 30 minutes.

Following the LOCA cycles, a pressure test was performed to identify any leakage from the unit. Small leakage was detected from some of the header/flange connections, but no leakage was found at any of the weld joints. Efforts to eliminate the leakage by refurbishing the flange connection or replacing the O-rings were not successful, but the resulting measured leakage was so small as to be insignificant to the measured performance of the unit. This was further confirmed during the remaining tests by the mass balance of the measured inlet and outlet flows to the PCC.

The simulated pneumatic tests were to be performed by pressurizing the PCC heat exchanger with air to 859 kPa with the PCC pool temperature at ambient conditions. A total of 300 cycles were planned. These tests were deferred following the discovery of the header/flange leakage to await a solution. However, following the completion of the PANTHERS/PCC Test Program, it was decided that the large number of thermal cycles which the unit experienced each test day subjected the PCC to stresses which bound these air cycle tests. On this basis, the simulated pneumatic tests were canceled.

The problem of the header/flange leakage was resolved and the test objective was met in that the LOCA cycles and thermal-hydraulic tests confirmed the structural integrity of the PCC design, especially, the tube-to-header welds. In order to qualify the design, further examination of the test article and review of the structural test results was done to identify the root cause of the leakage and determine an appropriate design change. An incorrect sizing of the O-ring grooves at the header flanges was found to be the cause of the small leakage. In addition with in-depth consultation with O-ring suppliers it was concluded a different type of O-ring, i.e., “spring energized”, will assist with any resulting stresses and distortion at the flange interface.

Table 2.1-1
PANTHERS/PCC Steady-State Performance Matrix – Steam Only Tests

[

Redacted

]

Table 2.1-2
PANTHERS/PCC Steady-State Performance Matrix – Air-Steam Mixture Tests

[

Redacted

]

Table 2.1-2 (cont'd)
PANTHERS/PCC Steady-State Performance Matrix – Air-Steam Mixture Tests

[

Redacted

]

Table 2.1-2 (cont'd)
PANTHERS/PCC Steady-State Performance Matrix – Air-Steam Mixture Tests

[

Redacted

]

Table 2.1-2 (cont'd)
PANTHERS/PCC Steady-State Performance Matrix – Air-Steam Mixture Tests

[

Redacted

]

Table 2.1-3
PANTHERS/PCC Noncondensible Buildup – Test Matrix

[

Redacted

]

Table 2.1-4
PANTHERS/PCC Pool Water Level Effects – Test Matrix

[

Redacted

]

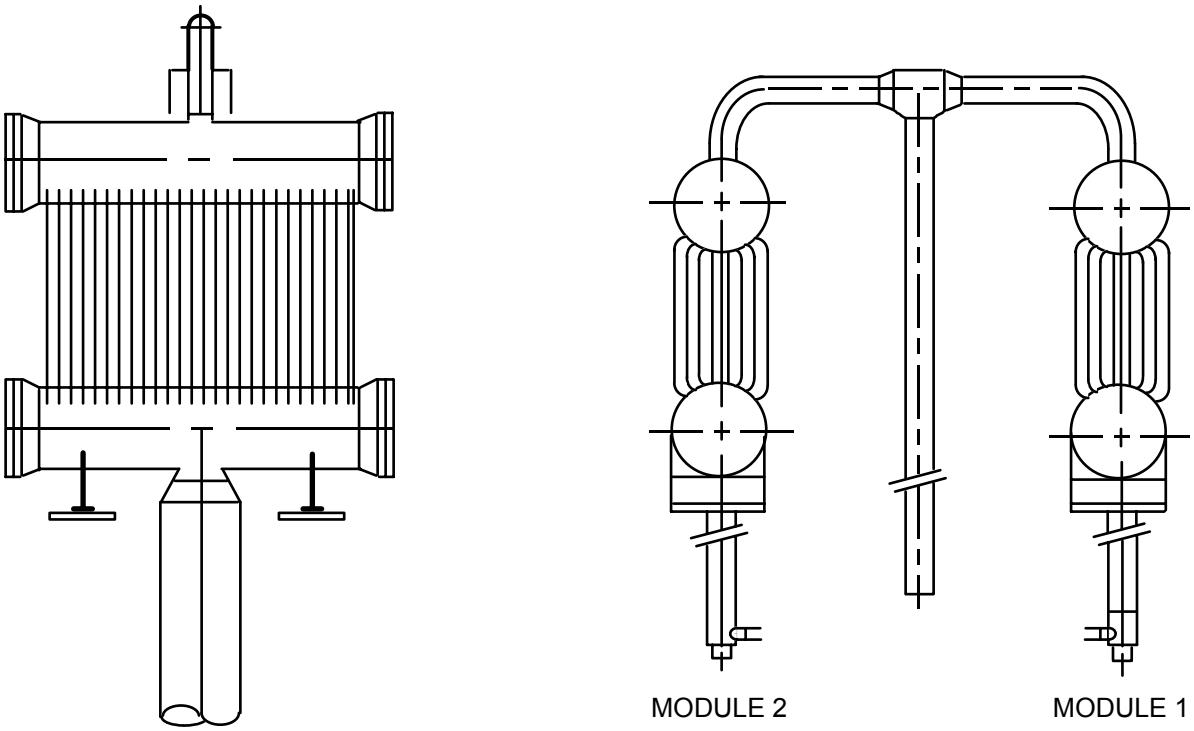

Figure 2.1-1: PANTHERS/PCC Test Article

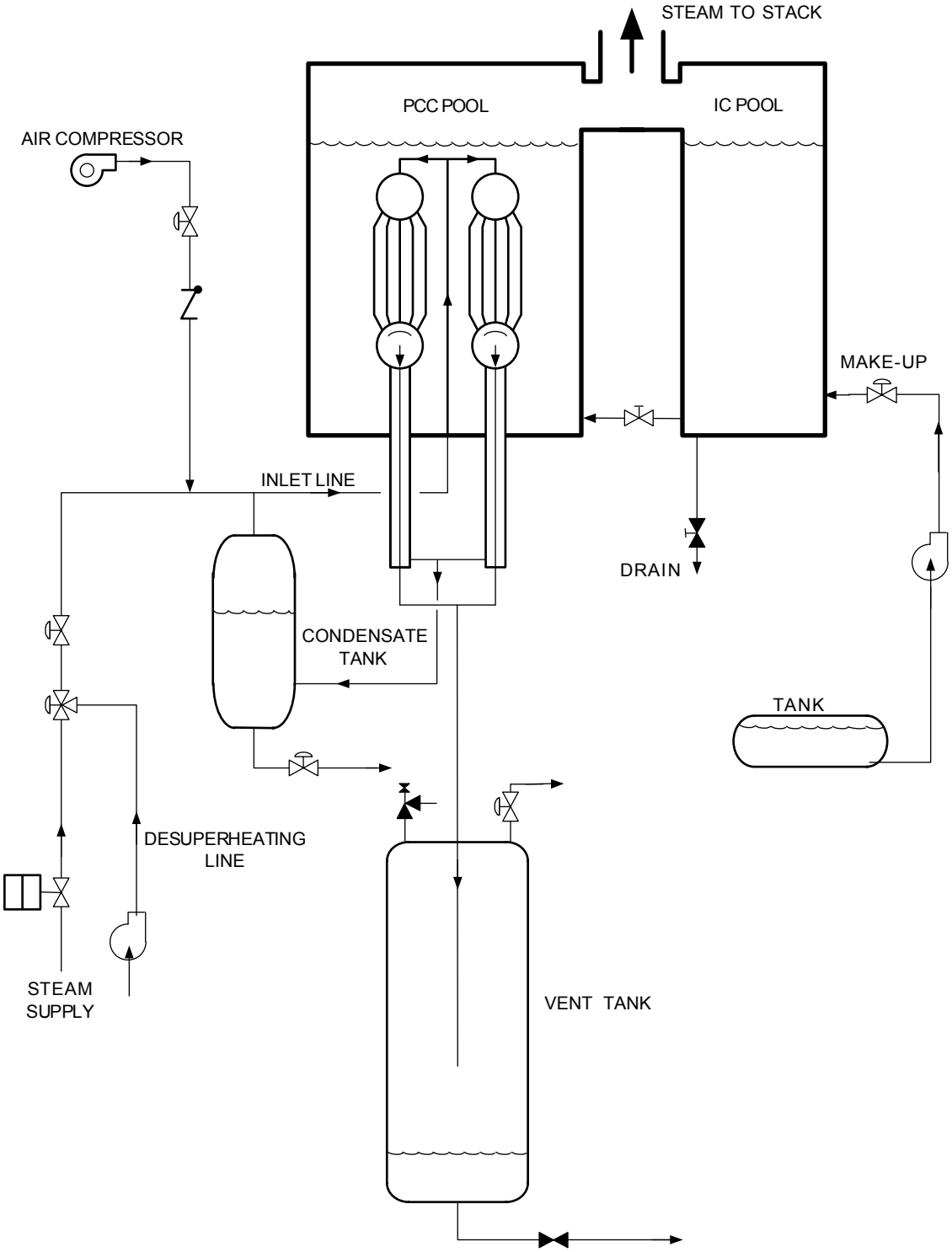

Figure 2.1-2: PANTHERS/PCC Test Facility Schematic

[

Redacted

]

Figure 2.1-3: PCC Operational Modes

[

Redacted

]

Figure 2.1-4: PANTHERS Representation of PCC Operational Modes

[

Redacted

]

Figure 2.1-5: TRACG PANTHERS/PCC Qualification Points

[

Redacted

]

Figure 2.1-6: PANTHER/PCC Power for Saturated Steam Tests

[

Redacted

]

Figure 2.1-7: PANTHERS/PCC Power for Air/Steam Tests

[

Redacted

]

Figure 2.1-8: Effect of Superheat on Condensation Efficiency for PANTHERS/PCC Air/Steam Tests

[

Redacted

]

Figure 2.1-9: Effect of Air Mass Fraction on Condensation Efficiency for PANTHERS/PCC Air/Steam Tests

[

Redacted

]

Figure 2.1-10: PANTHERS/PCC Test T54 Inlet Pressure Response to IC Pool Water Level

[

Redacted

]

Figure 2.1-11: PANTHERS/PCC Test T51 Tube Temperature Response with Air Injection

[

Redacted

]

Figure 2.1-12: PANTHERS/PCC Test T76 Tube 4A Temperature Response with Helium Injection

[

Redacted

]

Figure 2.1-13: PANTHERS/PCC Test T76 Tube 5Q Temperature Response with Helium Injection

[

Redacted

]

Figure 2.1-14: PANTHERS/PCC Pressure Transients for Air (Test T51) and Helium (Test T76) Buildup

2.2 PANTHERS/IC

2.2.1 Test Objectives

The objectives of the PANTHERS/IC (Isolation Condenser) Test Program were:

1. Demonstrate that the prototype IC heat exchanger is capable of meeting its design requirements for heat rejection. (Component Performance)
2. Provide a sufficient database to confirm the adequacy of TRACG to predict the quasi-steady heat rejection performance of a prototype IC heat exchanger over a range of operating pressures that span and bound the SBWR range. (Steady-State Separate Effects)
3. Demonstrate the startup of the IC unit under anticipated transient conditions. (Concept Demonstration)
4. Demonstrate the capability of the IC design to vent noncondensible gases and to resume condensation following venting. (Concept Demonstration)

The PANTHERS/IC test program also included an additional objective for structural component qualification. This is discussed in Section 2.2.6.

2.2.2 Test Description

PANTHERS/IC testing was performed at Societa Informazioni Esperienze Termoidrauliche (SIET) in Piacenza, Italy. The facility consisted of a prototype IC module, a steam supply vessel which simulates the SBWR reactor vessel, a vent volume, and associated piping and instrumentation sufficient to establish IC thermal-hydraulic performance.

The IC tested was one module of a full-scale, two-module vertical tube heat exchanger designed and built by Ansaldo. Only one module was tested because of the high energy rejection rate of the IC unit, and inherent limitations of facility and steam supply size. Figure 2.2-1 gives an outline drawing of the heat exchanger assembly. The IC was a prototype unit, built using prototype procedures and with prototype materials. The SBWR has six modules (three heat exchanger units). The IC was installed in a water pool having one half the appropriate volume for one SBWR IC assembly. Figure 2.2-2 is a schematic of the PANTHERS/IC facility.

For the steady-state tests, the steam supply to the steam vessel was regulated such that the vessel pressure stabilized at the desired value. A constant water level was maintained in the pressure vessel by draining condensate back to the power plant. Data were acquired for a period of approximately 15 minutes. Then the steam supply was increased or decreased to gather data at a different operating pressure, or testing was terminated. In all cases, flow into the IC was natural circulation driven, as is the case for the SBWR.

As with the PCC tests, transient tests were conducted by first establishing steady-state conditions and then either varying the water level in the IC pool or allowing the unit to fill up from an injection of noncondensible gases. The gases were subsequently purged through vent lines located on both the lower and upper headers.

2.2.3 Test Matrix

2.2.3.1 Steady-State Performance Tests

As with the PANTHERS/PCC tests, the majority of the IC tests were steady-state performance tests. Table 2.2-1 provides the PANTHERS/IC Steady-State Performance Test Matrix. A total of ten test conditions are specified. Tests T02 through T11 are identified as Test Group I1. These data established the IC heat rejection rate as a function of inlet pressure.

2.2.3.2 Transient Test Conditions

PANTHERS/IC transient tests demonstrated startup of the IC heat exchanger for full-scale thermodynamic conditions. These tests were designed to demonstrate heat exchanger performance; they were not intended to be integral systems tests.

Tables 2.2-2 and 2.2-3 give the PANTHERS/IC Transient Demonstration Test Matrix. Five test conditions are specified. Test Condition T16 (Test Group I2) was a set of two duplicate tests designed to demonstrate the startup and operation of the IC in a situation comparable to a reactor isolation and trip (Table 2.2-2). The tests were originally planned to initiate at a higher pressure (P1) to more closely simulate the slight pressure rise that would occur in the SBWR following RPV isolation. Those tests were deferred to the end of the test program because of the need to change the setpoint of the system relief valve. Prior to running these tests, the test program was suspended because of header/flange leakage (see Section 2.2.6) and never resumed. However, the intent of these tests and Test Objective 3 were met by the startup of two of the structural cycle tests which were performed.

Tests T12 and T13 (Test Group I3) had a nitrogen/helium mixture injected slowly after the steam vessel pressure had been reduced to the value specified as "inlet pressure" in Table 2.2-3. The IC was vented when the inlet pressure reached 7.75 MPa or when the pressure peaked, when at a lower value. Re-establishment of condensation following venting was recorded.

Tests T14 and T15 (Test Group I4) had the same constant steam flows as Tests T12 and T13, but in Tests T14 and T15 the water level in the IC pool was allowed to drop, exposing the IC tubes (Table 2.2-3). Both the IC pool level and the IC inlet pressure were monitored as a function of time.

The results from these tests meet the test objectives as discussed below:

- Test Group I2 demonstrated startup of the IC under near prototype conditions, provided heat rejection data at a higher pressure than the data from Test Group I1, and demonstrated test repeatability. Tests T12 and T13 demonstrated restart of condensation in the IC following venting of noncondensible gases and meets Test Objective 4. Tests T14 and T15 established the degradation of heat rejection ability of the IC as the IC pool water level decreases.

- Test Groups I1 and I2 were compared with design requirements to meet Test Objective 1.

- Test Groups I1, I2, and I4 provided a database for TRACG qualification and meets Test Objective 2.

- Test Group I2 demonstrated startup of the IC and meets Test Objective 3.

2.2.4 Applicability of Data to SBWR

2.2.4.1 Steady-State Tests

The independent variable for the PANTHERS/IC steady-state tests is the isolation condenser inlet pressure, which is equal to the steam vessel pressure. The isolation condenser is a natural circulation unit.

The IC inlet pressures tested (Table 2.2-1) span the entire operating range of the SBWR. The SBWR range is bounded by the SRV setpoints at 8.12 MPa and the vessel depressurized state. This is consistent with the test pressures. The low pressure (0.3 MPa) corresponds to a typical operating state during a loss-of-coolant accident (LOCA) when the vessel has depressurized to the containment pressure.

2.2.4.2 Transient Tests

[

Redacted

]

For the pool water level tests (T14 and T15), the water level was lowered to approximately 1.4 and 1.6m (respectively) above the pool floor, uncovering more than half the tube heat transfer area. Bounding calculations based on long-term decay heat rejection indicate that no more than one-third of the IC tube height will be uncovered during a 72-hour post-scram period. Consequently, the tests bounded the SBWR range of conditions and provided useful data to qualify TRACG for IC performance evaluation with the tubes partially uncovered.

The PANTHERS/IC transient tests were component, not system, tests. The purpose of the transient tests was to measure the change in performance of the IC with: (a) a known quantity of noncondensible gas present, or (b) a change in pool water level. Although the test facility was similar to the arrangement found in the SBWR, with the steam supply and condensate return line connected to a large pressure vessel, the transient tests did not exactly match the operating condition an IC would experience in the SBWR. For example, steam and noncondensible gases were "metered" into the test facility, while in the plant the conditions at the inlet of the heat exchanger depend on the conditions in the RPV and are not independent variables. However, the venting of the test unit closely matched the performance of the plant unit, and demonstrated that the IC can vent the gases and resume condensation at low pressure.

2.2.5 Key Results

2.2.5.1 Steady-State Tests

[

Redacted

]

2.2.5.2 Transient Tests

[

Redacted

]

[

Redacted

]

2.2.5.3 Closure with TAPD

All of the PANTHERS/IC thermal-hydraulic steady-state tests presented in TAPD [1.1], which cover the expected SBWR range of conditions, were conducted. All of the transient thermal-hydraulic tests were also conducted with the exception of the Startup and Operation Tests. However, as explained earlier, the intent and objectives of these tests were met by other tests. Therefore, all of the test objectives given in Section 2.2.1 were met. The IC was very well behaved, and there were no performance anomalies.

2.2.6 Component Demonstration Tests

[

Redacted

]

[

Redacted

}

Table 2.2-1: PANTHERS/IC
Steady-State Performance Test Matrix

[

Redacted

}

Table 2.2-2: PANTHERS/IC
Startup and Operation Test Matrix

[

Redacted

}

Table 2.2-3: PANTHERS/IC
Transient Performance Test Matrix

[

Redacted

}

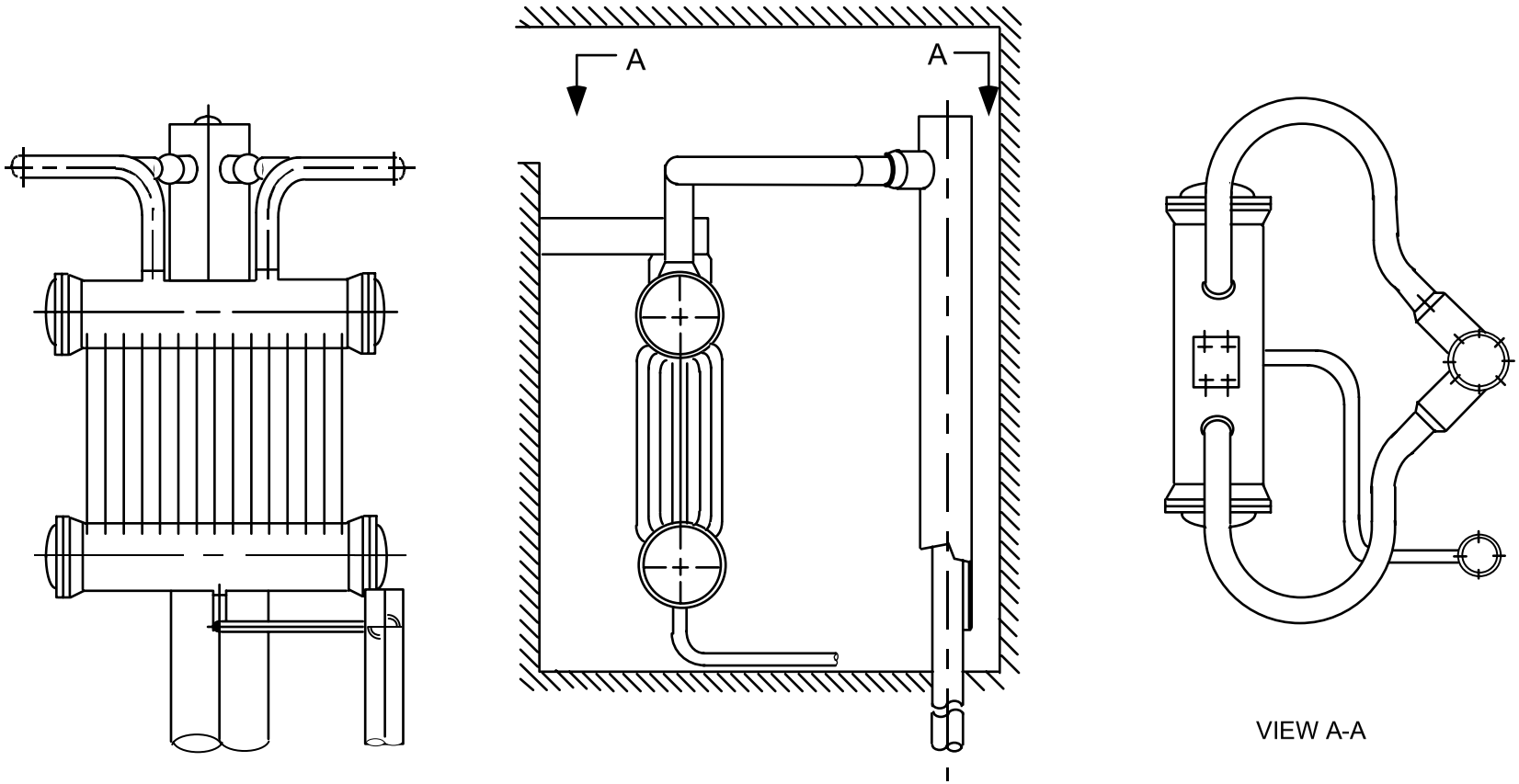

Figure 2.2-1: Isolation Condenser Test Article

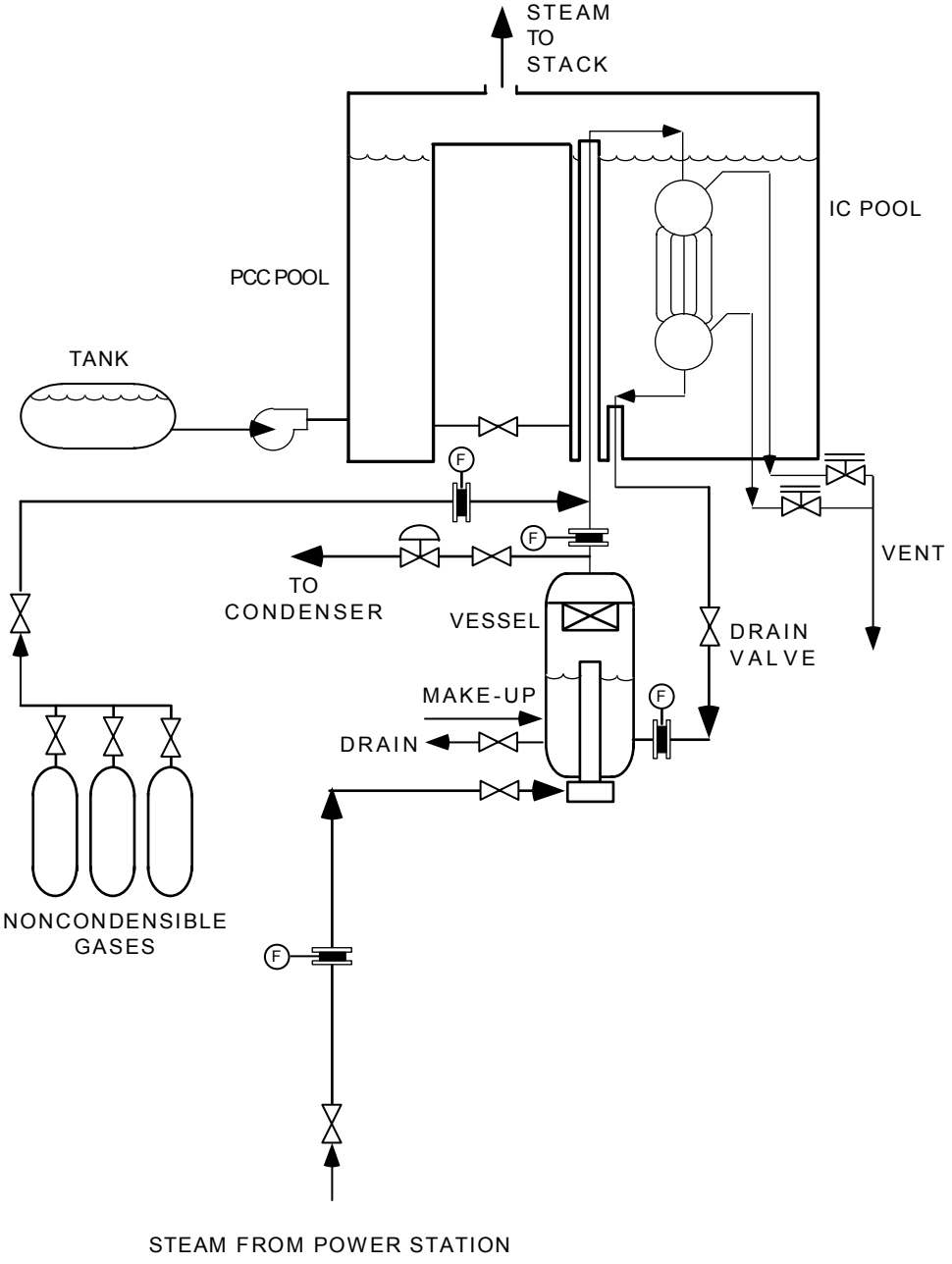

Figure 2.2-2: PANTHERS/IC Test Facility Schematic

[

Redacted

]

Figure 2.2-3: PANTHERS/IC Power for Saturated Steam Tests

[

Redacted

]

Figure 2.2-4: PANTHERS/IC Test T15 Inlet Pressure Response to PCC Pool Water Level

[

Redacted

]

Figure 2.2-5: PANTHERS/IC Inlet Pressure Response During Noncondensible Gas Venting Tests

2.3 PANDA

2.3.1 Test Objectives

The test objectives of the PANDA Test Program were:

1. Provide additional data to: (a) support the adequacy of TRACG to predict the quasi-steady heat rejection rate of a PCC heat exchanger, and (b) identify the effects of scale on PCC performance. (Steady-State Separate Effects)
2. Provide a sufficient database to confirm the capability of TRACG to predict SBWR containment system performance, including potential systems interaction effects. (Integral Systems Tests)
3. Demonstrate startup and long-term operation of a Passive Containment Cooling System. (Concept Demonstration)

2.3.2 Test Description

PANDA testing was performed as a joint effort by GE and the Paul Scherrer Institut (PSI) in Wuerenlingen, Switzerland. Figure 2.3-1 presents an isometric view of the PANDA facility.

The test facility is a large-scale integrated containment structure which is a 1/25 volumetric, full-scale height simulation of the SBWR containment system. It is a modular facility with separate pressure vessels representing the reactor pressure vessel (RPV), drywell (DW), wetwell (WW), and GDCS pool. The facility was equipped with three scaled PCC heat exchangers and one isolation condenser (IC) unit (representing two SBWR IC units), each with its own water pool.

The RPV volume was equipped with electrical heaters and heater controls to simulate decay heat and thermal capacitance of the SBWR RPV and internals.

The test facility also has interconnecting piping arrangements sufficient to establish configurations and thermal-hydraulic conditions representative of the SBWR Main Steam Line Break post-LOCA conditions covering a time period from approximately 1000 seconds (transition from the GDCS injection to long-term PCCS cooling phase) to more than 20 hours after a LOCA.

Figure 2.3-2 shows a schematic of the PANDA test facility and the arrangement of the PANDA test vessels. Two interconnected vessels are used for the DW and WW volumes in order to simulate potential asymmetric effects.

Figure 2.3-3 shows the IC and PCC units, which are essentially the same, except the IC tube outside diameter, thickness and pitch are slightly greater than the PCC values.

In addition to its transient capabilities, PANDA also had temporary piping connections such that a PCC heat exchanger could be tested in a steady-state manner. In this case, a temporary swing connection was made from the IC piping supply line to the inlet of PCC3.

For the PCC heat exchanger steady-state performance tests, the facility was configured to inject a measured flow rate of steam or a mixture of air/steam to the PCC, and the condensate was returned to the steam supply (RPV), while the PCC vent line was either closed for pure steam tests or open to the WW for the air/steam mixture tests. The pressure was established for the air/steam tests by controlling the venting rate from the WW air space. For the pure steam tests, the pressure was allowed to come to the steady-state equilibrium value consistent with the steam flow rate. Once the conditions were at the steady-state equilibrium values consistent with the specified input conditions, data were collected for 15 minutes. The time averaged data were reported [3.12, 3.13] and evaluated [3.24].

In general, for the transient tests, once the initial conditions for a given test had been established, all control was terminated except for automatic control of the WW-to-DW vacuum breaker position and the electric heater simulation of the RPV structure stored energy release and core power decay. The PANDA containment was then allowed to function without operator intervention, consistent with the SSAR assumptions for the SBWR. The only exceptions to the methodology described above were for Tests M3A and M3B, which included operator action to maintain PCC pool level, and Test M6/8 during which the operator established a DW-to-WW flowpath (bypass leakage) during the test and later valved the IC unit out of service. Details are contained in the Test Plans [3.3-3.6] and Data Transmittal Reports (DTRs) [3.25-3.33] for these tests.

2.3.3 Test Matrix

2.3.3.1 Steady-State Performance Tests

[

Redacted

]

[

Redacted

]

2.3.3.2 Transient Integral Systems Tests

[

Redacted

]

[

Redacted

]

[

Redacted

]

2.3.4 Applicability of Data to SBWR

2.3.4.1 Steady-State Tests

[

Redacted

]

[

Redacted

]

2.3.4.2 Transient Integral Systems Tests

[

Redacted

]

[

Redacted

]

[

Redacted

]

[

Redacted

]

[

Redacted

]

[

Redacted

]

2.3.5 Key Results

2.3.5.1 Steady-State Tests

[

Redacted

]

2.3.5.2 Transient Integral Systems Tests

[

Redacted

]

2.3.5.2.1 Base Case

[

Redacted

]

[

Redacted

]

[

Redacted

]

2.3.5.2.2 Asymmetric Break and PCC Configuration

[

Redacted

]

[

Redacted

]

2.3.5.2.3 IC Operation and Drywell-To-Wetwell Leakage

[

Redacted

]

[

Redacted

]

2.3.5.2.4 PCCS Startup

[

Redacted

]

2.3.5.2.5 GDCS Injection Phase

[

Redacted

]

[

Redacted

]

2.3.5.3 Closure with TAPD

[

Redacted

]

Table 2.3-1: PANDA Steady-State PCC Performance Test Matrix

[

Redacted

]

Table 2.3-2: PANDA Transient System Performance Test Matrix

M3 Series:	
M3	Base Case (Main steam line break LOCA + 1 hour)
M3A	Repeatability (PCC/IC pools isolated)
M3B	Repeatability (PCC/IC pools interconnected)
M7	PCC Startup (Bounding noncondensible gas concentrations)
M2	Asymmetric Case 1 (relative to M3 Series) (Total steam flow to DW2)
M10 Series:	Asymmetric (Two PCC units only)
M10A	Asymmetric Case 2 (DW1 essentially isolated, slow gas migration from DW1 to DW2)
M10B	Asymmetric Case 3 (Good mixing in both DWs)
M6/8	System Interaction with IC operation (M6) and DW-to-WW bypass leakage (M8)
M9	Early Start / GDCS injection into RPV (LOCA + 1040 seconds rather than LOCA + 3600 seconds)

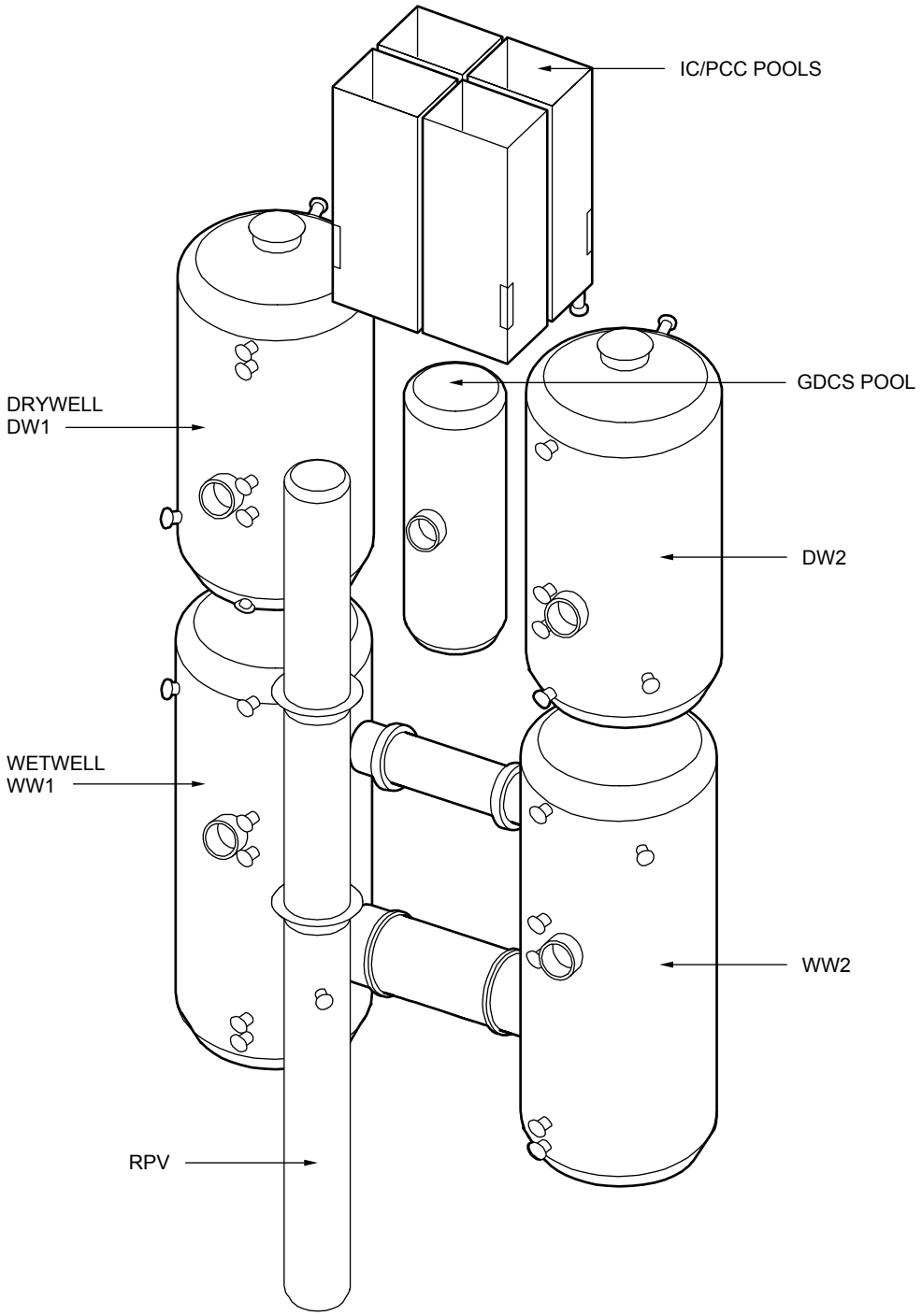

Figure 2.3-1: Isometric View of the PANDA Facility

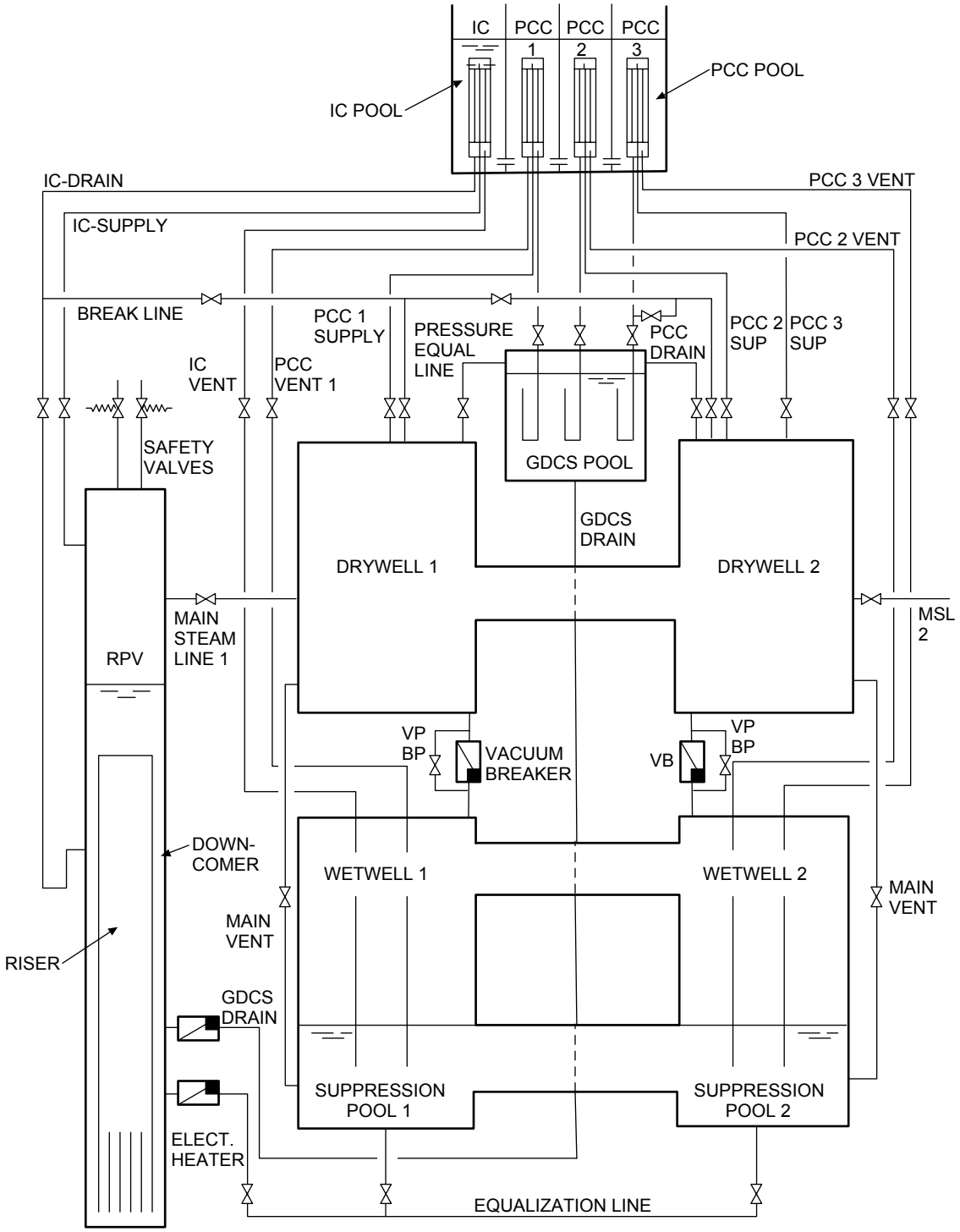

Figure 2.3-2: PANDA Facility Schematic

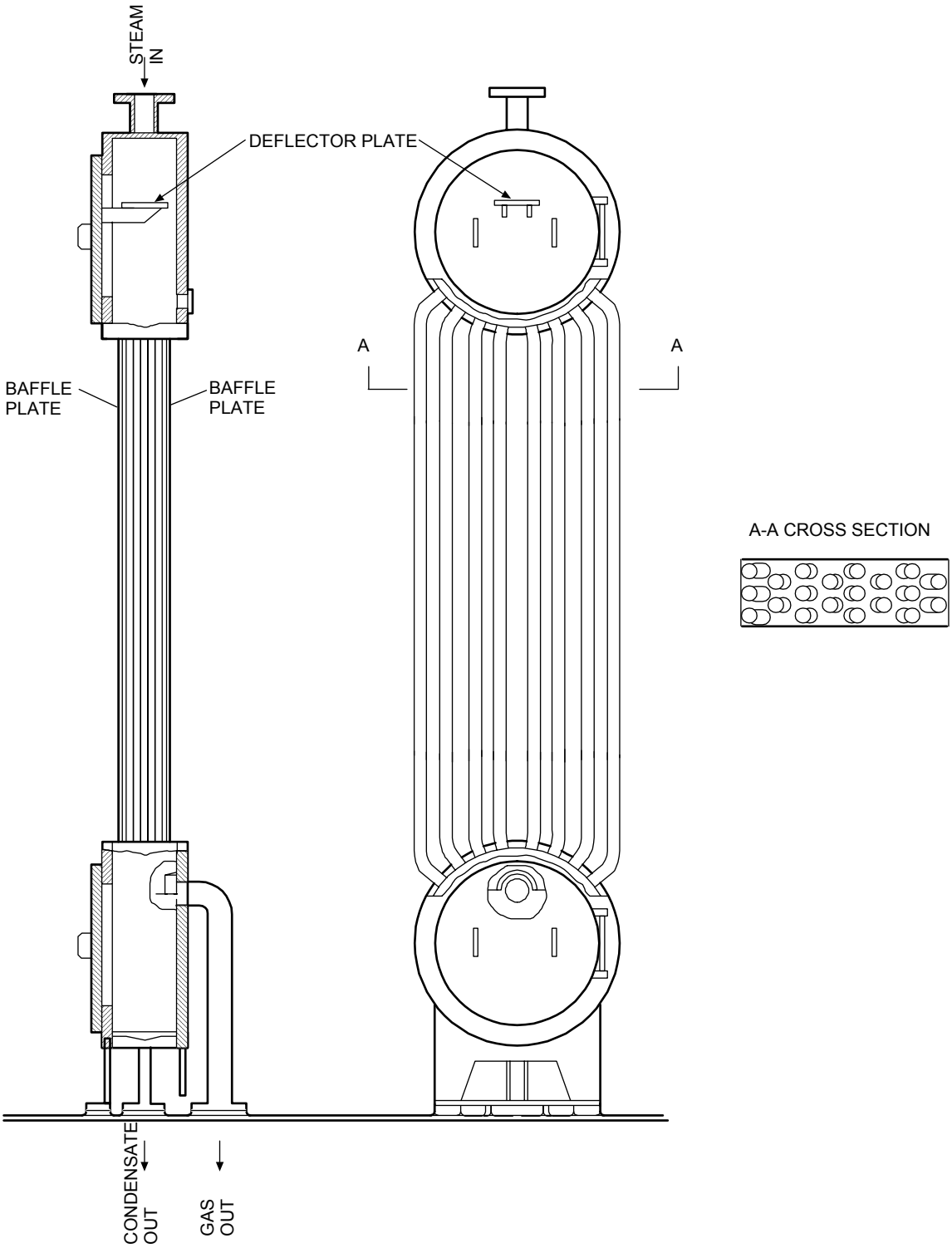

Figure 2.3-3: PANDA Facility: IC/PCC Test Units

[

Redacted

]

Figure 2.3-4: Effect of Air Mass Fraction on PANDA S-series Tests

[

Redacted

]

Figure 2.3-5: PANDA Tests M3, M3A, M3B Drywell Pressure Response

[

Redacted

]

Figure 2.3-6: PANDA Test M3 PCC1 Inside Tube Gas Temperatures

[

Redacted

]

Figure 2.3-7: PANDA Test M3 PCC1 Inside Gas and Wall Tube Temperatures

[

Redacted

]

Figure 2.3-8: PANDA Test M3B PCC1 Inside Tube Gas Temperatures

[

Redacted

]

Figure 2.3-9: PANDA Tests M3 and M2 Drywell Pressure Response

[

Redacted

]

Figure 2.3-10: PANDA Tests M10A, M10B, & M3 Drywell Pressure Response

[

Redacted

]

Figure 2.3-11: PANDA Tests M10A & M10B WW1 Upper Gas Temperature Response

[

Redacted

]

Figure 2.3-12: PANDA Test M10A PCC2 Inside Tube Gas Temperatures

[

Redacted

]

Figure 2.3-13: PANDA Test M10B PCC2 Inside Tube Gas Temperatures

[

Redacted

]

Figure 2.3-14: PANDA Test M6/8 and M3 Drywell Pressure Response

[

Redacted

]

Figure 2.3-15: PANDA Test M6/8 IC and PCC Pool Levels

[

Redacted

]

Figure 2.3-16: PANDA Tests M9 and M3 Drywell Pressure Response

[

Redacted

]

Figure 2.3-17: PANDA Test M9 GDCS and Average PCC Pool Levels

2.4 GIST

2.4.1 Test Objectives

The objectives of the GIST Test Program were:

1. Demonstrate the technical feasibility of the GDCS concept. (Concept Demonstration)
2. Provide a sufficient database to confirm the adequacy of TRACG to predict GDCS flow initiation times, GDCS flow rates, and RPV water levels. (Integrated Systems Test)

2.4.2 Test Description

The Gravity-Driven Integrated Systems Test (GIST) was performed by GE Nuclear Energy in San Jose, California, in 1988. The GIST facility was a section-scaled simulation of the 1987 SBWR design configuration, with a 1:1 vertical scale and a 1:508 horizontal area scale of the RPV and containment volumes. Because of the 1:1 vertical scaling, the tests provided real-time response of the 1987 SBWR pressures and temperatures.

The integrated systems test program included the effects of various plant conditions on GDCS initiation and performance. Figure 2.4-1 provides a facility schematic, and Figure 2.4-2 shows the major interconnecting lines. The GIST facility consisted of four pressure vessels: the RPV, upper drywell (UDW), lower drywell (LDW) and the wetwell (WW). The wetwell included the GDCS fluid. The RPV included internal structures, an electrically heated core, and bypass and chimney regions.

The GIST facility modeled SBWR plant behavior during the final stages of the RPV blowdown. The tests started with the RPV at 791 kPa (100 psig) and continued until the GDCS flow initiated and flooded the RPV.

2.4.3 Test Matrix

The GIST Test Matrix is shown in Table 2.4-1. Twenty-six test conditions were specified. These 26 individual tests were divided into four test types, three of them loss-of-coolant accidents:

- Bottom Drain Line Break (BDLB)
- Main Steam Line Break (MSLB)
- GDCS Line Break (GDLB)
- No-Break (NB)

A broad spectrum of test parameters was varied within each one of these test types. In each one of the four test categories, a base test was performed, and then subsequent tests were run where only one parameter at a time was varied from that used in the base case.

2.4.4 Applicability of Data to SBWR

2.4.4.1 Introduction

The GIST facility was a simulation of the SBWR design as it existed in 1987. Several differences exist between the GIST configuration and the final SBWR 670 MWe design. These differences are listed and reconciled in the SBWR Scaling Report [1.2]. Below is a summary of that discussion related to the geometrical differences between the GIST facility and the final SBWR design.

2.4.4.2 GDCS Driving Pressure

The major difference between the 1987 and final SBWR 670 MWe design is that, in the earlier version, a single pool was used to provide both containment pressure suppression (i.e., the suppression pool) and the source of the GDCS water. In the final SBWR design, the water inventories for GDCS and pressure suppression are separated. The suppression pool (SP) is in the WW, and the GDCS inventory is equally divided among three pools located on the diaphragm floor within the drywell (DW). A second difference is the addition of six depressurization valves (DPVs) discharging directly to the DW, to supplement the Automatic Depressurization System (ADS) function performed by the SRVs discharging to the SP.

An important parameter determining vessel reflood behavior is the upward force acting against the gravity head of the coolant in the downcomer. This depends on the pressures in the RPV steam dome and at the GDCS flow injection point. The differences in the older design tend to inhibit GDCS injection in GIST, relative to what would be expected in the present SBWR. This can be understood by recognizing that the DW and WW pressures in the SBWR are not independent variables. During the entire blowdown, the DW pressure exceeds the WW pressure by, at least, the hydrostatic head required to open the top main vent (about 15 kPa). This means that the GDCS pool overpressure in GIST was actually lower, relative to the RPV pressure, than it would be in the plant (alternatively, the pressure in the RPV steam dome was higher). Blowdown through the DPVs in the SBWR tends to sustain main vent flow and ensures that DW pressure remains above WW pressure up to the time GDCS flow initiates. The top of the GDCS pool, which is directly connected to the DW, is therefore at a relatively higher pressure in the SBWR.

The presence of the PCCS condensers in the SBWR has a small effect on the absolute pressure in the DW, but does not significantly change the pressure difference that is acting to reflood the vessel. Similarly, the ICS condenser loop, absorbing some steam from the RPV dome, tends to reduce the absolute pressure in the RPV, but not the pressure difference causing reflood.

2.4.4.3 RPV Water Level

The parameters controlling RPV water level during the reflood period were distorted in GIST. The high resistance (and therefore low flow) in the GDCS line had two results. First, the reflood rate was slower than the SBWR reflood rate. This is not particularly significant because the behavior during the reflood is well understood. Before the reflood begins, however, the subcooling due to the GDCS is of the same order as the decay heat. This indicates that stored energy release played a role in the two-phase level at the time of GDCS initiation. During the tests, it was observed that the swollen water level collapsed faster in GIST than expected in the SBWR because there was insufficient stored energy release near the time of GDCS initiation. As a result, the two-phase level fell lower in GIST than it would in the SBWR.

2.4.4.4 Summary of Data Applicability

[

Redacted

]

2.4.5 Key Results

[

Redacted

]

2.4.5.1 Series BDLB

[

Redacted

]

2.4.5.2 Series MSLB

[

Redacted

]

2.4.5.3 Series GDLB

[

Redacted

]

2.4.5.4 Series NB

[

Redacted

]

2.4.5.5 Closure with TAPD

[

Redacted

]

Table 2.4-1
GIST Test Matrix Initial Conditions (RPV at 791 kPa)

[

Redacted

]

Table 2.4-1 (cont'd)
GIST Test Matrix Initial Conditions (RPV at 791 kPa)

[

Redacted

]

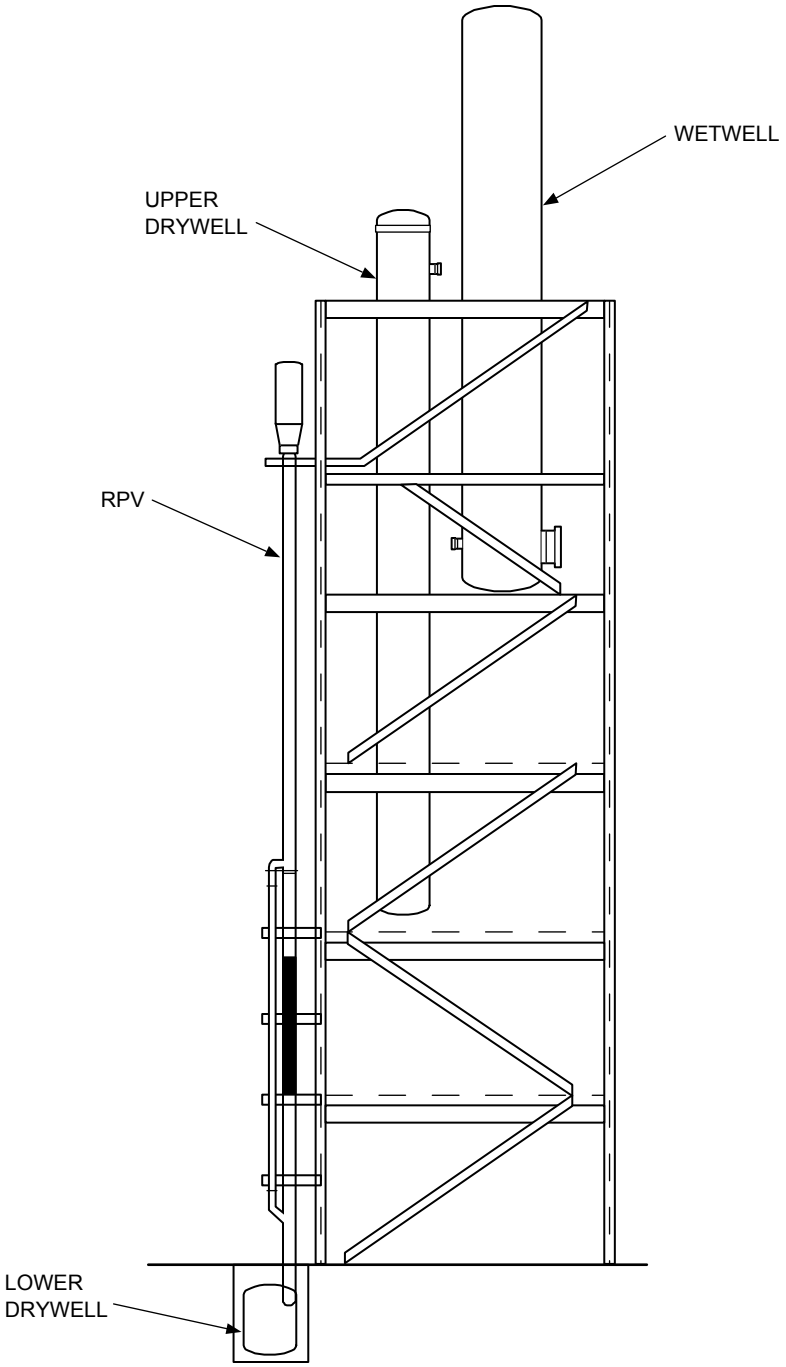

Figure 2.4-1: GIST Facility Schematic

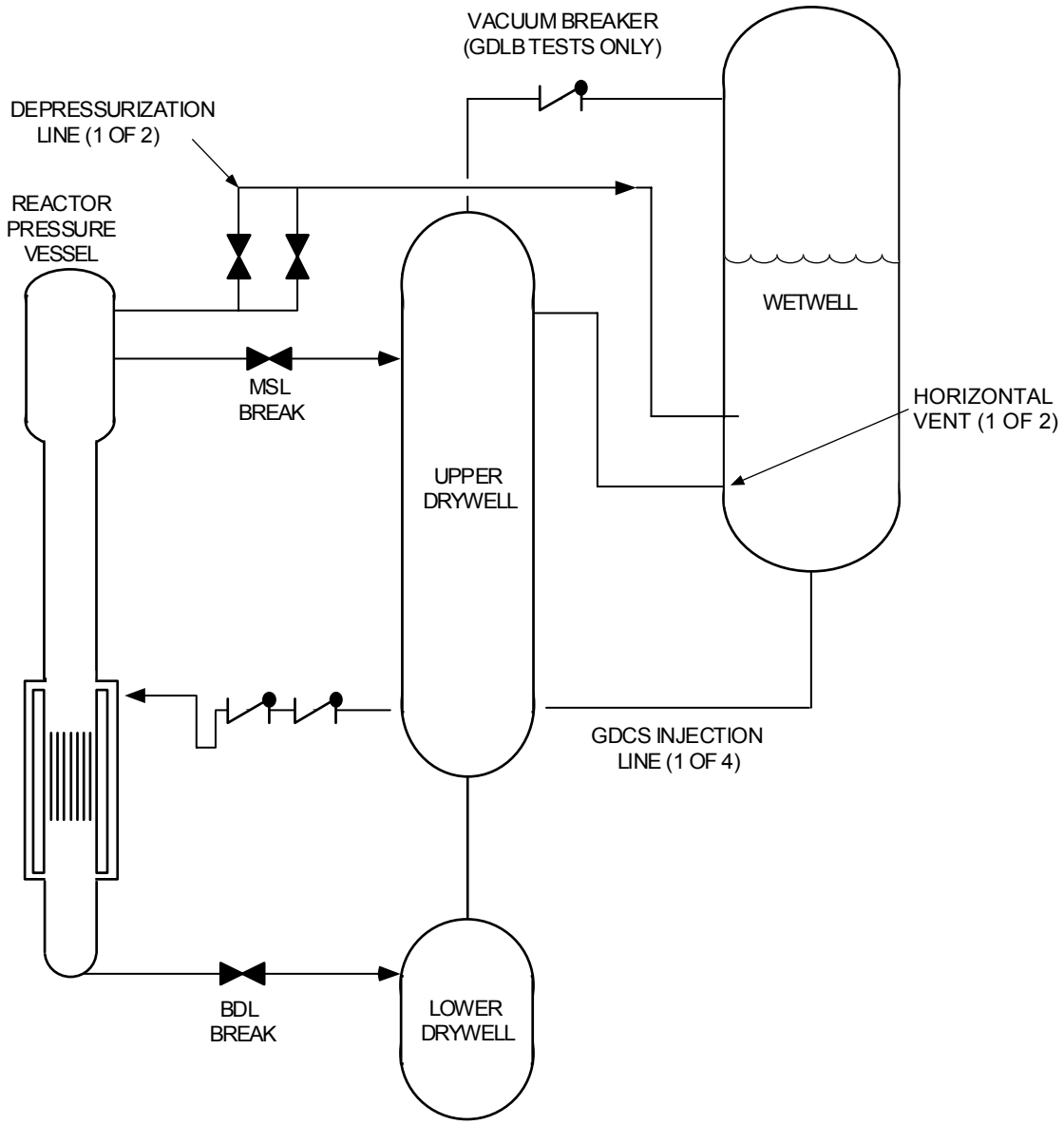

Figure 2.4-2: GIST Facility Piping Arrangement

[

Redacted

]

Figure 2.4-3: GIST RPV Pressure for GDCS Line Break Base Case Test (C01A)

[

Redacted

]

Figure 2.4-4: GIST RPV Inventory and GDCS Flow for GDCS Line Break Base Case Test (C01A)

2.5 GIRAFFE/Helium

2.5.1 Test Objectives

The test objectives of the GIRAFFE/Helium Test Program were:

1. Demonstrate the operation of a passive containment cooling system with the presence of a lighter-than-steam noncondensible gas, including demonstrating the process of purging noncondensible gases from the PCC.
2. Provide a database to confirm the adequacy of TRACG to predict SBWR containment system performance in the presence of a lighter-than-steam noncondensible gas, including potential systems interaction effects.
3. Provide a tie-back test, which includes the appropriate Quality Assurance documentation, to repeat a previous GIRAFFE test.

2.5.2 Test Description

GIRAFFE/Helium testing was performed as a joint effort by GE and Toshiba in Kawasaki City, Japan. The GIRAFFE facility is a large scale, integral system test facility designed to exhibit post-LOCA thermal-hydraulic behavior similar to the SBWR systems that are important to long-term containment cooling following a LOCA. Figure 2.5-1 shows a schematic of the GIRAFFE facility for the helium test program.

The global volume scaling of the facility is approximately 1:400, with a nominal height scaling of 1:1. The SBWR components simulated in the facility are: reactor pressure vessel (RPV), Passive Containment Cooling System (PCCS), Gravity-Driven Cooling System (GDCS), drywell (DW), wetwell (WW), and the connecting piping and valves. Five separate vessels represent the SBWR RPV, DW, WW, GDCS pools and the PCCS pool. The facility was equipped with one PCC (Figure 2.5-2), approximately scaled to represent the three SBWR PCCS condensers. Electric heaters provide a variable power source to simulate the core decay heat and the stored energy in the reactor structures.

For the helium series tests, once the test initial conditions were established, all control (except for the decay of RPV power and helium injection, if called for) was terminated, and the GIRAFFE containment was allowed to function without operator intervention (except that the vacuum breaker (VB) was operated manually to simulate automatic operation in SBWR and minor WW microheater power adjustments were made to compensate for facility heat losses).

2.5.3 Test Matrix

2.5.3.1 Helium Test Series

[Redacted]

[

Redacted

]

2.5.3.2 Tie-Back Test Series

[

Redacted

]

[

Redacted

]

2.5.4 Applicability of Data to SBWR

2.5.4.1 Test Facility Design

[

Redacted

]

2.5.4.2 Choice of the Base Case (H1)

[

Redacted

]

2.5.4.3 Other Tests

[

Redacted

]

2.5.5 Key Results

2.5.5.1 Nitrogen vs. Helium Tests (H1 and H2)

[

Redacted

]

[

Redacted

]

2.5.5.2 Nitrogen with Helium Tests (H3 and H4)

[

Redacted

]

2.5.5.3 Tie-Back Tests (T1 and T2)

[

Redacted

]

2.5.5.4 Closure with TAPD

[

Redacted

]

Table 2.5-1: GIRAFFE/Helium Test Series Test Matrix

[

Redacted

]

Table 2.5-2: GIRAFFE/Helium Test Series Initial Conditions

[

Redacted

]

Table 2.5-3: GIRAFFE/Helium Tieback Tests Initial Conditions

[

Redacted

]

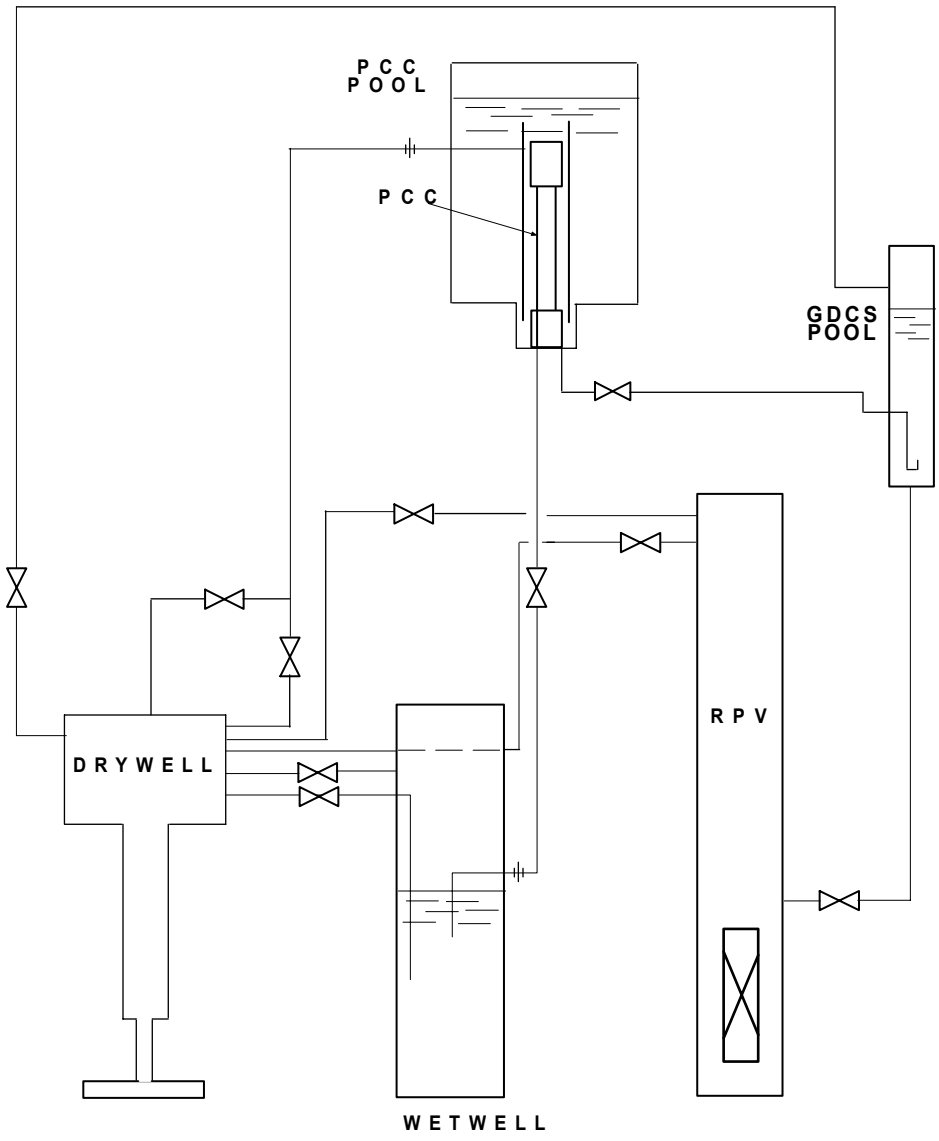

Figure 2.5-1: GIRAFFE/Helium Test Facility Schematic

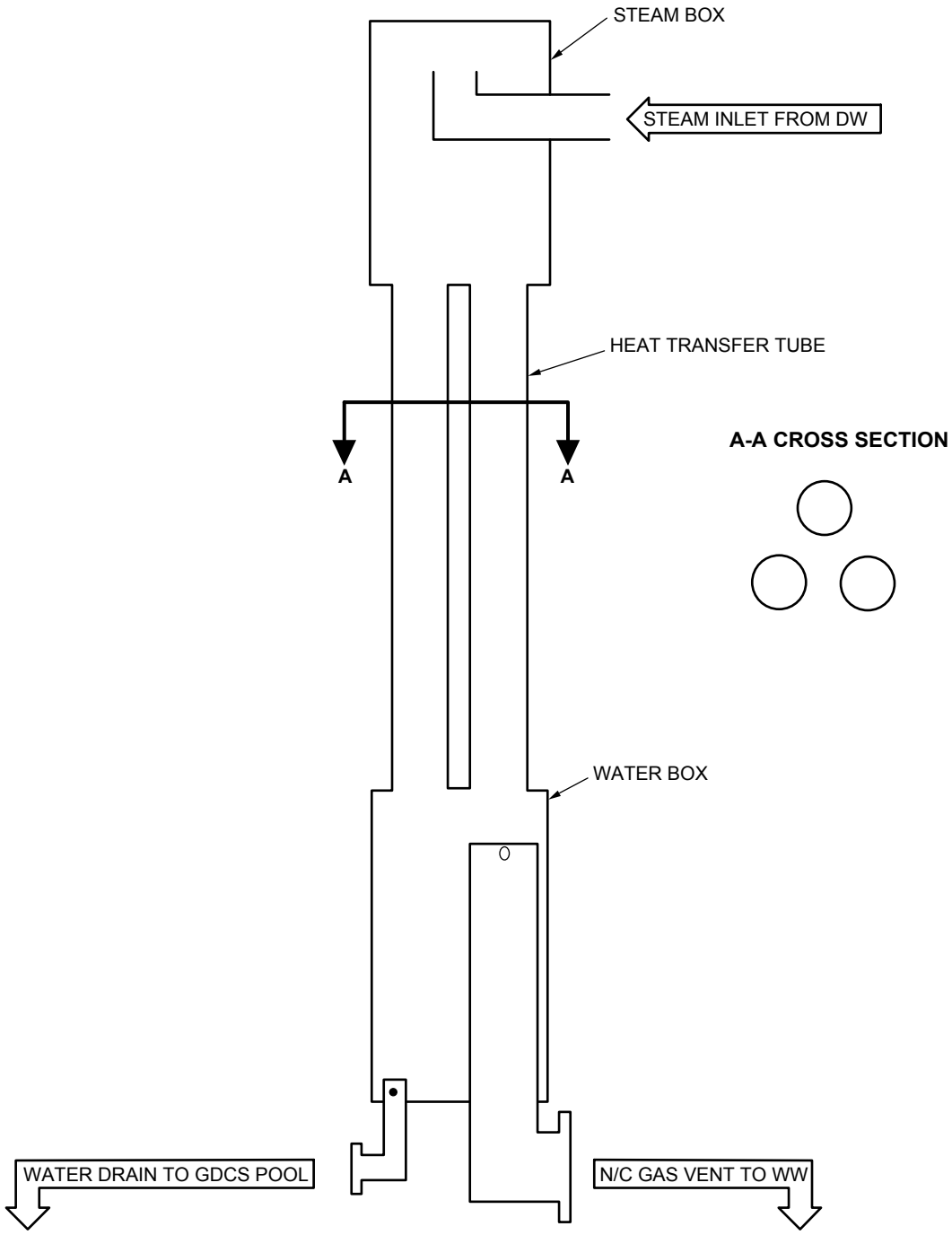

Figure 2.5-2: PCC Unit for GIRAFFE/Helium and SIT Tests

[

Redacted

]

Figure 2.5-3: GIRAFFE /Helium Tests Drywell Pressure Response

[

Redacted

]

Figure 2.5-4: GIRAFFE /Helium Test H1 PCC Tube Bulk Fluid Temperatures

[

Redacted

]

Figure 2.5-5: GIRAFFE /Helium Test H2 PCC Tube Bulk Fluid Temperatures

2.6 GIRAFFE/SIT

2.6.1 Test Objective

The objective of the GIRAFFE/SIT Test Program was:

Provide a database to confirm the adequacy of TRACG to predict the SBWR ECCS performance during the late blowdown/early GDCS phase of a LOCA, with specific focus on potential systems interaction effects.

2.6.2 Test Description

A series of four transient systems tests was conducted to provide an integral systems database for potential systems interaction effects in the late blowdown/early GDCS period. All four tests were liquid breaks: three GDCS line breaks and one bottom drain line break. Tests were performed with and without the ICS and PCCS in operation, and two different single failures were considered.

The post-LOCA thermal-hydraulic behavior (especially the RPV pressure transient and water level transient), the GDCS injection characteristics and possible systems interactions were simulated in the SIT. The test facility, therefore, models the whole containment system of the SBWR. The SBWR components which are modeled in the facility are: the RPV, ICS, GDCS, PCCS, DW, WW and the connecting piping and valves. Major portions of the SBWR primary containment (DW, WW and GDCS pool, as well as IC pool and PCCS pool) are modeled using separate vessels. Figure 2.6-1 is a facility schematic.

The PCC unit is the same as that used for the GIRAFFE/Helium Tests (Figure 2.5-2) and consists of a steam box, heat transfer tubes and a water box. The PCC has three heat transfer tubes corresponding to the scaled volume. The heat transfer tubes are full height, and the internal tube flow area is almost the same as the scaled SBWR flow area.

One scaled IC is mounted above the DW vessel. The IC has three tubes, two of which are plugged in order to reduce the heat transfer surface of the unit. This single condenser represents two IC condensers found in the SBWR. Figure 2.6-2 shows the IC test unit.

Testing followed a methodology very similar to that used in PANDA and GIRAFFE/Helium. Once the initial conditions for a given test were established, all controls (except for the decay of RPV power) were terminated. The GIRAFFE RPV and containment were allowed to function without operator intervention, mirroring the SSAR assumptions for the SBWR. The GDCS pool-to-DW flow was manually terminated at one hour in the GDCS break cases to avoid an inappropriate emptying of the pool. This was necessary since a single pool in GIRAFFE simulated the three SBWR pools, only one of which would have pool-to-DW flow. Manually stopping GDCS flow to the DW in GIRAFFE simulates the end of draining for that

one pool in the SBWR and maintains the simulation of flow from the remaining pools to the RPV.

2.6.3 Test Matrix

[

Redacted

]

[

Redacted

]

2.6.4 Applicability of Data to SBWR

2.6.4.1 Test Facility Design

[

Redacted

]

2.6.4.2 Choice of the Base Case Test (GS1)

[

Redacted

]

2.6.4.3 Other Tests

[

Redacted

]

2.6.4.4 Test Initiation

[

Redacted

]

2.6.5 Key Results

[

Redacted

]

2.6.5.1 Effect of IC/PCC (GS1 and GS2)

[

Redacted

]

2.6.5.2 Effect of Break Type (GS2 and GS3)

[

Redacted

]

[

Redacted

]

2.6.5.3 Effect of Single Failure Assumption (GS2 and GS4)

[

Redacted

]

2.6.5.4 Effect of GDCS Flow on PCCS Operation (GS2)

[

Redacted

]

[

Redacted

]

2.6.5.5 Closure with TAPD

[

Redacted

]

Table 2.6-1: GIRAFFE/SIT Test Matrix

Test	Break	Single Failure	IC/PCCS on?
GS1	GDL	DPV	No
GS2	GDL	DPV	Yes
GS3	BDL	DPV	Yes
GS4	GDL	GDCS	Yes

GDL = Gravity Drain Line
BDL = Bottom Drain Line
DPV = Depressurization Valve
GDCS = GDCS Injection Valve

Table 2.6-2: GIRAFFE/SIT Test Conditions

[

Redacted

]

Table 2.6-3:
Basis for GIRAFFE/SIT Test Conditions

[

Redacted

]

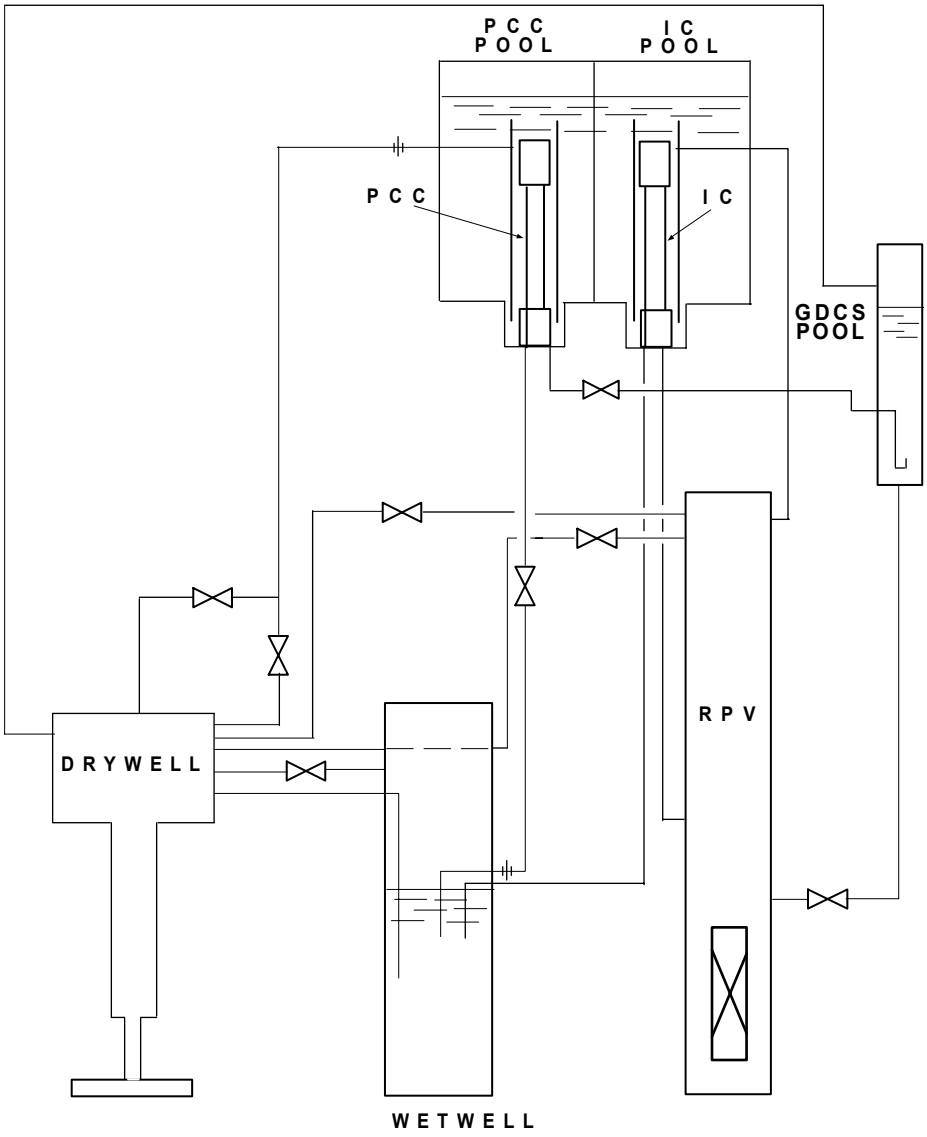

Figure 2.6-1: GIRAFFE/SIT Test Facility Schematic

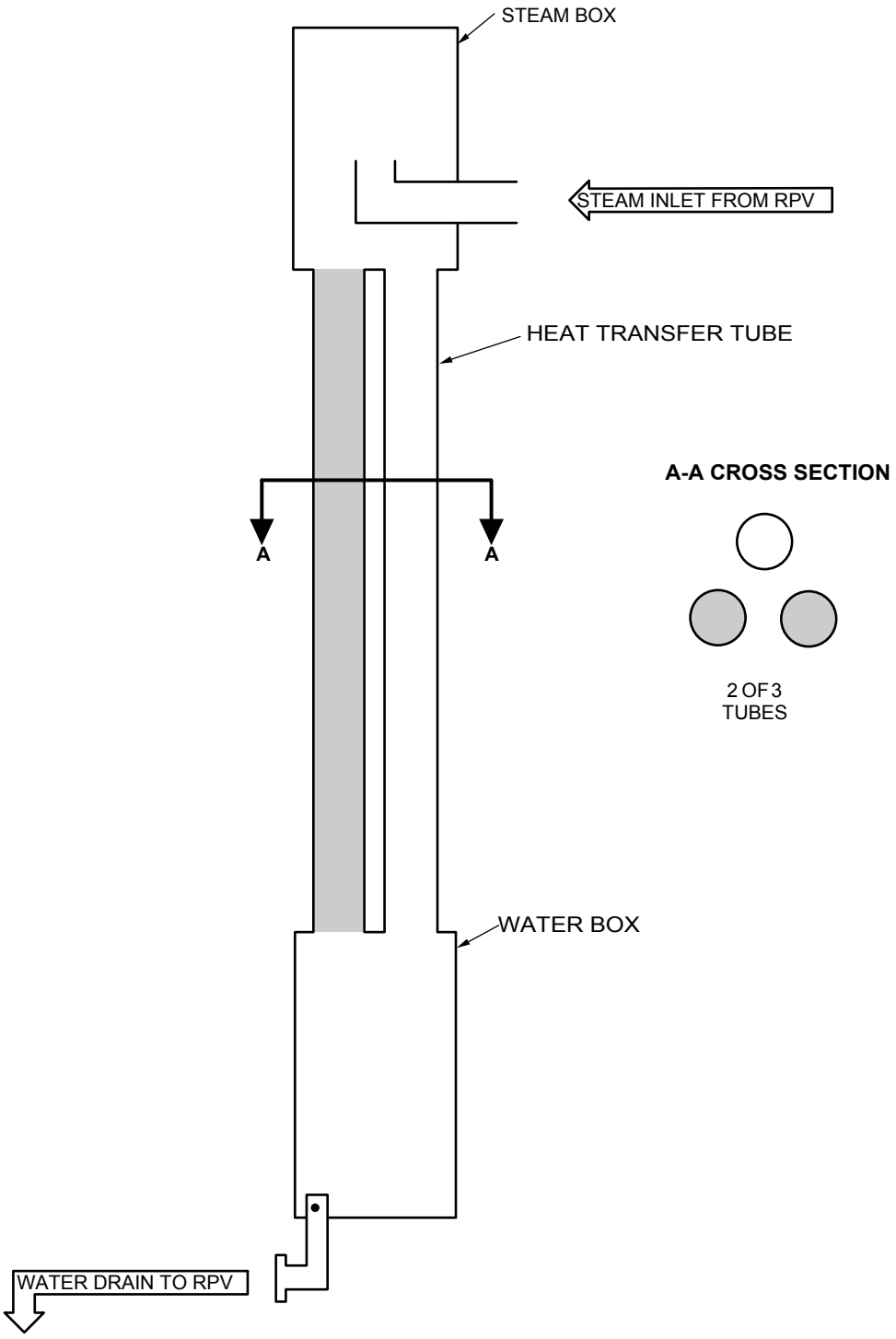

Figure 2.6-2: GIRAFFE/SIT IC Unit

[

Redacted

]

Figure 2.6-3: GIRAFFE/SIT RPV Pressure Response to IC/PCCS Operation

[

Redacted

]

Figure 2.6-4: GIRAFFE/SIT RPV Inventory Response to IC/PCCS Operation

[

Redacted

]

Figure 2.6-5: GIRAFFE/SIT RPV Pressure Response to Break Location

[

Redacted

]

Figure 2.6-6: GIRAFFE/SIT RPV Inventory Response to Break Location

[

Redacted

]

Figure 2.6-7: GIRAFFE/SIT RPV Pressure Response to Single Failure Assumption

[

Redacted

]

Figure 2.6-8: GIRAFFE/SIT RPV Inventory Response to Single Failure Assumption

[

Redacted

]

Figure 2.6-9: Effect of GDCS Flow on Containment Pressure and PCCS Operation in GIRAFFE/SIT Test GS2

3. PIRT EVALUATION

The *SBWR Test and Analysis Program Description* (TAPD) [1.1] provided a comprehensive integrated plan that addressed the testing elements needed for analysis of SBWR steady-state and transient performance. The TAPD provided the technical basis for validating the performance of the plant transients and accidents and provided the rationale for the diverse experimental and analytical efforts in support of SBWR certification based on the Phenomena Identification and Ranking Tables (PIRT). These tables listed the phenomena and interactions between systems important to SBWR transient and accident analysis.

Section 6 of the TAPD presented a road-map of the remaining activities to qualify TRACG for SBWR application. Table 6.1-1 in the TAPD showed how the SBWR tests discussed in this report meet the qualification needs for TRACG qualification.

The qualification needs identified in TAPD as coming from PANTHERS (IC and PCC), PANDA (steady state and transient), and GIRAFFE (Helium and SIT) are discussed in this section to evaluate whether the specified phenomenon was addressed in its respective test program. Elements relevant to these tests from TAPD Table 6.1-1 are reproduced here as Table 3.0-1 (PANTHERS), Table 3.0-2 (PANDA), and Table 3.0-3 (GIRAFFE). GIST testing is not discussed because the results have already been utilized for TRACG qualification.

Table 6.1-1 of TAPD [1.1] also included qualification needs from non-SBWR test programs (e.g., CRIEPI, Dodewaard, etc.).

The needs for these tests were all listed as high priority needs in TAPD. Results from these tests show that some of these phenomena, while present in the tests, are not very important to the modeling of the SBWR.

Table 3.0-1
TRACG Qualification Needs from PANTHERS

[

Redacted

]

Table 3.0-2
TRACG Qualification Needs from PANDA

[

Redacted

]

Table 3.0-3
TRACG Qualification Needs from GIRAFFE

[

Redacted

]

3.1 PANTHERS/PCC

Table 3.0-1 qualification needs are satisfied by the PANTHERS/PCC broad database of various steam flowrates, air flowrates, and inlet pressures. The results from these tests are discussed in Section 2.1.5 and documented in References 2.5 and 2.6. From its test matrix, nine steam/air mixture steady-state tests and three steam only steady-state tests were chosen for post-test analysis by TRACG [1.1].

[

Redacted

]

3.1.1 PCC Flow and Pressure Drop (PC1)

[

Redacted

]

[

Redacted

]

3.1.2 Condensation on Primary Side - Degradation by Noncondensible Gases (PC2)

[

Redacted

]

3.1.3 Secondary Side Heat Transfer (PC3)

[

Redacted

]

[

Redacted

]

3.1.3.1 Pool Temperature Distribution

[

Redacted

]

3.1.3.2 Pool Void Distribution

[

Redacted

]

3.1.3.3 Natural Circulation

[

Redacted

]

[

Redacted

]

3.1.4 Parallel PCC Tube Effects (PC4)

[

Redacted

]

[

Redacted

]

3.1.5 Parallel PCC Module Effects (PC5)

[

Redacted

]

Table 3.1-1
Key Results from PANTHERS/PCC Tests
with 5 kg/sec Steam Flow and 330 kPa Inlet Pressure

[

Redacted

]

Table 3.1-2
PANTHERS/PCC Pool Temperatures

[

Redacted

]

Table 3.1-3
PANTHERS/PCC Tube Temperatures
(Test T09-9)

[

Redacted

]

[

Redacted

]

Figure 3.1-1: PCC Module Pressure Drops at PANTHERS

3.2 PANTHERS/IC

The qualification needs listed in Table 3.0-1 are satisfied by the PANTHERS/IC broad database of tests. The results from these tests are discussed in Section 2.2.5 and documented in Reference 2.9. From this test matrix, three steady-state tests and three transient tests were chosen for post-test analysis by TRACG [1.1].

3.2.1 IC Pressure Drop (Q1)

[

Redacted

]

3.2.2 IC Capacity (Q2)

[

Redacted

]

3.2.3 Stratification in IC Drums (Q3)

[

Redacted

]

3.2.4 IC Pool Stratification (Q4) and Secondary Side Heat Transfer (Q5)

[

Redacted

]

3.3 PANDA

The qualification needs listed in Table 3.0-2 are satisfied by the PANDA steady-state and transient integral system tests broad database of various test conditions and configurations. Sections 3.3.1 through 3.3.4 discuss the qualification needs for the PCC performance. These needs are satisfied by both the steady-state (S-series) tests and the transient integral systems (M-series) tests. The remaining qualification needs (Sections 3.3.5 through 3.3.15) are satisfied by the transient integral systems tests.

3.3.1 PCC Flow and Pressure Drop (PC1)

[

Redacted

]

3.3.2 Condensation on Primary Side-Degradation by Noncondensible Gases (PC2)

[

Redacted

]

3.3.3 Secondary Side Heat Transfer (PC3)

[

Redacted

]

[

]

3.3.3.1 Pool Temperature Distribution

[

Redacted

]

3.3.3.2 Pool Void Distribution

[

Redacted

]

3.3.3.3 Natural Circulation Distribution

[

Redacted

]

3.3.4 Parallel PCC Tube Effects (PC4)

[

Redacted

]

[

Redacted

]

3.3.5 Three-Dimensional Effects (DW3)

[

Redacted

]

{

}

3.3.5.1 Phase Distribution

[

Redacted

]

3.3.5.2 Noncondensible Gas Distribution

[

Redacted

]

[

Redacted

]

3.3.5.3 Buoyancy/Natural Circulation

[

Redacted

]

3.3.6 Condensation on Reactor Outflows (DW4)

[

Redacted

]

3.3.7 Wetwell Free Surface Condensation/Evaporation (WW4)

[

Redacted

]

[

Redacted

]

3.3.8 Pool Mixing and Stratification (WW6)

[

Redacted

]

3.3.9 Three-Dimensional Effects in Gas Space (WW7)

[

Redacted

]

[

Redacted

]

3.3.9.1 Temperature Distribution

[

Redacted

]

3.3.9.2 Noncondensible Gas Distribution

[

Redacted

]

3.3.10 Drywell Spray Condensation (FPS1, WW8)

[

Redacted

]

[

Redacted

]

3.3.11 Parallel PCC Unit Effects (PC5/XC5)

[

Redacted

]

3.3.12 PCCS Startup with Noncondensible Gas (PC8)

[

Redacted

]

3.3.13 Leakage between Drywell and Wetwell (DWB1)

[

Redacted

]

[

Redacted

]

3.3.14 System Interactions - IC/GDCS/PCC (XC2)

[

Redacted

]

[

Redacted

]

3.3.15 System Interactions - Multiple PCC units (XC5)

[

Redacted

]

[

Redacted

]

Figure 3.3-1: PANDA Test M3 PCC1 Mid-Tube Wall Temperatures

[

Redacted

]

Figure 3.3-2: PANDA Test M3 PCC Feed Mass Flow Rates

[

Redacted

]

Figure 3.3-3: PANDA Test M7 Drywell 1 Air Mass Fraction and PCC Pool Water Level

3.4 GIRAFFE/Helium

The TRACG qualification needs listed in Table 3.0-3 for the GIRAFFE/Helium tests are satisfied by these tests. The results from these tests are discussed in Section 2.5.5 and documented in Reference 5.2.

3.4.1 System Interaction - Light Noncondensible Gas DW/PCCS/WW (XC6)

[

Redacted

]

[

Redacted

]

3.4.2 Three-Dimensional Effects (DW3)

[

Redacted

]

3.4.2.1 Phase Separation (DW3)

[

Redacted

]

3.4.2.2 Noncondensible Gas Stratification (DW3)

[

Redacted

]

[

Redacted

]

3.4.2.3 Buoyancy/Natural Circulation (DW3)

[

Redacted

]

[

Redacted

]

3.4.3 PCCS Startup with Noncondensible Gas (PC8)

[

Redacted

]

Table 3.4-1
GIRAFFE/Helium Drywell Temperatures at 7200 sec

[

Redacted

]

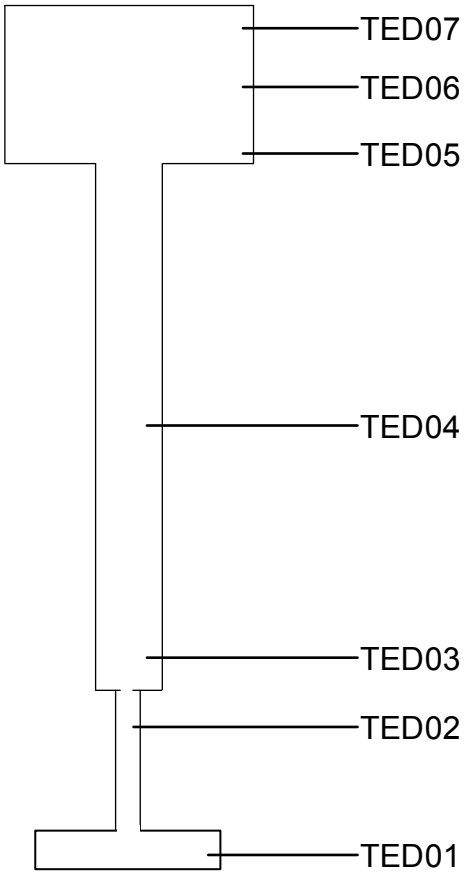

3.5 GIRAFFE/SIT

Table 3.0-3 lists the TRACG qualification needs from GIRAFFE/SIT. The results from these tests are discussed in Section 2.6.5 and documented in Reference 6.1. For the most part, the TRACG qualification needs associated with GIRAFFE/SIT concern the RPV response to loss-of-coolant accidents (LOCAs).

3.5.1 Break Uncovery (E1)

[

Redacted

]

3.5.2 Void Profile/Two-Phase Level in Downcomer (E2)

[

Redacted

]

3.5.3 Cold Water Injection Below Two-Phase Level (E3)

[

Redacted

]

3.5.4 Cold Water Injection Above Two-Phase Level (E7)

[

Redacted

]

[

Redacted

]

3.5.5 Void Distribution/Two-Phase Level in Chimney (F1)

[

Redacted

]

3.5.6 System Interaction - GDCS/System Depressurization (XL3)

[

Redacted

]

3.5.7 System Interaction - RPV/DW/WW/IC/DPV/PCCS/GDCS (XL4)

[

Redacted

]

[

Redacted

]

Figure 3.5-1: GDL Break Uncovery in GIRAFFE/SIT Test GS2

[

Redacted

]

Figure 3.5-2: RPV Temperatures in GIRAFFE/SIT Test GS2

4. INTEGRATION OF TESTS AND CONFIRMATION OF SCALING

In order to study SBWR-unique or performance critical features of the plant, the SBWR test program encompassed a broad range of tests that span and bound the important SBWR parameters. While a major objective of these tests is to provide qualification data for the TRACG computer code, it is also the program philosophy to test in multiple scales whenever possible. Multiple scale testing is useful, since it validates the scaling approach and allows a better understanding of the thermal-hydraulic phenomena involved. These tests, therefore, also provide data to examine the scaling criteria employed in the design and operation of the various test facilities.

Reference 1.2 documents the scaling study applicable to the SBWR-related tests. That study showed that the test facilities were scaled well for their intended purpose and that the distortions identified should not significantly impact the test behavior.

This study quantifies the analytical approach given in Reference 1.2 and demonstrates that the experimental observations from the test programs are representative of predicted SBWR behavior. The results from this study support the conclusions given in the analytical scaling study, namely that:

- All dominant phenomena are preserved in the experiments for various LOCA phases.
- No new phenomena are introduced by the scaled experiments.
- Scaling distortions do not exclude the essential phenomena.
- The experimental results are appropriate for TRACG qualification.

[

Redacted

]

[

Redacted

]

4.1 Steady-State Component Tests

A key feature in the SBWR design is the use of passive steam condensers to remove decay heat from the reactor pressure vessel (RPV) and containment during postulated accidents. During isolation transients, isolation condensers (IC) on the RPV are activated to control pressure by removing steam, condensing it, and returning the condensate to the RPV. Following a LOCA and pressurization of the containment, the Passive Containment Cooling System (PCCS) performs the same function by taking steam from the top of the drywell (DW), condensing it, and routing the condensate to the Gravity-Driven Cooling System (GDCS) pool for return to the RPV.

As part of the prototype test program, various scaled models of these condensers were constructed and tested. In these component tests, the condensers were supplied with a constant flow of steam or steam/gas mixture, and their performance was measured. The noncondensible gas used was either air (PANTHERS and PANDA) or nitrogen (GIRAFFE). The inlet pressure was either allowed to reach its equilibrium value, which results in complete condensation, or set at a specific value and the condensation efficiency (ratio of condensate to inlet steam) measured.

In PANTHERS, full-scale prototypes of both the PCC and the IC were tested (Sections 2.1 and 2.2). The test articles, therefore, exactly matched the SBWR design units in all aspects, including tube material, pitch, length, diameter, and wall thickness.

In PANDA, one of the three scaled PCC units was tested separately (Section 2.3). This 20-tube test unit was designed to represent a slice of one tube bundle at approximately 1:25 scale. The tubes had prototypical characteristics of material, pitch, length, diameter, and wall thickness.

In GIRAFFE, the scaled IC/PCC unit used in the early tests (prior to the GIRAFFE/Helium and GIRAFFE/SIT test programs) was tested. The three-tube test unit was designed to be approximately 1:400 scale of the total capacity of the PCCS. This unit was built before the SBWR unit was designed and did not match the final SBWR design in several areas. The tube wall thickness and length were somewhat greater than that of the SBWR design; however, the tube outside diameter was the same [1.1]. Table 4.1-1 gives the GIRAFFE Phase 1, Step 1 test matrix.

In this section, comparisons are made of steady-state data from the PANTHERS/PCC, PANTHERS/IC, PANDA S-series, and GIRAFFE Phase 1, Step 1 tests. These comparisons demonstrate that the key performance parameters for steam condensers are appropriately scaled by the scaling study [1.2].

4.1.1 Pure Steam Tests

[

Redacted

]

[

Redacted

]

4.1.2 Heat Removal Degradation by Noncondensible Gas

[

Redacted

]

[

Redacted

]

4.1.3 Correlating the PCC Performance Data

[

Redacted

]

[

Redacted

]

[

Redacted

]

Table 4.1-1
GIRAFFE Phase 1, Step 1 Test Matrix

[

Redacted

]

Table 4.1-2
Deduced Scale Factors for the PCC at SBWR Test Facilities

[

Redacted

]

[

Redacted

]

Figure 4.1-1: Effect of Pressure on Pure Steam Condenser Tests

[

Redacted

]

Figure 4.1-2: Effect of Noncondensible Concentration on Normalized Power

[

Redacted

]

Figure 4.1-3: Scaling Comparison of Air/Steam Condenser Tests Using a Simple Heat Transfer Correlation

4.2 Integral System Transient Tests

[

Redacted

]

[

Redacted

]

4.2.1 Short-term RPV Behavior

[

Redacted

]

4.2.1.1 RPV Liquid Mass

[

Redacted

]

[

Redacted

]

[

Redacted

]

[

Redacted

]

[

Redacted

]

4.2.1.2 RPV Blowdown Pressure

An additional parameter which is important for the Late Blowdown/GDCS phase is the RPV pressure. It is important because it determines the time at which injection of GDCS flow to

the RPV can begin. The pressure rate equation is developed in the scaling report [1.2, Eq. 2.5-3]. The nondimensional form is

$$\Pi_P f_2^+ V^+ \frac{dP^+}{dt^+} = \sum_i \Pi_{\dot{Q},i} Q_i^+ - \Pi_{\dot{V}} P^{*+} \frac{dV^+}{dt^+} + \sum_i \Pi_{Wh,i} W_i^+ h_i^+ + \frac{P^{*+}}{\rho^+} \sum_i \Pi_{mech,i} W_i^+ - V^+ \sum_j \Pi_{y,j} \left(f_{1,j}^+ \frac{dy_j^+}{dt^+} \right) \tag{4.2.1-5}$$

where

$$P^* = P + \left.\frac{\partial e}{\partial v}\right|_{P,y_j}$$

$$f_{1,j} = \frac{1}{v} \left.\frac{\partial e}{\partial y_j}\right|_{P,v,y}$$

$$f_2 = \frac{1}{v} \left.\frac{\partial e}{\partial P}\right|_{v,y_j}$$

are thermodynamic properties, and

$$\Pi_P = \frac{\Delta P_o}{\Delta P_r}$$

$$\Pi_{Wh,i} = \frac{t_r W_{i,o} \Delta h_{i,o}}{\Delta P_r V_r f_{2,r}}$$

$$\Pi_{mech,i} = \frac{t_r W_{i,o} P_r^*}{\Delta P_r V_r f_{2,r} \rho_r}$$

$$\Pi_{\dot{Q},i} = \frac{t_r \dot{Q}_{i,o}}{\Delta P_r V_r f_{2,r}}$$

$$\Pi_{\dot{v}} = \frac{P_r^* \Delta V_r}{\Delta P_r V_r f_{2,r}}$$

$$\Pi_{y,j} = \frac{f_{1,j,o} \Delta y_{j,o}}{\Delta P_r f_{2,r}}$$

are PI numbers, and

$$P^+ = \frac{P - P_o}{\Delta P_o}; \quad V^+ = \frac{V}{V_r}; \quad dV^+ = \frac{dV}{\Delta V_r} \quad t^+ = \frac{t - t_o}{t_r};$$

$$\dot{Q}_i^+ = \frac{\dot{Q}_i}{\dot{Q}_{i.o}}; \quad W_i^+ = \frac{W_i}{W_{i.o}}; \quad h_i^+ = \frac{h_i - h}{\Delta h_{i.o}}; \quad y_j^+ = \frac{y_j - y_{j,o}}{\Delta y_{i.o}};$$

$$P^{*+} = \frac{P^*}{P_r^*}; \quad \rho^+ = \frac{\rho}{\rho_r}; \quad f_{1,j}^+ = \frac{f_{1,j}}{f_{1,j,o}}; \quad f_2^+ = \frac{f_2}{f_{2,r}}$$

are nondimensional variables.

Equation 4.2.1-5 has been modified from the form in Reference 1.2 to include a global pressure PI-group, Π_P. This allows the use of a global reference pressure (ΔP_r) change that may have more meaning on a system-wide basis while still using a local value (ΔP_o) in P^+ to maintain it at order 1.

The specific form of the pressure equation for the RPV is

$$
\begin{aligned}
\Pi_P f^+_{2,R} V^+_R \frac{dP^+_R}{dt^+} = & \sum_i \Pi_{\dot{Q},i} \dot{Q}^+_i && \text{(i = decht - losses, stored)} \\
& + \sum_i \Pi_{Wh,i} W^+_i h^+_i && \text{(i = ADS, break, GDCS, ICin, ICdrain)} \\
& + \frac{P^{*+}_R}{\rho^+_R} \sum_i \Pi_{mech,i} W^+_i && \text{(i = ADS, break, GDCS, ICin, ICdrain)} \qquad (4.2.1\text{-}6) \\
& + \Pi_{\dot{V}} P^{*+}_R \frac{dV^+_R}{dt^+} \\
& - V^+_R \sum_j \left[\Pi_{y,j} f^+_{1,R,j} \frac{dy^+_{R,j}}{dt^+} \right] && \text{(j = SW, NC)}
\end{aligned}
$$

The following abbreviations are used in the equation:

R	-	RPV
decht-losses	-	decay heat minus heat losses through RPV wall
stored	-	stored energy release from walls and structures
ADS	-	SRVs and DPVs
break	-	broken main steam line
ICin	-	IC inlet flow
ICdrain	-	IC drain flow
SW	-	combination of steam and liquid in vessel
N/C	-	noncondensible gases

[

Redacted

]

[

Redacted

]

4.2.2 Containment Performance

[

Redacted

]

4.2.2.1 Containment Behavior Overview

[

Redacted

]

[

Redacted

]

[

Redacted

]

4.2.2.2 Wetwell Behavior

[

Redacted

]

[

Redacted

]

4.2.2.2.1 WW Pressure

WW Pressure Rate Equation

The general nondimensional form of the pressure equation is the same as for the RPV given in Equation 4.2.1-5. The specific form for the WW is

$$\begin{aligned}
\Pi_P f_{2,w}^+ V_w^+ \frac{dP_W^+}{dt^+} = & \sum_i \Pi_{Wh,i} W_i^+ h_i^+ && (i = G/L_{sp},\ G/L_{walls},\ MV,\ VB,\ PCV,\ ICV) \\
& + \frac{P_W^{*+}}{\rho_W^+} \sum_i \Pi_{mech,i} W_i^+ && (i = G/L_{sp},\ G/L_{walls},\ MV,\ VB,\ PCV,\ ICV) \\
& + \sum_i \Pi_{\dot{Q},i} \dot{Q}_i^+ && (i = G/L_{sp},\ G/L_{walls}) \\
& - \Pi_{\dot{V}} \ P_R^{*+} \frac{dV_W^+}{dt^+} \\
& - V_W^+ \sum_j \Pi_{y,j} f_{1,W,j}^+ \frac{dy_{W,j}^+}{dt^+} && (j = S,\ N/C)
\end{aligned} \tag{4.2.2-1}$$

The following abbreviations are used in Equation 4.2.2-1:

W	-	WW gas space
PCV	-	PCC vent
ICV	-	IC vent
VB	-	vacuum breaker flow - leakage or normal
MV	-	main vent
SP	-	surface of suppression pool
Walls	-	surfaces where condensation occurs
G/L	-	gas/liquid interfaces
S	-	steam
N/C	-	noncondensible gases

The right side of the equation contains terms for enthalpy additions, mechanical compression from mass additions, heat additions, compression due to volume changes and changes in component mass fractions.

[

Redacted

]

With these modifications, the reduced WW pressure equation is

$$\Pi_P f_{2,w}^{+} V_w^{+} \frac{dP_W^{+}}{dt^{+}} = \sum_i \Pi_{Wh,i} W_i^{+} h_i^{+} \qquad (i = G/L_{sp},\ G/L_{walls},\ VB,\ PCV)$$

$$+ \frac{P_W^{*+}}{\rho_W^{+}} \sum_i \Pi_{mech,i} W_i^{+} \qquad (i = G/L_{sp},\ G/L_{walls},\ G/L_{misc}, VB,\ PCV)$$

$$+ \sum_i \Pi_{\dot{Q},i} \dot{Q}_i^{+} \qquad (i = misc)$$

$$- \Pi_{\dot{V}} \quad P_W^{*+} \frac{dV_W^{+}}{dt^{+}}$$

$$- V_W^{+} \sum_j \Pi_{y,j} f_{1,W,j}^{+} \frac{dy_{W,j}^{+}}{dt^{+}} \qquad (j = S,\ N/C)$$

(4.2.2-2)

[

Redacted

]

[

Redacted

]

[

Redacted

]

[

Redacted

]

[

Redacted

]

4.2.2.2.2 Suppression Pool Temperature

[

Redacted

]

4.2.2.3 DW Behavior

[

Redacted

]

[

Redacted

]

DW Pressure Equation

The general nondimensional form of the pressure equation is the same as for the RPV and WW, as given in Equation 4.2.1-7. The specific formula for the DW is

$$\Pi_P f_{2,D}^+ V_D^+ \frac{dP_D^+}{dt^+} = \sum_i \Pi_{Wh,i} W_i^+ h_i^+ \qquad (i = G/L_{RPV}, G/L_B, G/L_{LGB}, G/L_{walls}, MV, VB, PC, IC)$$

$$+ \frac{P_D^{*+}}{\rho_W^+} \sum_i \Pi_{mech,i} W_i^+ \quad (i = G/L_{RPV}, G/L_B, G/L_{LGB}, G/L_{walls}, MV, VB, PC, IC)$$

$$+ \sum_i \Pi_{\dot{Q},i} \dot{Q}_i^+ \qquad (i = G/L_{RPV}, G/L_B, G/L_{LGB}, G/L_{walls})$$

$$- \Pi_{\dot{V}} \; P_D^{*+} \frac{dV_D^+}{dt^+}$$

$$- V_D^+ \sum_j \Pi_{y,j} f_{1,D,j}^+ \frac{dy_{D,j}^+}{dt^+} \quad (j = S, N/C)$$

(4.2.2-6)

The following abbreviations are used in Equation 4.2.2-6:

D	-	DW plus RPV volume
PC	-	PCC inlet
IC	-	IC inlet
VB	-	vacuum breaker
RPV	-	surface of liquid in RPV
LGB	-	broken GDCS line to DW
B	-	broken line to DW from RPV
Walls	-	surfaces where condensation occurs
G/L	-	gas/liquid interfaces
S	-	steam
N/C	-	noncondensibles

The right side of the equation contains terms for enthalpy additions, mechanical compression from mass additions, heat additions, compression due to volume changes and changes in component mass fractions.

[

Redacted

]

[

Redacted

]

[

Redacted

]

[

Redacted

]

4.2.2.4 Summary of Containment Behavior and Scaling

[

Redacted

]

Table 4.2-1 Reference Values and PI-Groups for RPV Liquid Mass

[

Redacted

]

Table 4.2-2 Reference Values and PI-Groups for RPV Pressure During Late Blowdown and GDCS Transition Phases

[

Redacted

]

Table 4.2-3 Reference Values and PI-Groups for WW Pressure During PCC Phase

[

Redacted

]

Table 4.2-4 Reference Values and PI-Groups for DW Pressure During PCC Phase

[

Redacted

]

[

Redacted

]

Figure 4.2-1: PI-Group Magnitudes for RPV Liquid Mass Equation During Three Early Phases

[

Redacted

]

Figure 4.2-2: Nondimensional Comparison of RPV Mass Equation for SBWR, GIST and GIRAFFE

[

Redacted

]

Figure 4.2-3: PI-Group Magnitudes for RPV Depressurization - Late Blowdown

[

Redacted

]

Figure 4.2-4: Nondimensional Comparison of RPV Pressure for SBWR, GIST and GIRAFFE

[

Redacted

]

Figure 4.2-5: Comparison of WW Pressures for SBWR, PANDA and GIRAFFE - MSLB

[

Redacted

]

Figure 4.2-6: Comparison of DW Pressures for SBWR, PANDA and GIRAFFE - MSLB

[

Redacted

]

Figure 4.2-7: Comparison of SP Temperatures for SBWR, PANDA and GIRAFFE - MSLB

[

Redacted

]

Figure 4.2-8: Comparison of WW Pressures for SBWR and GIRAFFE - GDLB

[

Redacted

]

Figure 4.2-9: Comparison of DW Pressures for SBWR and GIRAFFE - GDLB

[

Redacted

]

Figure 4.2-10: Comparison of SP Temperatures for SBWR and GIRAFFE - GDLB

[

Redacted

]

Figure 4.2-11: Nondimensional Comparison of WW Pressure for SBWR, PANDA and GIRAFFE

[

Redacted

]

Figure 4.2-12: PI-Group Magnitudes for WW Pressure Phenomena - PCCS Phase

[

Redacted

]

Figure 4.2-13: WW Pressure Increases with Increases in Noncondensible Partial Pressures

[

Redacted

]

Figure 4.2-14: Time Dependent Behavior of Dominant WW Phenomena for SBWR, PANDA and GIRAFFE - PCCS Phase

[

Redacted

]

Figure 4.2-15: Nondimensional Comparison of DW Pressure for SBWR, PANDA and GIRAFFE - PCCS Phase

[

Redacted

]

Figure 4.2-16: PI-Group Magnitudes for DW Pressure Phenomena - PCCS Phase

[

Redacted

]

Figure 4.2-17: Time Dependent Behavior of Dominant DW Phenomena for SBWR, PANDA and GIRAFFE - PCCS Phase

4.3 Helium Tests

[

Redacted

]

[

Redacted

]

4.4 Scaling Distortions

4.4.1 Background

Simulation of the SBWR transient performance using scaled models and tests invariably introduces nonprototypicalities in some of the many processes that occur during a transient. These can lead to scaling distortions that need to be examined to determine if they significantly influence the overall system performance simulation. This section examines the distortions that exist in the SBWR test facilities. Distortions that are important need to be accounted for in the code validation and design certification process, whereas scaling distortions that are deemed unimportant can be ignored.

[

Redacted

]

4.4.2 Scaling Issues Considered

[

Redacted

]

4.4.3 Scaling Issue Evaluation

[

Redacted

]

4.4.3.1 Heat Release from RPV Structures

[

Redacted

]

[

Redacted

]

[

Redacted

]

[

Redacted

]

[

Redacted

]

4.4.3.2 Heat Release from DW Structures

[

Redacted

]

[

Redacted

]

[

Redacted

]

4.4.3.3 Drywell Mixing

[

Redacted

]

[

Redacted

]

[

Redacted

]

[

Redacted

]

4.4.4 Discussion of Safety Parameters

[

Redacted

]

[

Redacted

]

Table 4.4-1
List of Perceived Scaling Distortions and Evaluation Results for SBWR Related Test Facilities

[

Redacted

]

Table 4.4-1
List of Perceived Scaling Distortions and Evaluation Results for SBWR Related Test Facilities (Continued)

[

Redacted

]

Table 4.4-1
List of Perceived Scaling Distortions and Evaluation Results for SBWR Related Test Facilities (Continued)

[

Redacted

]

Table 4.4-2
Calculated Specific Time Ratios for Drywell Mixing

	SBWR	GIRAFFE/He	PANDA
Time ratio (forced jet)	>20	140	70
Time ratio (buoyant plume)	>10	160	50

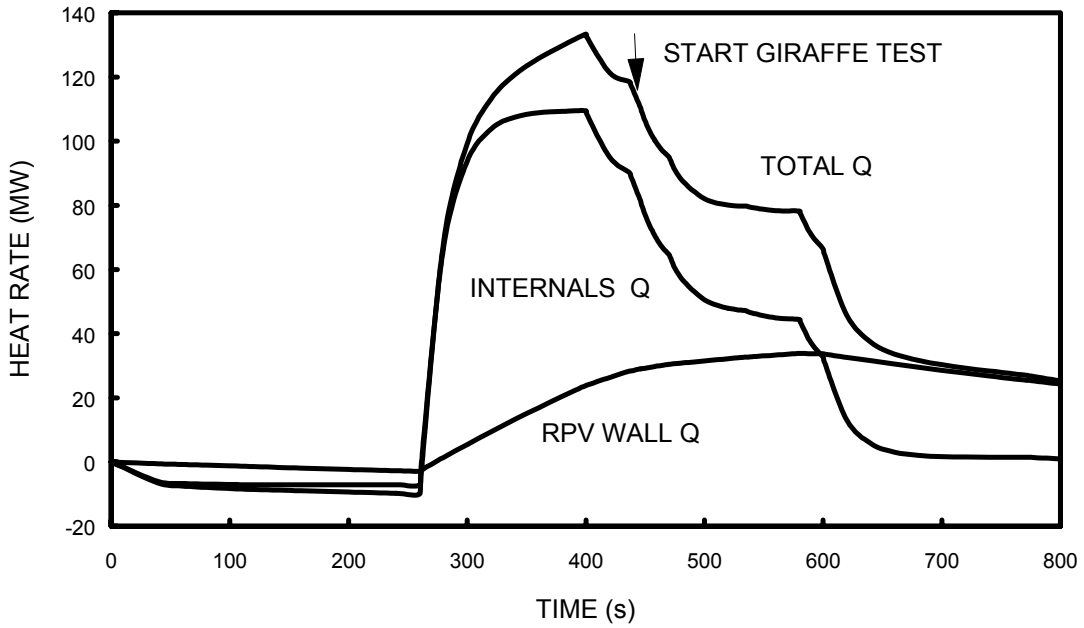

Figure 4.4-1: SBWR Structural Heat Release Rates for Blowdown Transient

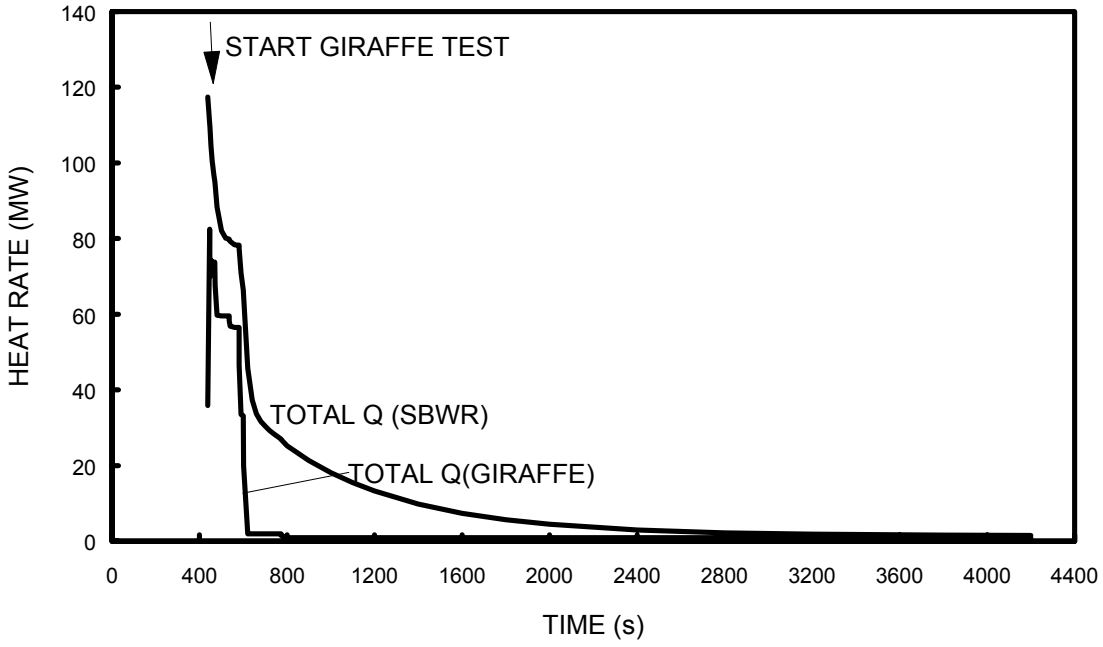

Figure 4.4-2: Comparison of Structural Heat Release Rates for SBWR and GIRAFFE

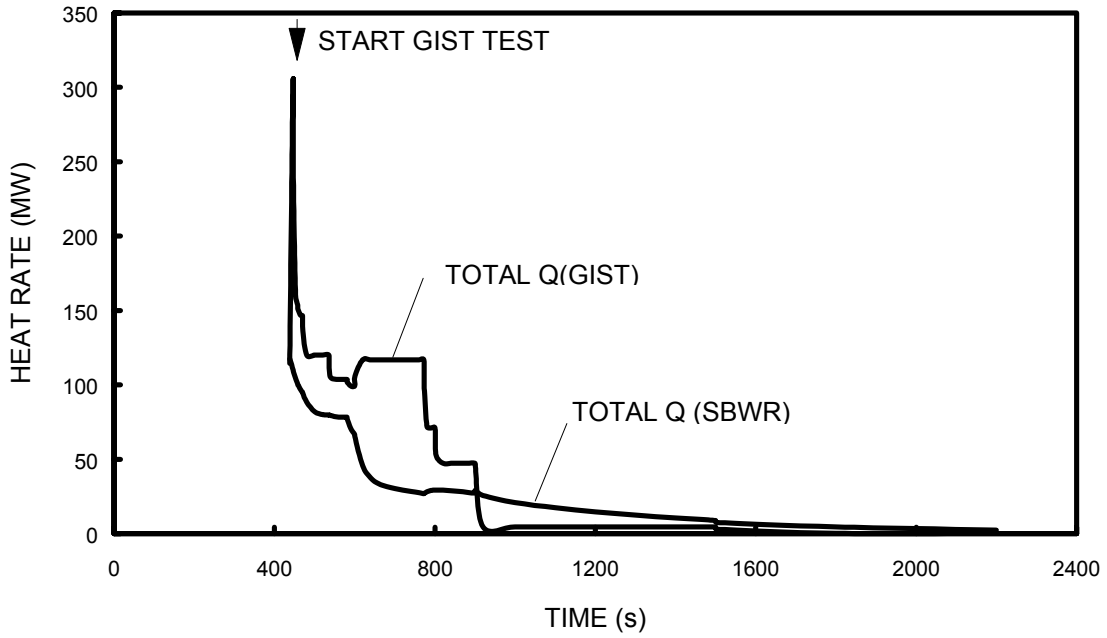

Figure 4.4-3: Comparison of Structural Heat Release Rates for SBWR and GIST

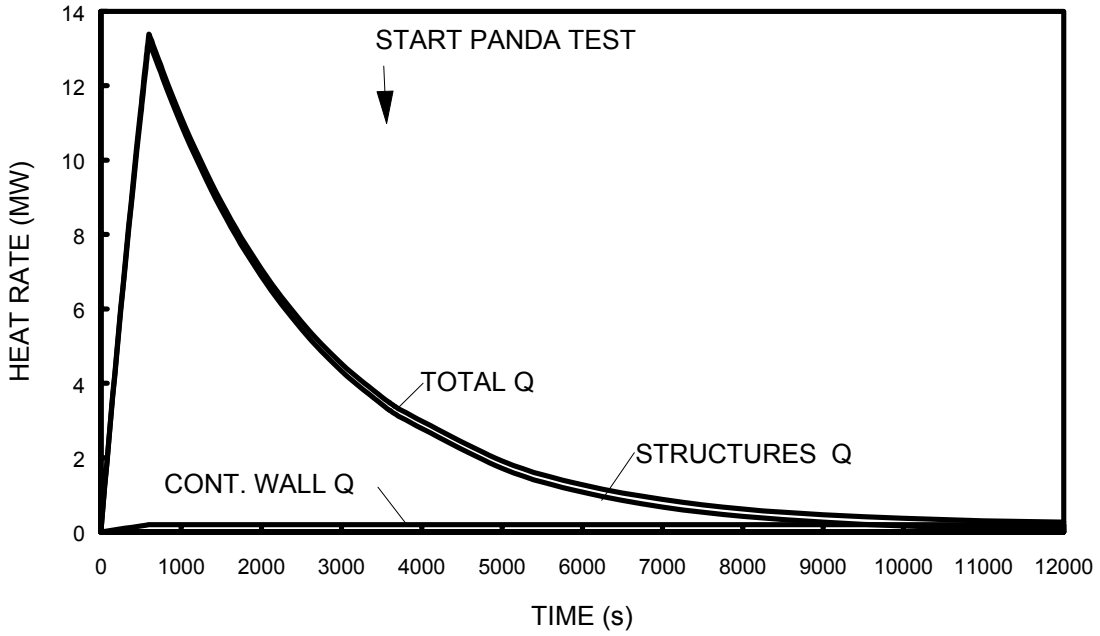

Figure 4.4-4: SBWR DW Heat Loss Rates for Transient

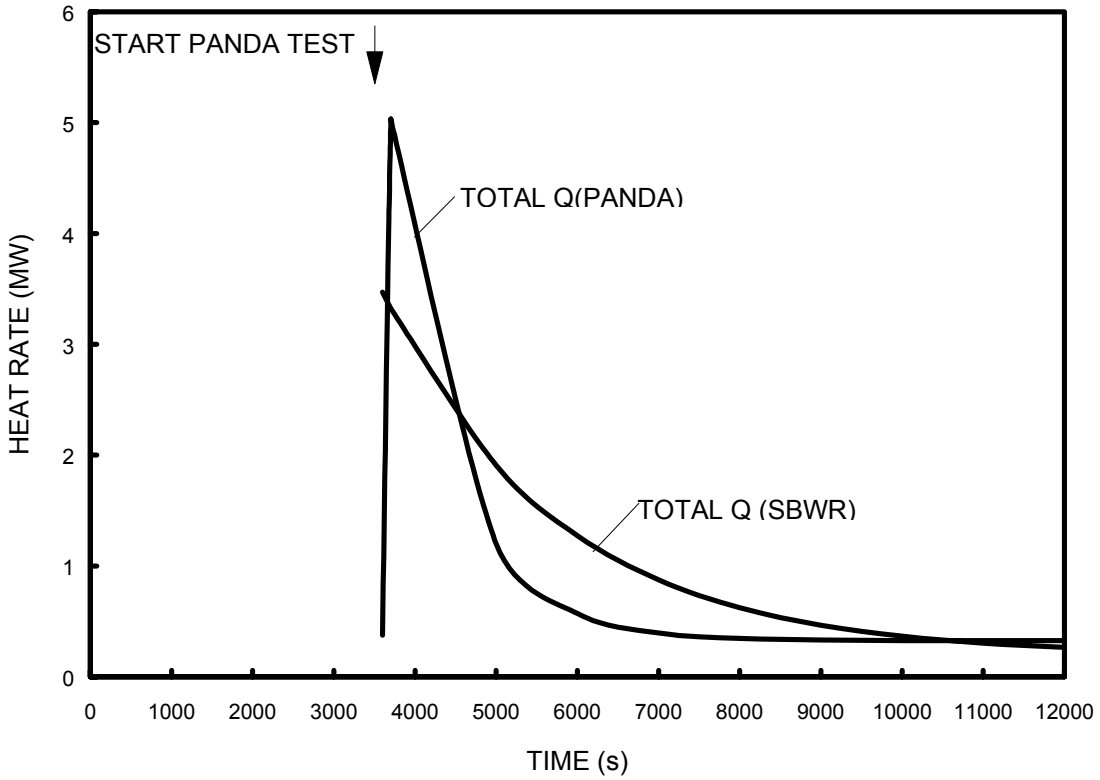

Figure 4.4-5: Comparison of DW Structural Heat Loss Rates for SBWR and PANDA

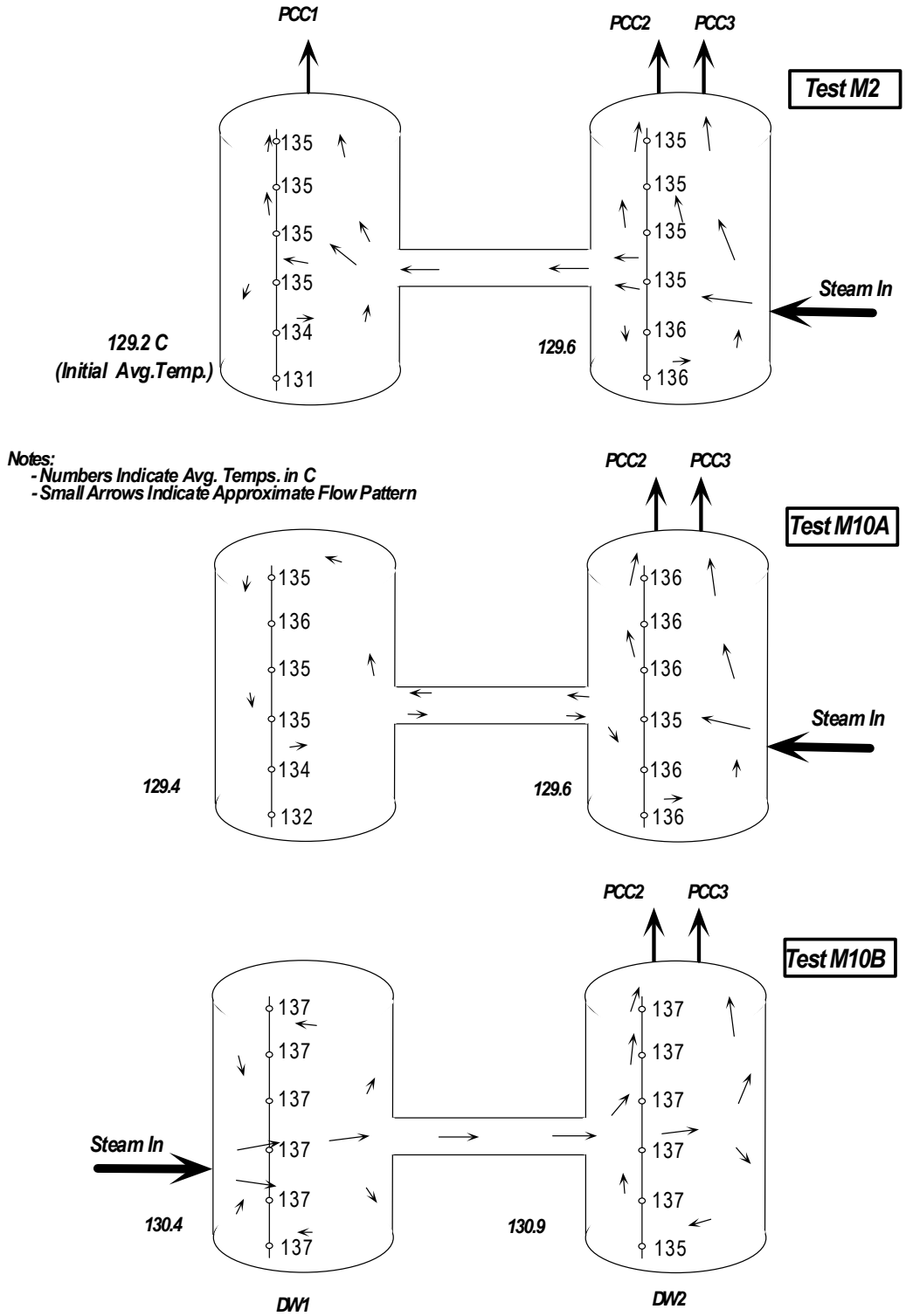

Figure 4.4-6: PANDA DW Axial Temperatures for Asymmetry Tests at 20,000 sec

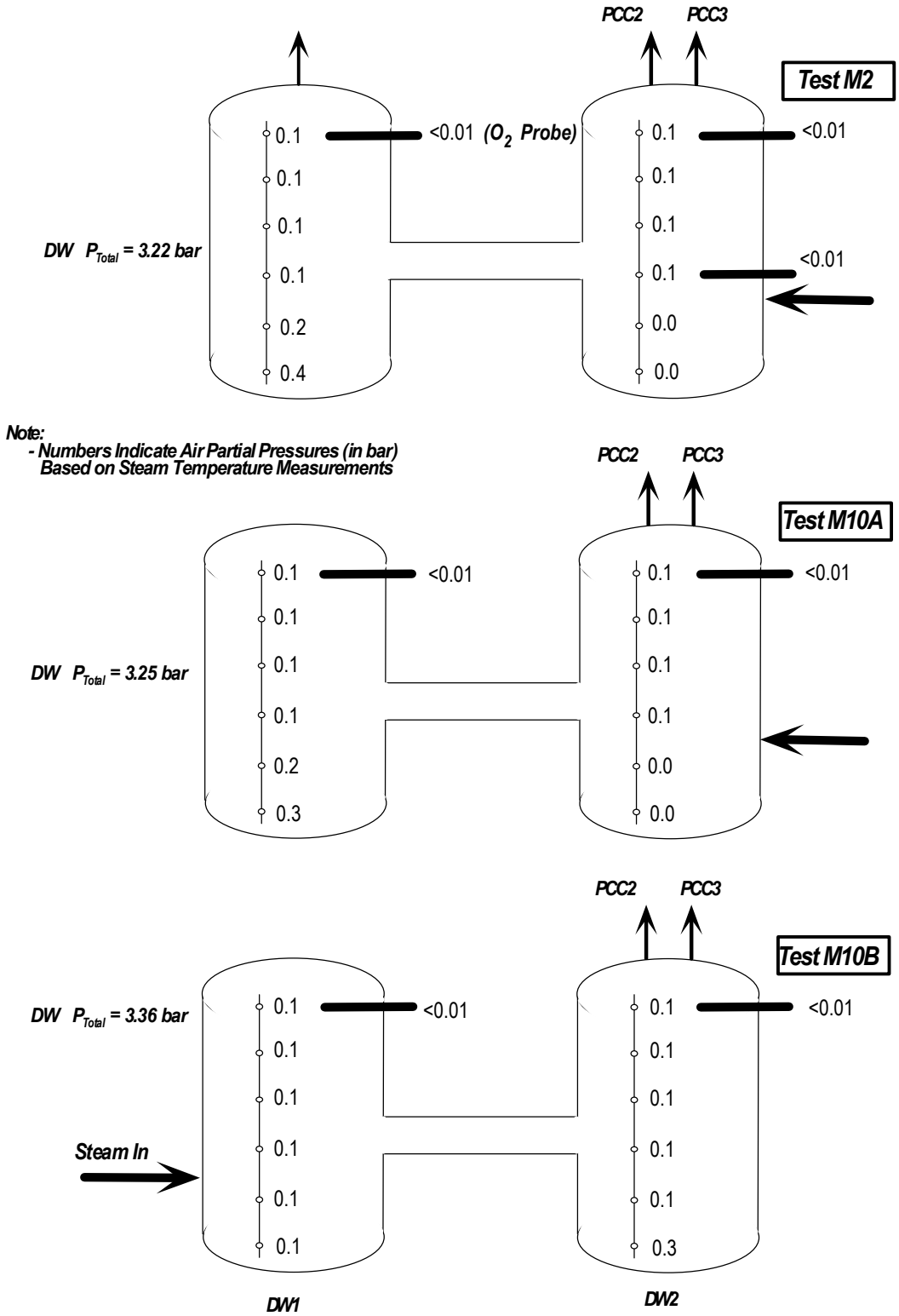

Figure 4.4-7: PANDA DW Air Partial Pressures for Asymmetry Tests at 20,000 sec

5. CONCLUSIONS

This *SBWR Testing Summary Report* summarizes the extensive database generated by GE and its associates from the SBWR-unique thermal-hydraulic test programs. A major objective of these test programs was to provide test data to qualify the GE computer code TRACG for SBWR applications. Both component and integral systems transient tests were conducted to gather this data and study the phenomena of interest. In addition to meeting that objective, the following conclusions were drawn from these test programs:

[

Redacted

]

[

Redacted

]

6. REFERENCES

General Documents

[1.1] *SBWR Test and Analysis Program Description,* GE Nuclear Energy, NEDC-32391, Rev. C, August 1995.

[1.2] *Scaling of the SBWR Related Tests,* GE Nuclear Energy, NEDC-32288P, Rev. 1, October 1995.

[1.3] *Heat and Mass Transfer,* A.F. Mills, IRWIN, Chicago, 1995.

[1.4] *SBWR Containment Response to LOCA: Passive Heat Removal System Performance,* B.S. Shiralkar, R.E.Gamble, G. Yadigaroglu, Beijing Conference., 1997.

[1.5] Letter, R.H. Buchholz (GE) to USNRC, *Submittal of Additional Information on Licensing Topical Reports (NEDE-32176P, NEDE-32177P and NEDE-32178P)*, September 20, 1994, Docket No. 52-004, MFN-096-94.

[1.6] *Scaling and Analysis of Mixing in Large Stratified Volumes,* P.F. Peterson, Int. J. Heat and Mass Transfer. Vol 37, Suppl. 1, 1994.

[1.7] Letter, Theodore E. Quay (NRC) to J. E. Quinn (GE), *Staff Evaluation of General Electric's (GE's) Test and Analysis Program Description, NEDC-32391, Revision C*, July 11, 1996, Docket No.52-004.

PANTHERS Documents

[2.1] *Isolation Condenser and Passive Containment Condenser Test Requirements,* GE Nuclear Energy, 22A6999, Rev. 5, October 23, 1995.

[2.2] *PANTHERS/PCC Test Plan & Procedures,* SIET document No. 0098 PP 91, Rev. 1, July 12, 1994.

[2.3] *Technical Specification For IC & PCC Instruments Installation,* SIET document No. 00157ST92, Revision 1, January 1, 1994.

[2.4] *PANTHERS/PCC Test Facility Instrumentation, Data Acquisition, & Processing Specification,* SIET document No. 00095RS91, Revision 1, June 8, 1994.

[2.5] *Thermal-Hydraulic Data Report of PANTHERS/PCC Tests,* SIET document No. 00393RP95, Rev. 1, January 24, 1996.

[2.6] *PANTHERS/PCC Data Analysis Report,* SIET document No. 0039RA95, Rev. 0, June *20, 1995.*

[2.7] *PANTHERS-IC Test Plan*, SIET document No. 00396RI95, Rev. 1, February 7, 1996.

[2.8] *PANTHERS-IC Test Procedures*, SIET document No. 00395PP95, Rev. 1, February 15, 1996.

[2.9] *PANTHERS-IC Test Report,* SIET document No. 00458RP95, Rev. 0, April 19, 1996.

[2.10] *PANTHERS/PCC Apparent Test Results,* MFN 063-95, April 25, 1995.

[2.11] *PANTHERS-IC Apparent Test Results, Phase 1,* MFN 246-95, October 25, 1995.

[2.12] *PANTHERS-IC Apparent Test Results, Phase 3,* MFN 005-96, January 9, 1996.

PANDA Documents

[3.1] *PANDA Test Specification,* GE Nuclear Energy, 25A5587, Rev. 1, January 26, 1995.

[3.2] *PANDA Steady State PCC Performance Tests, Test Plan and Procedures,* Paul Scherrer Institut, document No. ALPHA-410-2, May 16, 1995.

[3.3] *PANDA Test Plan for M3, M3A, M3B, M4, M7;* GE Nuclear Energy, 25A5764, Rev. 3, November 15, 1995.

[3.4] *PANDA Test Plan for M2, M10A, M10B;* GE Nuclear Energy, 25A5785, Rev. 0, November 21, 1995.

[3.5] *PANDA Test Plan for M6/8;* GE Nuclear Energy, 25A5788, Rev. 0, December 7, 1995.

[3.6] *PANDA Test Plan for M9;* GE Nuclear Energy, 25A5824, Rev. 0, December 12, 1995.

[3.7] *M3, M3A, M3B Integral System Test Procedure,* Paul Scherrer Institut, document No. ALPHA-520-2, October 24, 1995.

[3.8] *M7 Integral System Test Procedure,* Paul Scherrer Institut, document No. ALPHA-521-0, November 14, 1995.

[3.9] *M2, M10A, M10B Integral System Test Procedure,* Paul Scherrer Institut, document No. ALPHA-527-0, November 21, 1995.

[3.10] *M6/8 Integral System Test Procedure,* Paul Scherrer Institut, document No. ALPHA-529-0, December 8, 1995.

[3.11] *M9 Integral System Test Procedure,* Paul Scherrer Institut, document No. ALPHA-528-0, December 18, 1995.

[3.12] *S1 through S6 PCC Performance Apparent Test Results,* Paul Scherrer Institut, document No. ALPHA-509-1, October 3, 1995.

[3.13] *S10 through S13 PCC Performance Apparent Test Results,* Paul Scherrer Institut, document No. ALPHA-522-0, February 8, 1996.

[3.14] *M3 Integral System Test Apparent Test Results,* Paul Scherrer Institut, document No. ALPHA-601-0, March 18, 1996.

[3.15] *M3A Integral System Test Apparent Test Results,* Paul Scherrer Institut, document No. ALPHA-604-0, March 29, 1996.

[3.16] *M3B Integral System Test Apparent Test Results,* Paul Scherrer Institut, document No. ALPHA-605-0, April 11, 1996.

[3.17] *M7 Integral System Test Apparent Test Results,* Paul Scherrer Institut, document No. ALPHA-607-0, April 17, 1996.

[3.18] *M2 Integral System Test Apparent Test Results,* Paul Scherrer Institut, document No. ALPHA-608-0, April 25, 1996.

[3.19] *M10A Integral System Test Apparent Test Results,* Paul Scherrer Institut, document No. ALPHA-610-1, June 12, 1996.

[3.20] *M10B Integral System Test Apparent Test Results,* Paul Scherrer Institut, document No. ALPHA-611-1, June 12, 1996.

[3.21] *M6/8 Integral System Test Apparent Test Results,* Paul Scherrer Institut, document No. ALPHA-612-1, June 12, 1996.

[3.22] *M9 Integral System Test Apparent Test Results,* Paul Scherrer Institut, document No. ALPHA-614-0, May 10, 1996.

[3.23] *PANDA Facility, Test Program and Data Base General Description,* Paul Scherrer Institut, document No. ALPHA-606-0, May 31, 1996.

[3.24] *PANDA Steady State Data Transmittal Report,* Paul Scherrer Institut, document No. ALPHA-609-0, May 31, 1996.

[3.25] *M3 Integral System Test Data Transmittal Report,* Paul Scherrer Institut, document No. ALPHA-613-0, June 18. 1996.

[3.26] *M3A Integral System Test Data Transmittal Report,* Paul Scherrer Institut, document No. ALPHA-615-0, June 28, 1996.

[3.27] *M3B Integral System Test Data Transmittal Report,* Paul Scherrer Institut, document No. ALPHA-616-0, July 2, 1996.

[3.28] *M7 Integral System Test Data Transmittal Report,* Paul Scherrer Institut, document No. ALPHA-617-0, July 2, 1996.

[3.29] *M2 Integral System Test Data Transmittal Report,* Paul Scherrer Institut, document No. ALPHA-618-0, July 2, 1996.

[3.30] *M10A Integral System Test Data Transmittal Report,* Paul Scherrer Institut, document No. ALPHA-619-0, July 12, 1996.

[3.31] *M10B Integral System Test Data Transmittal Report,* Paul Scherrer Institut, document No. ALPHA-620-0, July 16, 1996.

[3.32] *M6/8 Integral System Test Data Transmittal Report,* Paul Scherrer Institut, document No. ALPHA-621-0, July 22, 1996.

[3.33] *M9 Integral System Test Data Transmittal Report,* Paul Scherrer Institut, document No. ALPHA-622-0, July 30, 1996.

[3.34] *PANDA Facility Characterization: Vessel Heat Loss Measurements,* Paul Scherrer Institut, document No. ALPHA-519-0, document in process.

[3.35] *PANDA Facility Characterization: System Line Loss Coefficient Measurements,* Paul Scherrer Institut, document No. ALPHA-517-0, February 15, 1996.

GIST Documents

[4.1] *Test Requirements and Test Specification for GDCS Integrated Systems Test,* GE WA No. XVS841875, Rev. 1, October 30, 1987.

[4.2] *Testing of the Gravity-Driven Cooling System for the Simplified Boiling Water Reactor, Final Test Report,* NEDO-31680, July 1989.

[4.3] *GIST Final Test Report, SBWR Program Gravity-Driven Cooling System Integrated Systems Test,* GEFR-00850, October 1989.

GIRAFFE-HE Documents

[5.1] *GIRAFFE Test Specification, GE Nuclear Energy*, 25A5677, Rev. 1, May 10, 1995.

[5.2] *GIRAFFE SBWR Helium Series Test Report*, GE Nuclear Energy, NEDC-32608P, June 1996.

[5.3] *GIRAFFE Test Helium Series Tests H1 through H4, T1 and T2 Apparent Test Results Reports,* MFN 038-96, March 14, 1996.

GIRAFFE-SIT Documents

[6.1] *GIRAFFE SBWR Systems Interaction Test Report,* NEDC-32540P, June 1996.

[6.2] *GIRAFFE Test GS1 Apparent Test Results Report,* NEDC-32541P, March 1996.

[6.3] *GIRAFFE Test GS2 Apparent Test Results Report,* NEDC-32542P, March 1996.

[6.4] *GIRAFFE Test GS3 Apparent Test Results Report,* NEDC-32543P, March 1996.

[6.5] *GIRAFFE Test GS4 Apparent Test Results Report,* NEDC-32544P, March 1996.

[6.6] *GE Nuclear Energy GIRAFFE System Interaction Test Specification,* Document 25A5772 Rev. 0, September 27, 1995.

APPENDIX A

DEVELOPMENT OF RPV LIQUID MASS EQUATIONS

The dimensional and non-dimensional forms of the mass equation were developed in the Scaling Report [1.2], but the specific formulas for the liquid mass in the RPV were not developed. This appendix provides the development of these formulas.

The basic mass conservation equation for the liquid phase in the RPV volume, V_{RPV}, is

$$\frac{dM_l}{dt} = \sum_i W_{l,i} - \dot{M}_{fg} \tag{A-1}$$

where:

M_l = is the liquid mass

$W_{l,i}$ = are liquid flows entering or exiting

$\dot{M}_{fg}$ = are the net vapor generation term

Equation B.1.4-5 of Reference 1.2 provides the net vapor generation equation

$$\dot{M}_{fg} = \frac{1}{h_{fg}} \sum_i \dot{Q}_i + \frac{1}{h_{fg}} \sum_i (h_{l,i} - h_f)\ W_{l,i} + \frac{1}{h_{fg}} \frac{dP}{dt} \left[V_{RPV} - \left(M_f \frac{dh_f}{dP} + M_g \frac{dh_g}{dP} \right) \right] \tag{A-2}$$

Substituting this into equation A-1 yields

$$\frac{dM_l}{dt} = \sum_i W_{l,i} - \sum_i \frac{\dot{Q}_i}{h_{fg}} + \sum_i \frac{\left(h_f - h_{l,i}\right)}{h_{fg}} W_{l,i} - \frac{1}{h_{fg}} \left[V_{RPV} - \left(M_l h_f' + M_g h_g' \right) \right] \frac{dP}{dt} \tag{A-3}$$

where primes (′) indicate derivatives with respect to pressure along the saturation line.

The vapor mass in the control volume, M_g, can be related to the liquid mass by

$$M_g = \rho_g V_g = \rho_g \left(V_{RPV} - V_l \right) = \rho_g \left(V_{RPV} - \frac{M_l}{\rho_l} \right) \tag{A-4}$$

Then equation A-3 becomes

$$\frac{dM_l}{dt} = -\sum_i \frac{\dot{Q}_i}{h_{fg}} + \sum_i W_{l,i} + \sum_i \frac{\Delta h_{sub,i} W_{l,i}}{h_{fg}} - \frac{1}{h_{fg}} \left[V_{RPV} \left(1 - \rho_g h_g^{'} \right) + M_l \left(\frac{\rho_g}{\rho_l} h_g' - h_f' \right) \right] \frac{dP}{dt} \tag{A-5}$$

where,

$$\Delta h_{sub,i} = h_f - h_{l,i}$$

The nondimensionalization and normalization procedure and the nomenclature used are defined below. Consider:

- the *local* variable, z_n, (e.g., the particular flow rate n entering a volume)
- a local scale, $z_{n,o}$:

  $z_{n,o}$ is typically an initial or boundary or average value or some other proper scale for that particular local variable.
- the global scale, z_r, for all the variables z (e.g., for all flow rates):

  z_r is typically the most important value of z (e.g., the blowdown flow rate when the Blowdown phase of the accident is considered) or the sum of the local scales, $z_{n,o}$.

  One then defines:
- the *locally* scaled variable,

$$z_n^+ \equiv \frac{z_n}{z_{n,o}}$$

- the local normalizing factor or weight,

$$z_n^+ \equiv \frac{z_n}{z_{n,o}}$$

and obtains:

$$z_n = \left(\frac{z_n}{z_{n,o}} \right) \left(\frac{z_{n,o}}{z_r} \right) z_r = z_n^+ z_n^o z_r$$

First define the new thermodynamic variables

$$f_3 = 1 - \rho_g h'_g$$

$$f_4 = \frac{\rho_g}{\rho_l} h'_g - h'_f$$

Now define the nondimensional variables

$$M_l^+ = \frac{M_l - M_{l,o}}{\Delta M_{l,o}}$$

$$\dot{Q}_i^+ = \frac{\dot{Q}_i}{\dot{Q}_{i,o}}$$

$$t^+ = \frac{t}{t_r}$$

$$W_{l,i}^+ = \frac{W_{l,i}}{W_{l,i,o}} \tag{A-6}$$

$$h_{sub,i}^+ = \frac{\Delta h_{sub,i}}{\Delta h_{sub,i,o}} \quad ; \quad h_{fg}^+ = \frac{h_{fg}}{h_{fg,r}}$$

$$f_3^+ = \frac{f_3}{f_{3,r}} \quad ; \quad f_4^+ = \frac{f_4}{f_{4,r}}$$

$$P^+ = \frac{P - P_o}{\Delta P_r}$$

Then the nondimensional form of Equation A-5 is

$$\begin{aligned}\left(\frac{\Delta M_{l,r}}{W_r t_r}\right)\left(\frac{\Delta M_{l,o}}{\Delta M_{l,r}}\right) h_{fg}^+ \frac{dM_l^+}{dt^+} = {} & \frac{-\dot{Q}_r}{W_r h_{fg,r}} \sum_i \left(\frac{\dot{Q}_{i,o}}{\dot{Q}_r}\right) \dot{Q}_i^+ + \left(\frac{W_{l,r}}{W_r}\right) h_{fg}^+ \sum_i \left(\frac{W_{l,i,o}}{W_{l,r}}\right) W_{l,i}^+ \\ & + \left(\frac{W_{l,r}}{W_r} \frac{\Delta h_{sub,r}}{h_{fg,r}}\right) \sum_i \left(\frac{\Delta h_{sub,i,o}}{\Delta h_{sub,r}}\right)\left(\frac{W_{l,i,o}}{W_{l,r}}\right) h_{sub,i}^+ W_{l,i}^+ \\ & - \left[\frac{V_{RPV} f_{3,r}}{W_r h_{fg,r}} \frac{\Delta P_r}{t_r} f_3^+ + \frac{\Delta M_{l,o} f_{4,r}}{W_r h_{fg,r}} \frac{\Delta P_r}{t_r} f_4^+ \left(M_l^+ + \frac{M_{l,o}}{\Delta M_{l,o}}\right)\right] \frac{dP^+}{dt^+}\end{aligned} \tag{A-7}$$

where we have divided the entire equation by $W_r\, h_{fg,r}$.

This can be written for the RPV as,

$$\Pi_t \Pi_{GM} h_{fg}^{+} \frac{dM_l^{+}}{dt^{+}} = -\Pi_{PCH} \sum_i \dot{Q}_i^{o} \dot{Q}_i^{+} + \Pi_W h_{fg}^{+} \sum_i W_{l,i}^{o} W_{l,i}^{+} + \Pi_{sub} \sum_i \Delta h_{sub,i}^{o} W_{l,i}^{o} h_{sub,i}^{+} W_{l,i}^{+}$$
$$-\Pi_t \Pi_{GM} \Pi_{\dot{P}} \left[\Pi_V f_3^{+} + f_4^{+} \left(M_l^{+} + \Pi_M \right) \right] \frac{dP_R^{+}}{dt^{+}} \tag{A-8}$$

where, following the nomenclature defined above, we find the following

$$\dot{Q}_i^{o} = \frac{\dot{Q}_{i,o}}{\dot{Q}_r}$$

$$W_{l,i}^{o} = \frac{W_{l,i,o}}{W_{l,r}}$$

$$h_{sub,i}^{o} = \frac{\Delta h_{sub,i,o}}{\Delta h_{sub,r}}$$

which relate local reference values to global ones and the following PI numbers:

$$\Pi_t = \frac{\Delta M_{l,r}}{W_r t_r}$$

$$\Pi_{GM} = \frac{\Delta M_{l,o}}{\Delta M_{l,r}}$$

$$\Pi_{PCH} = \frac{\dot{Q}_r}{W_r h_{fg,r}}$$

$$\Pi_W = \frac{W_{l,r}}{W_r}$$

$$\Pi_{sub} = \frac{\Delta h_{sub,r}}{h_{fg,r}} \frac{W_{l,r}}{W_r}$$

$$\Pi_{\dot{P}} = \frac{f_{4,r} \Delta P_r}{h_{fg,r}}$$

$$\Pi_V = \frac{V_{RPV} f_{3,r}}{\Delta M_{l,o} f_{4,r}}$$

$$\Pi_M = \frac{M_{l,o}}{\Delta M_{l,o}}$$

By using local PI-groups and dividing through by Π_t, Equation A-8 can also be written as

$$\Pi_{GM} h_{fg}^{+} \frac{dM_l^{+}}{dt^{+}} = \left[-\sum_i \Pi_{PCH,i} \dot{Q}_i^{+} + h_{fg}^{+} \sum_i \Pi_{W,i} W_{l,i}^{+} + \sum_i \Pi_{sub,i} h_{sub,i}^{+} W_{l,i}^{+} \right] \Big/ \Pi_t$$
$$-\Pi_{GM} \Pi_{\dot{P}} \left[\Pi_V f_3^{+} + f_4^{+} \left(M_l^{+} + \Pi_M \right) \right] \frac{dP_R^{+}}{dt^{+}} \qquad \text{(A-9)}$$

where the local PI numbers are defined as

$$\Pi_{PCH,i} = \Pi_{PCH} \dot{Q}_i^{o} = \frac{\dot{Q}_{i,o}}{W_r h_{fg,r}}$$

$$\Pi_{W,i} = \Pi_W W_{l,i}^{o} = \frac{W_{l,i,o}}{W_r}$$

$$\Pi_{sub,i} = \Pi_{sub} \Delta h_{sub,i}^{o} W_{l,i}^{o} = \frac{\Delta h_{sub,i,o}}{h_{fg,r}} \frac{W_{l,i,o}}{W_r}$$

Equation A-9 is the same as Equation 4.2.1-2 found in Section 4.2.